Utilization of Surface-active Compounds and Microfibrillated Cellulose Particles from Argan Processing Residue as Sustainable Natural Emulsifiers

August 2020

Meryem BOUHOUTE

Utilization of Surface-active Compounds and Microfibrillated Cellulose Particles from Argan Processing Residue as Sustainable Natural Emulsifiers

A Dissertation Submitted to

the School of Integrative and Global Majors,

the University of Tsukuba

in Partial Fulfillment of the Requirements

for the Degree of Doctor of Philosophy in Food Innovation

(Doctoral Program in Life Science Innovation)

Meryem BOUHOUTE

Advisory committee:

Associate Professor. Dr. M.A. Neves
Food and Process Engineering

Professor. Dr. M. Nakajima
Appropriate Technology and Science for Sustainable Development

Professor. Dr. I. Kobayashi
Food and Process Engineering

Professor. Dr. H. Isoda
Food Functionality and Natural Compounds Drug Discovery

“Nothing in life is to be feared, it is only to be understood.
Now is the time to understand more, so that we may fear less.”

Marie Curie

Acknowledgment

I had the privilege to spend three fascinating years (2017-2020) in the Food Resources Engineering Laboratory at the University of Tsukuba. It was an enormous honor to pursue a Ph.D. based on a collaboration between Morocco and Japan and this could never be possible without the Japan Science and Technology Agency (JST) and the Japan International Cooperation Agency (JICA) funding SATEPS project international research. With my sincerest gratitude, I wish to begin my thesis by acknowledging those who kindly supported me during this dissertation.

First, I wish to thank Professor Nakajima Mitsutoshi and Professor Marcos Neves for providing me the opportunity to join their laboratory. Professor Nakajima openness for discussion was a relieve when research questions were getting complicated, learning from his experience was an honor for me. The degree of freedom that I could get to pursue my own ideas would have never been possible without him and I will be always grateful to him. Associate Professor Neves who helped me with his advices, supervision and fruitful discussions, trusting me with my ideas and supporting them.

Thank you to Professor Hiroko Isoda, leader of TLSI program, for providing me with the opportunity to join this prestigious program, for her dedication to each student research aswell as her dedication to the SATREPS project thrive.

I wish to thank Professor Kobayashi Isao for being a co-supervisor of this thesis. His advises through this three year were essential for this thesis and I am sincerely grateful for the time that he spend discussing with me rising more research questions and shaping my thoughts.

My sincere gratitude goes also to Professor Zahar Mohamed for facilitating my journey and helping before and after my acceptance to conduct this thesis.

Next, I had the pleasure to work with brilliant students, discussing with them and working with them, practicing in front of them was an essential part of this thesis. Many thanks to Noamane Taarji, Lenin Kandasamy, Sekove Vodo, Lorena De Filipe, Teetach Changwatchai, Khaiwenn Seah. I gain not only science and knowledge from them but real friendship.

Thank you to all the group members of Nakajima' Lab, Sohan, Cherry, Grace, Baggi, Samar, Potter, Sakata, Hakiki, Kubra, Yuntai, Aymen.

Thank you to Kawamoto san and all the TLSI office for all the administrative support and help.

Thank you to Dr. Youssef Habibi from Luxembourg Institute of Science and Technology for providing me with the opportunity to visit his lab in Beleaux. During my visit I met with inspiring people and made great discussion. Thank you to Reiner Dieden, Yves Fleming, Régis Vaudemont, and many others who helped me during this experience. A special thanks to Nejib and Abdoulah.

A special thank you to all the people I met during this journey, who inspired me for more, Michael and Alessandro, thank you.

Am thankful for the support of all my friends, my dear roommate Meriem and my dear friends Yllah, Sarah, Ola, Islem, Slim, Seif, Aymen, Riadh, Akram, Xue, Baggi, Lenin, Lorena, Rachid, Mehdi, Youssef. There are no words to describe all the support I received from them and I am so lucky I had to spend these three years with all of them.

Thank you to all JICA Tsukuba team especially Mcgoey san.

Last but not least, I would like to thank my parents, who stood behind me in every single step of my life and without whom I would never be able to reach even a smallest portion of this work. Mouna and Youssef for our fun moments and for pushing me to be the best. Farouk for being such wonderful cousin and friend. Oumaima my second sister and my dearest friend for all these years of support. All, Ouchrif and Bouhoute families, my sincerest thanks to all of you, I love you so much.

Finally, this work is dedicated to the memory of my dearest uncle Mohammed Ouchrif (Khali) who inspired all my childhood and with whom I had the most inspiring talks, I will always remember his excitement when I told him I want to pursue a PhD , you were one of a kind and the memory of you will always be in my heart, may you rest in peace.

Meryem BOUHOUTE

Tsukuba, May 2020

Abstract

Oil-in-water (O/W) emulsion is a system encountered in many commercial products such as food, cosmetic and pharmaceutic industries. This system is thermodynamically unstable consisting of two immiscible liquids, one dispersed into the other, that would rapidly separate to the initial homogenized components in the absence of stabilizers. Emulsion stabilizers can be categorized into surface-active emulsifiers (surfactants) and thickening or gelling agents. Furthermore, solid particles were also described to stabilize emulsions forming the so-called 'Pickering emulsions' that were first reported by Pickering (1907) [1]. Our research focus was to identify a new natural source of surface-active compounds and microfibrillated cellulose and utilize them to formulate and stabilize emulsions. First, a characterization of the extracted compounds by means of spectrophotometric methods, Fourier Transform infrared spectroscopy (FTIR), X-ray diffraction (XRD), nuclear magnetic resonance (NMR), thermogravimetric analysis (TGA), differential scanning calorimetry (DSC), interfacial tension and contact angle, scanning electron microscopy (SEM) and transmission electron microscopy (TEM), was conducted. Then, we focused on the utilization of the identified compounds to formulate and stabilize (O/W) emulsions, this involved high energy emulsification and monitoring physical stability under different environmental stress conditions.

Emulsions formulation and stability using natural emulsifiers is varying considerably due to the source and the type of surface-active compounds. This is even more the case when using crude extracts from plant material as emulsion stabilizers. Mostly, interfacial tension and composition are used to confirm the tendency of an emulsifier to formulate a stable emulsion. However, systemic studies also offer more reflection on the mechanism behind a successful stability. Our study showed the possibility of using crude argan shell extracts as natural emulsifiers. We confirmed that with the same starting material, under different extraction

conditions, all extracts were capable of producing submicron emulsions with a highly negative charge and good physical stability despite the variation in the composition of surface-active compounds. However only one extract (20% ethanolic extract) could form an emulsion with the lowest mean droplet size $d_{4,3} < 200$ nm. This means that the whole composition contributes to emulsion formation when using complex mixtures of surface-active compounds and emulsion trials have to be conducted in order to reveal this tendency.

The use of argan shell microfibrillated cellulose (AS-MFC) as oil-in-water (O/W) emulsions stabilizer was also investigated. The effect of particles concentration was assessed and led to long term stability (15 days) of O/W emulsions at high concentration of AS-MFC confirmed by droplet size $d_{4,3}$ and creaming index. This study also shows the oil concentration suitable to reach the maximum volume of emulsion using 1% w/w AS-MFC. The results show AS-MFC could stabilize 70% w/w MCT oil. Finally, CLSM shows the adsorption of AS-MFC at the oil-water interface and the formation of a 3D network surrounding oil droplets by larger fibrils. The raw material used in this research is extremely interesting due to different reasons. First, it's a by-product of an oil industry (argan oil). Argan shell is generally combusted by the local population without generating any value. Therefore, this research could lead to high-value products having a social and environmental impact. Furthermore, the oil industry referred to is of extreme importance in cosmetic products. Argan oil made a breakthrough in international markets due to its virtues. Argan tree tolerance for hard climate conditions of dry arid lands and poor precipitations procured to argan oil its high antioxidant, anti-cancer, and anti-acne properties. Developing a 100% product, simply from this tree is believed to have very high appreciation and demand internationally. The mechanism elucidated was the amphiphilic structure of solvent extract and the dual wettability of mechanically disintegrated cellulose.

Table of Contents

Jan-May 2020
Most of the time was spent in global fighting against
COVID-19 pandemic

List of tables

List of figures

Chapter 1 – Introduction

1.1.Historical background

Emulsions have been used by humans for centuries. Ancient Egyptians learned to use eggs, berry extracts and oils to form emulsified paints. History of food emulsions started with milk products such as butter and cheese. By 1756, mayonnaise was invented by a French chef [2]. The world emulsion emerged from the Latin words *emulgere* and *emulsum*, meaning to milk. Although, the ancient long history, the scientific studies related to emulsions are quite recent. Oil-in-water (O/W) and water-in-oil (W/O) have been described in the pioneer work of Ostwald, 1910. More recently, in 1961 Schulman & Montagne described the concept of micro and macroemulsions as important for the study of droplet absorption process in the intestine or delayed absorption of subcutaneous injections. Today, an extensive understanding of emulsions is necessary as many productions including drugs, paints and inks, cosmetics and foods along with functional foods are emulsions.

1.2.Emulsion systems

Emulsion systems are encountered in many commercial products such as food, cosmetic and pharmaceutic industries [5,6]. This systems are thermodynamically unstable consisting of at least two immiscible liquids (generally referred to as oil and water phases), one dispersed into the other as small spherical droplets, that would rapidly separate to the initial homogenized components in the absence of stabilizers [7]. Different terms were used to describe emulsions and it is important to clarify those meanings which are generally based on the dispersed phase diameter (Table 1).

Table 1: Droplet diameter and properties of different types of emulsions

Emulsion type	Droplet diameter	Appearance
Macroemulsion	0.1 – 100 μm	Turbid/opaque
Nanoemulsion	20 – 100 nm	Transparent
Microemulsion	5 -50 nm	Transparent

Emulsions classification is based on the spatial distribution of the oil and water phases in the mixture. When oil droplets are dispersed in the watery phase, the system is referred to as oil-in water (O/W) emulsion, whereas the opposite is called a water-in-oil (W/O) emulsion. These emulsions are conventional emulsions that are used to formulated various products. More sophisticated systems have also been described such as multiple emulsions e.g., oil-in-water-in-oil (O/W/O) or water-in-oil-in-water (W/O/W) emulsions [8], solid lipid nanoparticles or filled hydrogel particles, that may have novel applications and performance. Over time, emulsions tend to break down because they are thermodynamically unfavorable systems due to gravitational separation, flocculation, coalescence, partial coalescence, and/or Ostwald ripening [9]. Being able to formulate emulsions with sufficient long kinetic stability is the main challenge for emulsion technologists. By incorporating substances known as “stabilizers” kinetic stability can be enhanced [10].

Emulsion stabilizers can be categorized based on the mechanism of stability of the system, we distinguish:

- Emulsifier: it is a surface-active molecule adsorbing to the surface of oil droplet during homogenization. By adsorbing at the interface, emulsifiers facilitate oil disruption during emulsification process and prevent aggregation.

- Texture modifier: it is a substance able to thicken or gel the continuous phase. The stability of the system is maintained by preventing droplet movement.
- Weighting agent: when adding this substance to the droplets it allows a density match with the continuous phase therefore retarding creaming or sedimentation induced by gravitational separation
- Ripening retarder: being highly hydrophobic material it prevents Ostwald ripening when added to the dispersed phase.

In emulsion formulation the selection of appropriate stabilizers is highly important as it affects the shelf life and physicochemical properties of the of the formulated product [10].

1.3.Toward natural emulsifiers

One of the main concern of modern consumers is to be able to use and consume minimally processed products (food, beverage, creams) containing natural ingredient. The industrial trend toward answering consumer demand is described by “clean label” ingredients for products formulation. The use of natural emulsifiers (as one of the major ingredients for successful formulation) brings up many challenges to products developers, mainly due to their lower performance when compared to their synthetic counterparts. Chemical and synthetic emulsifiers still account for 67% of global market volume [11]. The reason is simply because the industry could not find natural emulsifier as effective and versatile as the synthetic ones and should be used in combination with other ingredients in order to emulsify effectively. However, research and development made significant advancement in this field and more innovative ingredients have been proposed [12].

1.4.Natural surface-active compounds as emulsion stabilizers

Surface-active emulsifiers have a strong tendency to adsorb at the oil-water interface, due to an appropriate amount of polar and non-polar groups in their chemical structure [13,14], the most common natural ones are described in Table 2.

Table 2: Description of natural surface-active emulsifiers [12]

Natural surface-actives	Source	Adsorption mechanism	Stabilization mechanism
Proteins	Bovine milk (caseins, whey proteins), animal proteins (gelatins), plant proteins (pea proteins, lupin proteins, soy proteins, corn germ proteins)	Hydrophilic and hydrophobic amino acids along their polypeptide chains	Electrostatic repulsion due to the presence of (–COO) or ($–NH3^{+}$) groups Stearic repulsions due to the formation of thick interfacial layer
Polysaccharides	Gum Arabic, pectin, galactomannans	Low surface-activity thereby increasing continuous phase viscosity	Droplet movement inhibition
Phospholipids	Cell membranes of animal, plant, and microbial species i.e. lecithin	Amphiphilic structure with hydrophilic head (phospholipid acid esterified with glycerol) and lipophilic tail (fatty acid)	Thin interfacial layer prone to coalescence
Saponins	Plant secondary metabolites	Hydrophilic sugar groups attached to non-polar aglycone groups.	Electrostatic repulsion due to the presence glucuronic acids

In order for surface-active compounds to be effective as emulsion stabilizers they require a number of physicochemical characteristics mainly i) appropriate ratio of polar and non-polar groups ii) rapid adsorption to the oil-water interface iii) interfacial tension reduction as to facilitate droplet disruption iv) droplet protection from aggregation via electrostatic or steric repulsions v) sufficient surface coverage.

1.5.Natural solid particles as emulsion stabilizers

Emulsions stabilized by solid particles are referred to as Pickering emulsions based on the description of Pickering in 1907. Research interest on this type of emulsions increased tremendously between 2000 and 2018 from 0.05% to 8.0% (source: data from Web of Science). The reason is directly linked to the enhanced properties in emulsion stabilization when compared to surface-active compounds. Pickering emulsions are hardly disrupted by the environmental conditions due to the irreversible adsorption of particles at the oil-water interface. In addition, this type of emulsions offer some advantages to reduce allergic effects and undesirable taste characteristics when compared to conventional emulsifiers [15]. Pickering emulsions stability, type, morphology and characters are highly influenced by the type of particles used [16]. Both organic and inorganic particles have been described to produce O/W Pickering emulsions. Particles such as silica (SiO_2) [17], calcium carbonate ($CaCO_3$) [18] and titanium dioxide (TiO_2) [19] maybe used in food as Pickering stabilizers. However, such particles face criticism due to the suitability for food and environmental related questions [20]. Therefore, sustainable food-grade particles are more appealing currently.

Among natural particles described for the stabilization of Pickering emulsions we distinguish natural polymers such as polysaccharide-based particles mainly starch, cellulose and chitosan. Furthermore, Lignin-based particles and proteins-based particles were also described as effective Pickering emulsions stabilizers.

1.6.Argania spinosa potential valorization route

Argan tree, endemically grown in Morocco, belongs to the monospecific genus (*Argania spinosa*). It is the only representative tree of the tropical family *Sapotaceae* remaining in subtropical zone [21]. Production of edible and cosmetic oil from argan fruit kernel is the main activity providing income to argan forest inhabitants (~3 million people) [22]. Argan oil represents ~3 wt% of the whole fruit (~50% dry weight kernels), with an annual production of 4800 tons [23]. In addition, oil industry produces large amounts of by-products that are not valorized: argan press cake, argan pulp and argan shell that represent ~2 wt%, ~43 wt% and ~52.6 wt% of the argan fruit respectively [24]. Figure 1 shows argan oil extraction process and its industrial by-products.

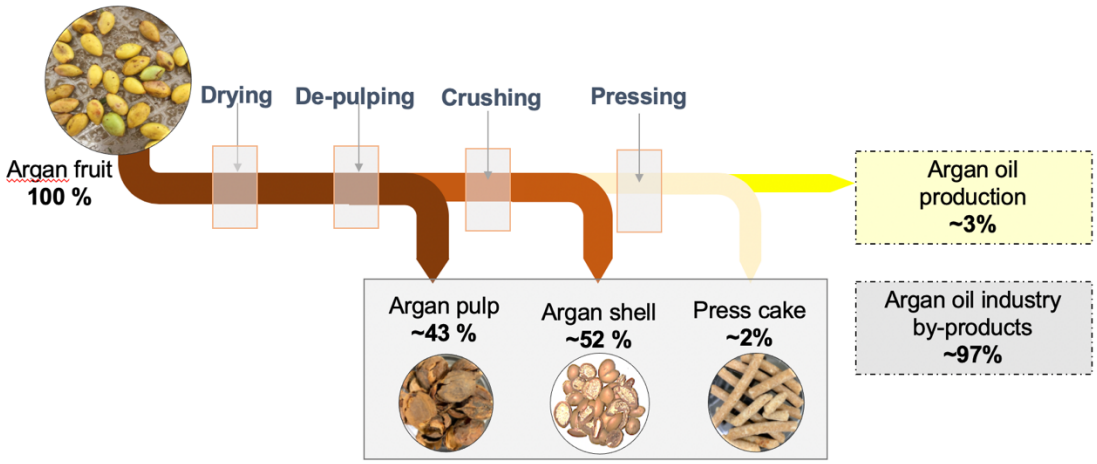

Figure 1: Argan oil extraction process and its industrial by-products

The industry generates large quantities of by-products that are poorly valorized either as cattle feed or combusted for energy purposes. Figure 2 shows the mass balance of argan industry products.

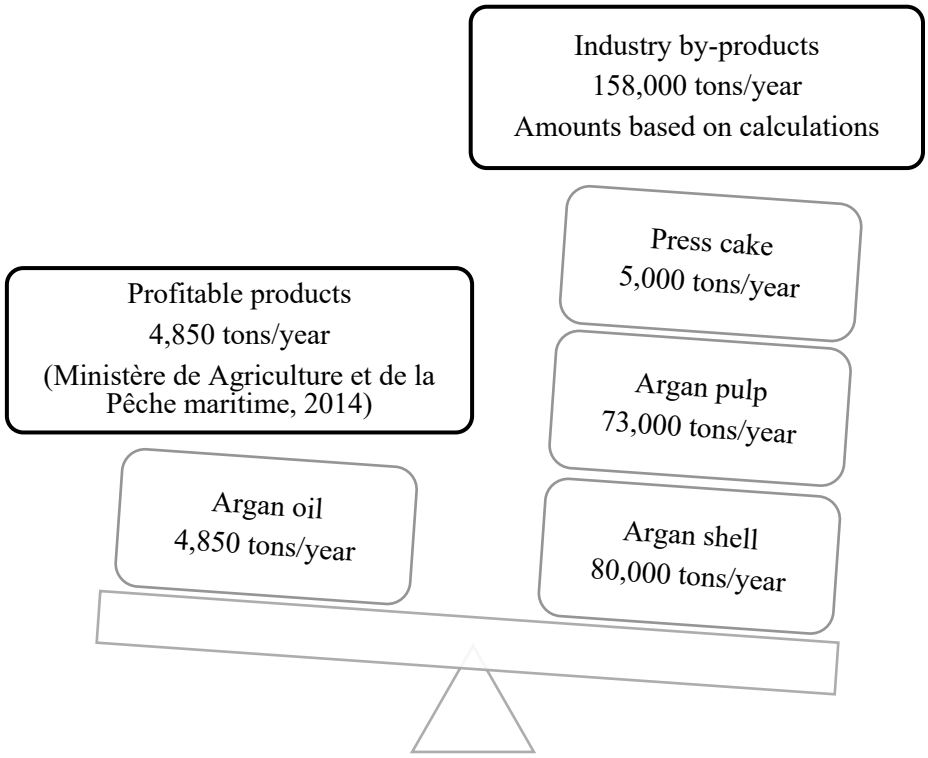

Figure 2: Argan industry products mass balance

Argan fruit shell is a lignocellulosic material representing the endocarp protecting the kernel of argan fruit. Large amounts of argan shell are produced annually (>80,000 tons based on calculations) and is mostly used as a source of energy by combustion [25]. El Monfalouti et al. (2012) reported about the polyphenol composition in argan shell and isolated (-)-epicatechin, iso-quercitrin, rutin, phloridzin, hyperoside, procyanidin B1 and B2, myricetin and quercitrin. Alaoui et al. (2002) studied triterpenoid saponins from methanol extract of argan shell. Their study described protobassic acid and 16α-protobassic acid as aglycons linked to the carbohydrate moieties in the chemical structure. Furthermore, the saponins content was reported to be 1% in argan shell (Guillaume & Charrouf, 2005). In addition, this material contains a high fiber content >78%. Hence, for the added-value income to the industry, argan

shell could be a potential candidate to produce natural emulsifiers considering the presence of saponins in its secondary metabolites and the high-content of fibers.

1.7.Aim and motivation of this thesis

Natural ingredients represent an important concern for food industrials in order to satisfy well aware consumers seeking clean label. Emulsifiers are one of the most utilized ingredients in food formulations, they can affect stability of emulsions depending on the type of adsorption at the oil-water interface. Researchers have recently reported about the utilization of plant extracts exhibiting surface-activity to stabilize oil-in-water (O/W) emulsions as well as the utilization of microfibrillated cellulose to produce Pickering type emulsions. Argan shell is a lignocellulosic material, representing an important by-product of the argan oil industry, it is composed mainly of fibers >78% but also contains low molecular weight compounds in its structure, thus, making it a good candidate to produce natural emulsifiers. In this study, our aim is to use argan shell to produce surface-active ingredients and microfibrillated cellulose (MFC) to be utilized separately to stabilize O/W emulsions.

Chapter 2 – Emulsification properties of aqueous-ethanolic extracts from Argan shell powder

---

Abstract

The aim of this work was to extract and characterize surface-active compounds from argan fruit shell. Argan shell extracts were used to prepare oil-in-water emulsions using soybean oil as dispersed phase. Formulation and stability of emulsions were investigated during storage time (30 days) at two different temperatures (5°C and 25°C). Extraction was conducted after size reduction of argan shell sample to a fine powder and carried out using a food-grade aqueous-ethanol solution (0 – 99.5 vol%). Then, solvents were evaporated, and extracts were freeze-dried. Argan shell extracts showed high concentrations of saponins, proteins and polyphenols. The five extracts against soybean oil showed similar reduction in interfacial tension values. Extracts were effective at producing submicron emulsions with a volume mean droplet size 200 nm < $d_{4,3}$ < 440 nm and good physical stability at the studied temperatures. ζ-potential values confirmed the adsorption of saponins on oil droplets. In addition, size distribution of emulsions showed a bimodal distribution that was maintained during storage. This is possibly due to the formation of a thick layer of proteins on oil droplets. Mechanism of stability of emulsions by argan fruit shell extracts is likely standing behind saponin-protein adsorption providing electrostatic and stearic repulsions.

This chapter is published as: Bouhoute, M., Taarji, N., Vodo, S., Kobayashi, I., Zahar, M., Isoda, H., Nakajima, M., Neves, M. A. (2020). Formation and stability of emulsions using crude extracts as natural emulsifiers from Argan shells. Colloids and Surfaces A: Physicochemical and Engineering Aspects, 591, 124536.

2.1.Introduction

Emulsions are among the most encountered systems in processed food and beverage. Salad dressings, butter, ice-cream, fortified energy drinks… are all emulsion systems consisting of two immiscible phases, one dispersed into the other, and surrounded by surface-active ingredients called emulsifiers [9]. Emulsions are effective delivery systems for functional ingredients incorporated in the dispersed phase, and isolated from the external environment by the continuous phase [28]. Successful formulation of such systems relies on the ability to appropriately select an emulsifier (based on chemical and structural properties) that can form and stabilize the two immiscible phases [5].

Natural food-grade emulsifiers are subject to an extensive work that answers consumers increasing demand for 'clean labels' in food and beverage products [13]. The most encountered ones are proteins, polysaccharides, phospholipids, and small molecule surfactants [13,14]. Oil-in-water (O/W) emulsions can be stabilized by the following mechanisms i) the ability to rapidly adsorb to oil droplets during homogenization process ii) decrease the oil-water interfacial tension and iii) create a protective layer that will stand as barrier to droplet coalescence [5]. In this field, efforts are still undergoing in order to identify novel sources of natural emulsifiers and thoroughly characterize and compare their performance in forming and stabilizing emulsions [7].

Saponins are small molecular weight emulsifiers that could be found in many plants of agricultural importance. They have an amphiphilic structure consisting of carbohydrate chains (hydrophilic), attached to aglycone groups of either a sterol or triterpene unit (hydrophobic) [29]. Recently, quillaja saponins from *Quillaja Saponaria* (Q-Naturale®) have been utilized to formulate and stabilize O/W emulsions [30]. This research led to an extensive work on saponins rich plants in order to increase the availability of this compound of interest. The main sources of saponins with industrial applications are, in addition to soap bark tree (*Quillaja*

saponaria), licorice (*Glycyrrhiza* species), gypsophila genus (*Gypsophila paniculata*), ginseng (*Panax* species), fenugreek (*Trigonellafoenum-graceum*), alfalfa (*Medicago sativa*), Mojave yucca (*Yucca schidigera*), horse chestnut (*Aesculus hippocastanum*), soapwort (*Saponaria officinaux*), and sarsaparilla (*Smilax species*) [31].

As an extension to saponins utilization as O/W emulsion stabilizers a new class of food grade-emulsifiers is being investigated. Crude natural plant extracts, containing saponins in their chemical structure have been utilized to formulate O/W emulsions. Recent studies have reported about crude extracts from sugar beet (*Beta vulgaris*), Yucca tree (*Yucca schidigera*), red beet (*Beta vulgaris*), oat bran (*Avena sativa* L.) and argan press cake (*Argania spinosa* L.) as natural emulsifiers (Ralla et al., 2017a, 2017b , 2018, Taarji et al., 2018). The crude extracts successfully generated O/W emulsions with a long shelf-life and ensured stability against environmental stresses. However, purity of saponins in those extracts was found to be significantly lower than quillaja saponins. For example, saponins content was reported to be 0.5% for sugar beet, 0.9% for red beet, 4,2% for argan press cake, 4.6% for oat bran, 9.5% for yucca tree and > 68% for quillaja saponins. Nevertheless, those extracts showed similar performance in emulsion formulation when compared to the highly pure molecule of quillaja. Authors suggest that not only saponins were responsible for emulsions formulation and stability but rather the biogenic saponins-proteins complexes (Ralla et al., 2017a, 2017b , 2018, Taarji et al., 2018).

Argan tree, endemically grown in Morocco, belongs to the monospecific genus (*Argania spinosa*). It is the only representative tree of the tropical family *Sapotaceae* remaining in subtropical zone [21]. Production of edible and cosmetic oil from argan fruit kernel is the main activity providing income to argan forest inhabitants (~3 million people) [22]. Argan oil represents ~3 wt% of the whole fruit (~50% dry weight kernels), and an annual production of 4800 tons [23]. In addition, oil industry produces large amounts of by-products that are not

valorized: argan press cake, argan pulp and argan shell that represent ~2 wt%, ~43 wt% and ~52.6 wt% of the argan fruit respectively [24]. Argan fruit shell is a lignocellulosic material representing the endocarp protecting the kernel of argan fruit. Large amounts of argan shell are produced annually (>80,000 tons based on calculations) and is mostly used as a source of energy by combustion [25]. El Monfalouti et al. (2012) reported about the polyphenol composition in argan shell and isolated (-)-epicatechin, iso-quercitrin, rutin, phloridzin, hyperoside, procyanidin B1 and B2, myricetin and quercitrin. Alaoui et al. (2002) studied triterpenoid saponins from methanol extract of argan shell. Their study described protobassic acid and 16α-protobassic acid as aglycons linked to the carbohydrate moieties in the chemical structure. Furthermore, the saponins content was reported to be 1% in argan shell [37]. Hence, for the added-value income to the industry, argan shell could be a potential candidate to produce natural emulsifiers considering the presence of saponins in its secondary metabolites. To the best of our knowledge, there is no scientific report describing the use of argan shell to produce natural emulsifiers so far.

Generally, studies reporting about crude extracts as natural emulsifiers, focus on a specific extract that reduces the interfacial tension to a minimum value, coupled to high saponins content. However, these studies have not compared between emulsions prepared using extracts produced under different extraction conditions. Here, we show that different argan shell extracts, prepared by different ethanol concentrations, led to different emulsion properties. First, we report about argan shell extraction yields and composition, focusing mainly on saponins, proteins and polyphenols content. Then, we investigate interfacial properties of those extracts by measuring the interfacial tension of extracts solutions against soybean oil. Droplet size, ζ-potential, size distribution and visual aspect of emulsions were used to shed the light on the mechanisms of emulsions stability. Finally, one extract was used to assess the effect of extract concentration and oil-mass fraction on emulsion formation and stability. Through this

systemic study, we highlight the importance of emulsion trials in order to assess the efficiency of a crude extract to formulate and stabilize emulsions beyond interfacial characteristics and composition.

2.2.Materials and methods

2.2.1. Materials

Two batches of argan fruit shell were provided by Argan oil-producing cooperatives located in the cities of Essaouira and Agadir, Morocco. Analytical-grade ethanol (99.5%), oleanolic acid standard (97%), vanillin, acetic acid, perchloric acid, sodium carbonate, sodium azide and refined soybean oil with a density at 25 °C of 0.92 mg/ml were purchased from FUJIFILM Wako Pure Chemical Corporation (Osaka, Japan). Folin & Ciocalteu's phenol reagent was prepared by MP Chemicals (Illkirch, France). Ultrapure water was produced using Arium® pro system (Sartorius, Goettingen, Germany) and used was to prepare all solutions and emulsions in the current study.

2.2.2. Extracts preparation

Argan shells with a size range of 25-40 mm were washed with deionized water to remove all impurities then left to dry at 50 °C. Size reduction was performed using Hammer mill Super-masscolloider (MKCA6-2, Masuko Sangyo Ltd., Saitama, Japan) at 3,000 rpm for 5 min including 15 min rest in between additions of sample. The powder produced was then sieved to obtain a homogeneous argan shell powder (< 0.5 mm). Solid-liquid extraction was conducted using ethanol/water mixtures 0/100, 20/80, 50/50, 80/20 or 99.5/0 v/v at a powder:solvent ratio of 1:10 to produce argan shell extracts (ASE) and were denoted as 0-ASE, 20-ASE, 50-ASE, 80-ASE and 99.5-ASE respectively. The suspensions were stirred using a magnetic stirrer over night at room temperature then centrifuged at 3,300 rpm for 30 min (Kubota 8420, Kubota

Corp, Tokyo, Japan) to separate the solid powder from the supernatant. Solvents were then evaporated at 40 °C and 49 hPa (Eyela EVP- 1100, Shanghai Co., Ltd., China). Extracts after evaporation were further purified by a redissolution in ultrapure water, stirring and centrifugation at 10,000 rpm for 20 min (MX-307, Tomy Digital Biology Co., Ltd., Tokyo, Japan) then filtration using syringe hydrophilic membrane filter (0.45 µm) to remove water insoluble fractions. The filtrates were freeze-dried and stored at -20 °C until further use. In all the study, ASE will be referring to freeze dried extracts from argan shell powder.

2.2.3. Extraction yield

Since the extraction was carried out in 2 steps extraction process, the authors defined two extraction yields. *EY1* represents the yield after evaporation of the solvent given by equation 1:

$$\mathrm{EY}_1\ (\%, \text{dry basis}) = \frac{\mathrm{W}_1}{\mathrm{W}_0} \times 100 \qquad (1)$$

W_1 represents the weight of the extract after evaporation of the solvent, W_0 represents the weight of raw argan shell powder.

EY2 represents the yield after freeze-drying of extract samples, calculated using equation 2:

$$\mathrm{EY}_2\ (\%, \text{dry basis}) = \frac{\mathrm{W}_{\mathrm{ASE}}}{\mathrm{W}_0} \times 100 \qquad (2)$$

$\mathrm{W}_{\mathrm{ASE}}$ represents the weight of the extract after freeze drying operation, W_0 represents the weight of raw argan shell powder.

2.2.4. Extracts analysis

Saponins content was determined spectrophotometrically (V-570, JASCO Co., Hachioji, Japan) according to the method reported by Xiang et al. (2001) [38] using oleanolic acid as a standard with slight modification. Briefly, 0.1 ml (0.5 or 1 %) of each argan shell extract were mixed with 0.1 ml of 5 % vanillin-acetic acid solution and 1.2 ml of 60 % perchloric acid then

incubated for 20 min at 70 ℃. After cooling down, 5 ml ethyl acetate was added. Absorbance was measured at 550 nm against a blank solution as reference.

Crude protein content was estimated from total nitrogen content using a nitrogen-to-protein conversion factor of 6.25 [39]. Nitrogen content was determined using an elemental analyzer (2400 II CHN, Perkin-Elmere, Waltham, Massachusetts, US).

Total polyphenols were determined spectrophotometrically by Folin–Ciocalteau method using gallic acid as standard [40] with minor modification. Briefly, 0.5 ml (0.025 or 0.05 %) were added to 0.5 ml Folin–Ciocalteau reagent and total volume was adjusted to 8.5 ml using ultrapure water. The mixture was incubated for 10 min at room temperature. Additional 1.5 ml of 20 % sodium carbonate was added and total mixture was incubated for 20 min at 40 ℃. Absorbance was measured at 755 nm against a blank solution as reference.

Viscosity and density were measured for 1 wt% argan shell extract solutions using viscometer and density meter (SVM^{TM} 3001, Anton Paar GmbH, Graz, Austria). This study reports dynamic viscosity and density as a function of ethanol concentration during extraction.

2.2.5. Interfacial tension measurements

Various solutions (0.005 – 3 wt%) were prepared using different samples of ASE. Interfacial tensiometer (DM-501, Kyowa Interface Science Co., Ltd., Saitama, Japan) was used to identify the effect of ASE concentration on interfacial tension (γ_{OW}) at soybean oil/water interface. Using pendant drop method, argan shell extract solutions were placed in syringe and a drop was formed by the needle until reaching its maximum volume. Interfacial tension was calculated based on the drop shape according to Young-Laplace equation, immediately after its formation.

2.2.6. O/W emulsions preparation

O/W emulsions were prepared using 1 wt% ASE or 0.1 – 4 wt% 20-ASE in ultrapure water as continuous phase (95 wt%, pH 5.8) and soybean oil as dispersed phase (5 wt%), sodium azide (0.02 wt%) was added in order to inhibit microbial proliferation during the storage. Coarse emulsions were prepared by high shear blending at 10,000 rpm for 5 min (Polytron PT-3100, Kinematica- AG, Luzern, Switzerland). Fine O/W emulsions were prepared under standardized conditions using high-pressure homogenization (NanoVater, NV200, Yoshida Kikai Co., Ltd., Japan) at 100 MPa for 4 passes. A selected extract (20-ASE) was used to assess the effect of the concentration of emulsifier (0.1 – 4 wt%) on volume mean droplet size of emulsions. The same extract (1 wt%) was then used to test the effect of oil mass fraction (5 – 30 wt%) on emulsions stability.

2.2.7. Droplet size measurement

Droplet size of emulsions was monitored using laser diffraction particle size analyzer (LS 13,320, Beckman Coulter, Brea, USA). Droplet size was expressed as volume-based mean diameter, $d_{43} (= \sum n_i \, {d_i}^4 / \sum n_i \, {d_i}^3)$ or surface-based mean diameter $d_{32} (= \sum n_i \, {d_i}^3 / \sum n_i \, {d_i}^2)$ where n_i is the number of droplets with diameter d_i.

2.2.8. Zeta-potential measurement

ζ-potential of emulsions was determined using electrophoretic light scattering instrument (Zetasizer, Nano ZS, Malvern Instruments Ltd., Worcestershire, UK) after 24 h settlement of emulsions. Samples were diluted (1:100) using ultrapure water in order to avoid multiple scattering effect, then loaded into a folded 1 ml capillary cell. Refractive index of the aqueous

phase (1 wt% argan shell extracts in ultrapure water) and dispersed phase was set to 1.330 and 1.432 respectively.

2.2.9. Optical microscopy

Morphological appearance of emulsions was assessed using an optical light microscope (DFC300FX, Leica Microsystems GmbH, Wetzlar, Germany). Emulsion samples were gently mixed before one drop was placed on an objective slide glass and covered by cover slip. Visual appearance of emulsions is also reported in this study.

2.2.10. Emulsions stability

Stability during storage was assessed by monitoring droplet size change over time. Emulsions were prepared, then stored at different temperature 5 °C or 25 °C for 30 days. Additionally, emulsions prepared to test the effect of oil mass fraction were kept for 10 days at 5 °C.

2.2.11. Statistical analyses

All experiments were conducted at least duplicates with a minimum 3 replicates, reported values are means and standard deviations calculated using Excel Office (One Microsoft Way, Redmond, Washington, U.S.). Furthermore, one-way analysis of variance (ANOVA) was performed using SPSS Statistics (IBM Corp., Armonk, New York, U.S.).

2.3.Results and discussion

2.3.1. Extraction yields and extracted saponins, proteins and polyphenols from argan fruit shell

Crude extraction yields after evaporation of different solvent mixtures (first extraction) and after freeze-drying of extracts (second extraction), EY_1 and EY_2 respectively, are shown in

Figure 3a EY_1 was maximized when using 50% and 80% ethanol and decreased when using 99.5% ethanol or water, although, there is no significant difference between the means ($p > 0.05$). The purification operations consisting of centrifugation and filtration, prior to freeze-drying of extracts, led to a decrease in EY_2 by 60-74% when compared to EY_1. Insoluble agglomerates in water were removed, and EY_2 was ranging between 1.1% and 2 %. Extraction yields varies generally due to multiple factors related to extraction conditions and extraction techniques [41–43]. Thus, our results show the effect of ethanol concentration on total compounds mixtures solubilized by the solvent. Those findings are supported by previous studies reporting that ethanol could affect the extraction of soluble components from different natural sources [44]. To the best of our knowledge, neither extraction yields from argan fruit shell powder using aqueous-ethanolic solvent nor the characterization of those extracts have been reported in previous studies. Therefore, we selected all extracts to be analyzed in order to determine the presence of surface-active compounds.

Surface-activity of plant extracts is correlated to the extract composition. Saponins and proteins detains surface-active properties due to the presence of hydrophilic and lipophilic moieties in their chemical structure [5]. In addition, physical properties of emulsions may be affected by the presence of some polyphenols in the continuous phase [45]. Therefore, ASE were characterized for their saponin, protein and polyphenol contents (Figure 3b).

Total saponin was maximum in 99.5-ASE (391.2 ± 5.8 mg/g) followed by 80-ASE and 50-ASE. The lowest saponins concentration was found in 0-ASE (104.7 ± 6.3 mg/g). These results show that while extraction yields decreased, total saponins increased with the increase of ethanol concentration during extraction. Solubility of saponins in water and aqueous ethanol varies depending on their aglycone structure and the properties of the extraction solvent [46]. Therefore, we suggest that argan fruit shell saponins are more soluble in ethanol or ethanol-

water mixtures than in water. These results are similar with those reported by Ko et al. (1992) about an increase in saponins yield from red ginseng with high ethanol concentration.

Protein content was ranging between 55.2 ± 18.7 mg/g and 76.6 ± 11.8 mg/g for 99.5-ASE and 0-ASE respectively. Proteins are well known to be highly soluble in water than in ethanol [47]. Thus, protein content was higher in water extract compared to ethanolic extracts. Furthermore, high molecular weight (HMW) proteins (i.e. >200 kDa) may have precipitated and removed by centrifugation and filtration processes, leading to the concentration of peptides in the samples. Further experiments are required in order to determine molecular weight of proteins in ASE.

Total polyphenol content (TPC) can be grouped into 2 levels: the highest contents (297.2 ± 46.0 - 320.9 ± 15.2 mg/g extract) for 99.5-ASE and 80-ASE respectively, and the lowest contents (153.7 ± 7.8 - 202.3 ± 21.1 mg/g extract) for 0-ASE and 20-ASE. Generally, authors suggest that 80 vol% aqueous ethanol is the optimum solvent for extraction of phenolics from plant material. Similarly, in our results we found the highest polyphenol content extracted using 80 vol% ethanol [48].

2.3.2. Interfacial tension of argan fruit shell extracts

Figure 4 shows that all ASE samples were able to reduce interfacial tension at oil/water interface with increasing their concentrations. At high concentration of 3 wt%, ASE reduced the interfacial tension to minimal average of 11.2 mN/m, noting a decrease by up to 45% when compared to interfacial tension between ultrapure water and soybean oil (25.5 mN/m). This indicate that surface-active compounds were adsorbed at the oil-water interface. Interestingly, the composition of ASE did not affect the reduction of interfacial tension, and the trend remained similar. The highest saponin content found in ASE prepared with ≥ 50 vol% ethanol did not further decrease the interfacial tension as expected. Those findings are consistent with

previous study on Korean Ginseng extracts that showed similar interfacial tension despite a different compositions [49]. In addition, reported plant extracts exhibiting surface-activity from argan press cake, sugar beet or *Quillaja* reduce the interfacial tension to minimal values of 5 – 16.3 mN/m (Ralla et al., 2017b; Taarji et al., 2018; Yang et al., 2013). This indicates that all ASE fall into the range of plant extracts utilized as effective emulsifiers. Other traditional natural emulsifiers such as proteins (β-casein), polysaccharide (gum arabic) or phospholipids (soy lecithin) reduce interfacial tension values to 19, 10 – 47 and 2 mN/m respectively [5,51]. This suggest that ASE were more efficient at reducing interfacial tension than proteins and polysaccharides.

The mechanism of adsorption of proteins is known to be time dependent, since they undergo conformational changes to expose hydrophobic side chain to the oil phase. In contrast, saponins tend to adsorb faster thus reducing interfacial tension in a shorter lag-time. Mixtures of saponins-proteins also result in a slower movement when compared to saponins alone [52–54]. Therefore, considering the reported values of interfacial tension taken immediately after the adsorption of ASE at the oil phase, we suggest that surface-activity of ASE is mainly based on the adsorption of saponins and/or saponins-proteins complexes.

2.3.3. Effect of argan fruit shell extracts on formation and characterization of O/W emulsions

Practically, when investigating new sources of emulsifiers it is more appealing to use the lowest amounts possible of emulsifier to stabilize emulsions [55]. Thus, we fixed a total emulsifier concentration of 1 wt% in order to test ASE effectiveness to forming and stabilizing emulsions. This concentration corresponds to an average interfacial tension value of 13 mN/m. Similar results were also reported by Taarji et al. (2018) when using 1 wt% argan press cake extracts and interfacial tension was reduced to an average 12.3 mN/m at soybean oil interface. In addition, we confirm that 1 wt% ASE does not affect the dynamic viscosity or density of

ultrapure water as shown in Figure 9. Emulsion viscosity is assumed to be proportional to the continuous phase viscosity [56]. Thus, the mechanism of emulsion formation is suggested to be based on molecular adsorption of surface-active compounds rather than rheological properties of ASE solutions.

As expected, all ASE were able to produce submicron emulsions with minimum d_{32} and d_{43} values (Figure 5). Hence, relative abilities of ASE as emulsifying agents at pH = 5.8 were found to lie in this order 20-ASE > 0-ASE > 80-ASE > 50-ASE > 99.5-ASE. Surprisingly, 20-ASE was the most effective emulsifier at producing small droplets during homogenization (d_{32} = 132 $\pm$ 11 nm; d_{43} = 201 $\pm$ 23 nm). This extract did not show the highest saponins and proteins concentration (235.3 $\pm$ 14.8 mg/g; 74.4 $\pm$ 11.7 mg/g respectively) nor the largest reduction in interfacial tension values (13 $\pm$ 0.7 mN/m). Additionally, 0-ASE also achieved rather small droplet size (d_{32} = 157 $\pm$ 3 nm; d_{43} = 242 $\pm$ 7 nm) with the lowest saponins concentration. This results are slightly different from the ones reported about argan press cake saponins. Taarji et al. (2018) showed that 50 vol% ethanol extract exhibiting the highest saponins of 4.2 % and < 1% proteins contents formed a droplet size of (d_{32} = 107 nm, 2 wt% extract, 5 wt% soybean oil).

ASE compositions play an important role in the adsorption of surface-active compounds at the interfacial layer. Competitive adsorption between saponins and proteins present in the extracts might have taken place during homogenization. In addition, other compounds like polyphenols could interact with proteins in the aqueous phase, through hydrophobic or hydrophilic interactions. This could lead to the formation of new complexes that could affect proteins adsorption. Results of ASE composition (Figure 1) confirms this hypothesis, since both 0-ASE and 20-ASE had low polyphenols content. Moreover, non-adsorbed emulsifiers in heterogeneous systems can also cause emulsion instability as a consequence of depletion flocculation mechanism. This phenomenon corresponds to an osmotic effect due to the

exclusion of free biopolymers from a narrow region surrounding oil droplets [57,58]. This was assessed by the optical microscopy images of the fresh emulsions (Figure 10) detecting small flocs for fresh emulsions prepared with ≥ 50 vol% ethanol. Similar results on aqueous garlic extracts prove that a higher concentration of surface-active compounds leads to depletion flocculation and bridging flocculation that impact droplet size of emulsions [59].

The electrical charge of emulsions formed with different ASE was found highly negative. ζ-potential was ranging between −46.3 and −51.5 mV (Figure 5). Electrical charge of oil droplets generates electrostatic repulsions between droplets preventing agglomeration and therefore creaming and phase separation of the emulsions. Thus, high values of ζ-potential can affect emulsions stability. Losso et al. (2005) described that values of ζ-potential of -41 to -50 mV have a good stability. Other authors suggest that in order to predict distinct stability, the absolute magnitude of ζ-potential should be at least 10 mV [61]. From our results, we can hypothesize that all extracts prepared with different concentrations of ethanol can stabilize emulsions, due to electrostatic repulsions between oil droplets. Nevertheless, we cannot predict any enhanced properties for one extract among the others due to the small difference between ζ-potential values.

Finally, ζ-potential values further confirm that saponins could be the major adsorbed component to the oil surface. Hydroxyl groups found in argan shell saponins structure [27] could interact with water molecules via hydrogen bonds thus leading to their ionization and therefore to the large magnitude in negative ζ-potential. Nevertheless, the negative charge could also result from ionic impurities or mineral composition of ASE. Similarly, Taarji et al. (2018) reported about the presence of glucuronic acids in argan press cake saponins as a source of negative charge of oil droplets at neutral pH, yet, the same study showed that at pH ≈ pKa (3.25) the emulsions maintained a relatively high negative charge. Further studies are

undergoing to assess the effect of pH and ionic strength on ζ-potential of emulsions prepared with ASE.

2.3.4. Influence of storage time and temperature on emulsions stability

The stability of the obtained emulsions using 1 wt% ASEs was assessed. Overall, no significant variation was observed up to 30 days storage at 5 ℃ when using ASE (Figure 6a). The difference was observed in the initial mean droplet size as reported in the previous section. Droplet size of emulsion was maintained during storage. For example, emulsions prepared using 20-ASE showed the lowest droplet size d_{43} of 201 $\pm$ 23 nm for fresh emulsions and d_{43} of 203 $\pm$ 14 nm after 30 days storage. Submicron emulsions with higher mean droplet size were observed for emulsions prepared with 99.5-ASE, values of 403 $\pm$ 33 and 437 $\pm$ 40 respectively for fresh emulsions and after 30 days storage. Similar results were also noted when emulsions were stored at 25 ℃ (Figure 6b). Thus, higher temperature did not affect the stability of emulsions, and volume-based mean droplet size of the different emulsions remained nearly unchanged.

A thin creamy layer appeared on the top of all emulsions prepared with 0 – 80 ASE (Figure 6c). The creaming was intensified for the emulsion prepared with 99.5-ASE and a serum of the continuous phase was visible after 30 days storage at 25 ℃. The creaming rate expressed by creaming velocity can be calculated from Stokes' law:

$$\nu = \frac{2gr^2(\rho_w - \rho_o)}{9\,\eta_w} \qquad (3)$$

ν represents the velocity of droplet, ρ is the density of continuous phase (w) and oil (o), respectively, r is droplet radius, η_w is the viscosity of continuous phase, and g is the acceleration due to gravity [62]. Since all extract's solutions (1 wt%) showed similar density and viscosity (Figure 9), creaming velocity of the prepared emulsions is only correlated to

emulsions radius. Thus, emulsions presenting higher droplet size are more exposed to creaming. The calculated creaming velocity of the samples is ranging between 3 – 12 mm for 30 days storage. This range corresponds to emulsions prepared by 20-ASE and 99.5-ASE respectively.

In addition, despite the highly negative ζ-potential values reported in the previous section, micrographs of emulsions showed flocculation after 30 days storage (Figure 10). Flocculation induced by bridging with an adsorbing emulsifier, or by depleting with non-adsorbing one is particularly applicable for protein-stabilized emulsions [63]. Therefore, we suggest that emulsions were also stabilized by proteins. Adsorbed proteins at the interface of oil droplets could interact with each other, thus, inducing flocculation. Other non-adsorbed molecules still present in the continuous phase could also affect the stability of the emulsions.

Droplet size distribution was assessed simultaneously by laser diffraction (Figure 7). Bimodal distributions were encountered independently of the type of extract utilized to stabilize emulsions. A first peak at around 100 nm and a second one around 400 nm were observed for all prepared emulsions, in addition a third peak at 1500 nm was encountered when using 99.5-ASE as emulsifier. Moreover, the overlay of size distribution matched strongly when comparing emulsions after 1 day and stabilized emulsions after one-month storage at 5 ℃ or 25 ℃. This might indicate that a thick layer of surface-actives has formed on oil droplets thus inhibiting coalescence via steric repulsion. Our results suggest that none of the extracts behave similarly at the interface of the oil droplets, despite similar values of interfacial tension described in section 3.2. Furthermore, 20-ASE showed the lowest mean droplet size, yet, the size distribution of its emulsions showed the presence of larger droplets that could lead to Ostwald ripening [64]. We suggest that not only saponins are responsible for small oil droplet formation during homogenization, rather a mixture of saponins and proteins interacting

strongly at the oil interface through electrostatic and hydrophobic interaction thus creating a thick layer at the oil interface.

The complexity of crude plant extracts composition renders adsorption mechanism of surface-active molecules challenging to understand, since they are non-purified compounds. Different structures could result from mixed emulsifier systems, thus affecting the stability of emulsions [65,66]. Xu et al. (2019) reported about combined hydrolyzed rice glutelin and quillaja saponin on formation and stability of emulsions. Their study showed that a thicker interfacial layer was formed due to the presence of proteins. It seems that the formulation and stability of emulsions using such kind of mixtures is highly dependent on the saponin:protein ratio. For example, mean droplet diameter of emulsions stabilized with quillaja saponin-hydrolyzed rice glutelin at a ratio 1:1 was the lowest (180 nm), and remained stable when increasing saponin content up to 4:1. Reichert et al. (2018) showed that Quillaja saponins interfacial behavior was more sensitive to the presence of proteins than lecithin due to molecular interactions leading to the formation of complexes at interfaces and/or in the continuous phase. To the best of our knowledge, adsorption mechanism of crude extracts has not yet been verified in previous studies.

2.3.5. Effect of selected extraction condition (20-ASE) on emulsion characteristics

The purpose of this section was to assess the effect of 20-ASE on emulsions stability as a model extract to be utilized in emulsion formulations. The reason behind selecting this extract was its ability to produce emulsions with the lowest mean droplet size. Therefore, the effect of oil mass fraction on mean droplet size up to 30 days and visual aspect were assessed.

Figure 8a displays the variations in mean droplet size (d_{43}) during storage at 5 ℃ of O/W emulsions prepared with 1 wt% 20-ASE in ultrapure water as continuous phase and a dispersed phase consisting of 10 - 30 wt% soybean oil. 20-ASE could stabilize 10 wt% soybean oil up to

30 days with an average d_{43} of 527 nm. As we increase the concentration of oil to 20 wt% we notice an increase in d_{43} values from 1009 $\pm$ 271 nm for the fresh emulsions to 1601 $\pm$ 25 nm after 30 days storage. The same trend was also observed when using 30 wt% of oil, d_{43} values were 1747 $\pm$ 361 nm and 2449 $\pm$ 30 nm respectively for fresh emulsions and after 30 days storage. Similar trend was also observed at 25 ℃ storage for 30 days (Figure 8b). Furthermore, emulsions showed creaming related to the increase in droplet size with time and an increase in emulsions viscosity and no oiling-off was observed (Figure 8c). The results show stable submicron emulsions prepared with 10 wt% oil up to 30 days at both studied temperature. Signals of instability when using over 20 wt% oil are probably related to insufficient concentration of ASE to fully stabilize oil droplets and/or increase of the viscosity of emulsion system preventing a size reduction of oil droplets during homogenization [9]. All in all, 20-ASE could stabilize emulsions with a concentration of oil up to 10 wt%. The stability is related to adsorption of surface-actives compounds on oil droplet. Emulsions stability with high concentrations of oil could be improved with higher concentrations of 20-ASE.

2.4.Conclusion

Emulsions formulation and stability using natural emulsifiers is varying considerably due to the source and the type of surface-active compounds. This is even more the case when using crude extracts from plant material as emulsion stabilizers. Mostly, interfacial tension and composition are used to confirm the tendency of an emulsifier to formulate a stable emulsion. However, systemic studies also offer more reflection on the mechanism behind a successful stability. Currently, there is still no clear understanding of stability mechanism of emulsions using crude extracts as emulsifiers. One of the challenges is the complexity of the extract composition at molecular level, both at the bulk phase and at the interface of oil droplets. When surface-active compounds adsorb at the oil interface, other compounds could interact to disrupt

this adsorption. Furthermore, purification of surface-actives does not ensure similar emulsifying performance. Hence, future work will have to be conducted in this field in order to understand the mechanisms behind the utilization of crude extracts as emulsifiers.

The study showed the possibility of using argan fruit shell aqueous-ethanolic extracts as natural emulsifiers. Composition and interfacial tension were determined prior to emulsion formulation. Our results showed that with the same starting material, but different extraction conditions, all extracts were capable of producing submicron emulsions with highly negative charge and good physical stability. The stability mechanism is believed to be electrostatic and stearic repulsion. The saponins at the interface provide the highly negative charge at the oil droplet surface. Furthermore, proteins possibly interacted with saponins to form a thick layer, thus inhibiting droplet coalescence. This work could be extended in order to evaluate the potential of argan fruit shell extracts to stabilize emulsions against environmental stresses such as pH, salt and temperature in order to be applied in the food industry.

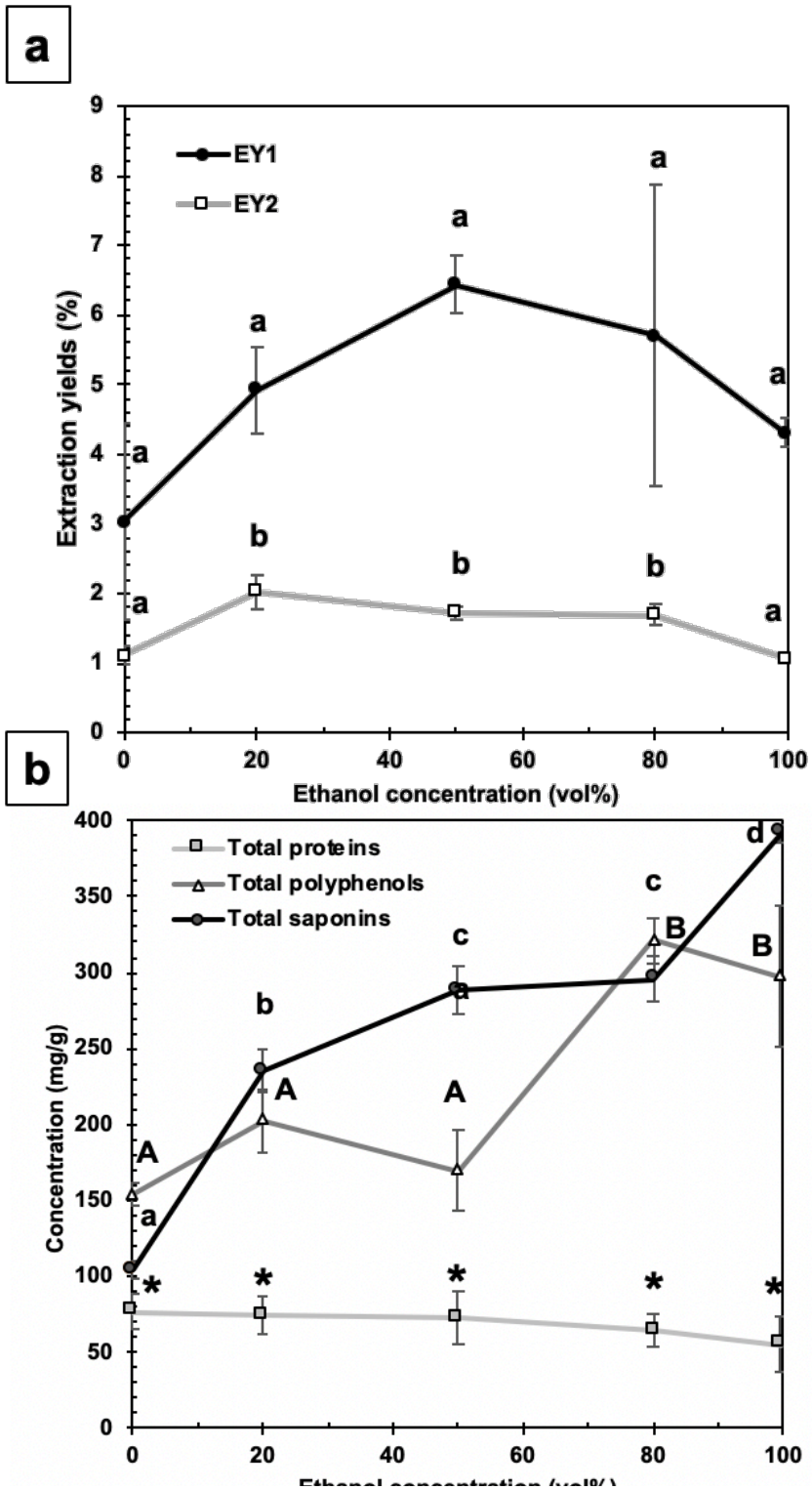

Figure 3: (a) Effect of ethanol concentration on (a) extractions yields from argan shell powder after evaporation of solvents (EY1) and after freeze-drying (EY2) and on (b) total saponins, polyphenols and proteins content in ASE. Means with the same letter/symbol are not significantly different at $p > 0.05$.

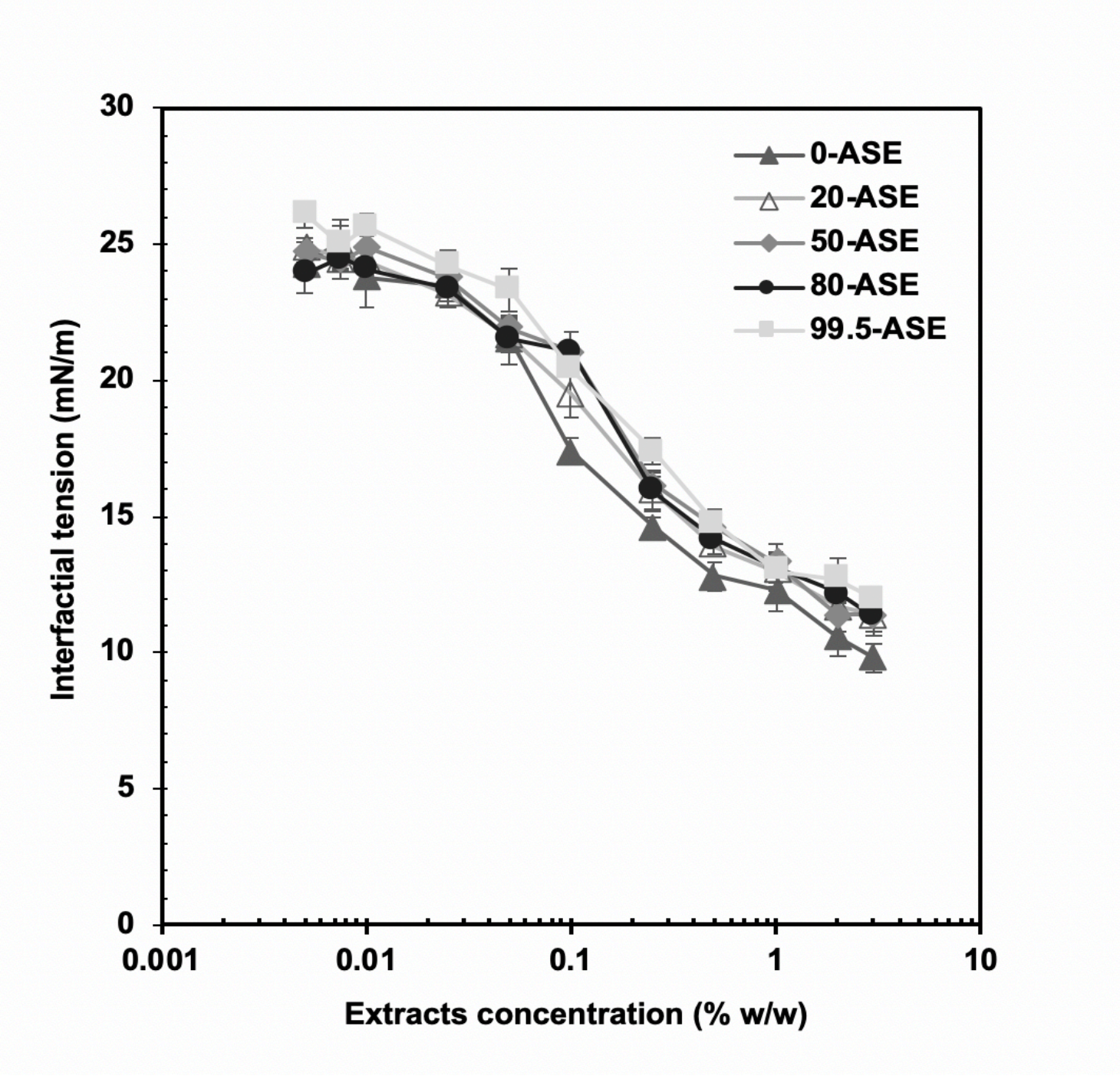

Figure 4: Influence of argan shell extracts prepared using 0-99.5 aqueous ethanol (0-ASE – 99.5-ASE) on interfacial tension (γ_{OW}) at soybean oil/water interface at room temperature.

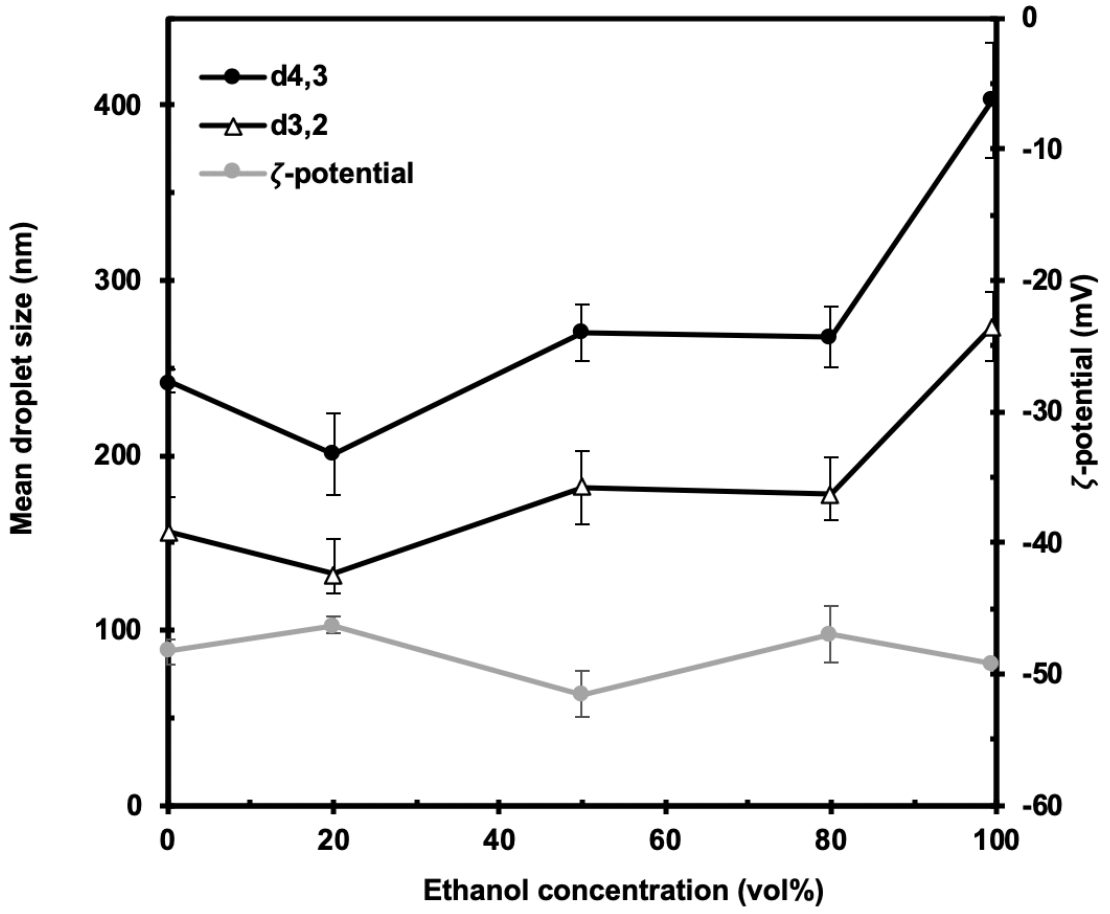

Figure 5: Effect of ethanol concentration during extaction on emulsion volume-base mean droplet size (d_{43}) and surface-mean droplet size (d_{32}) and ζ-Potential of 5 wt% soybean oil-in water emulsions.

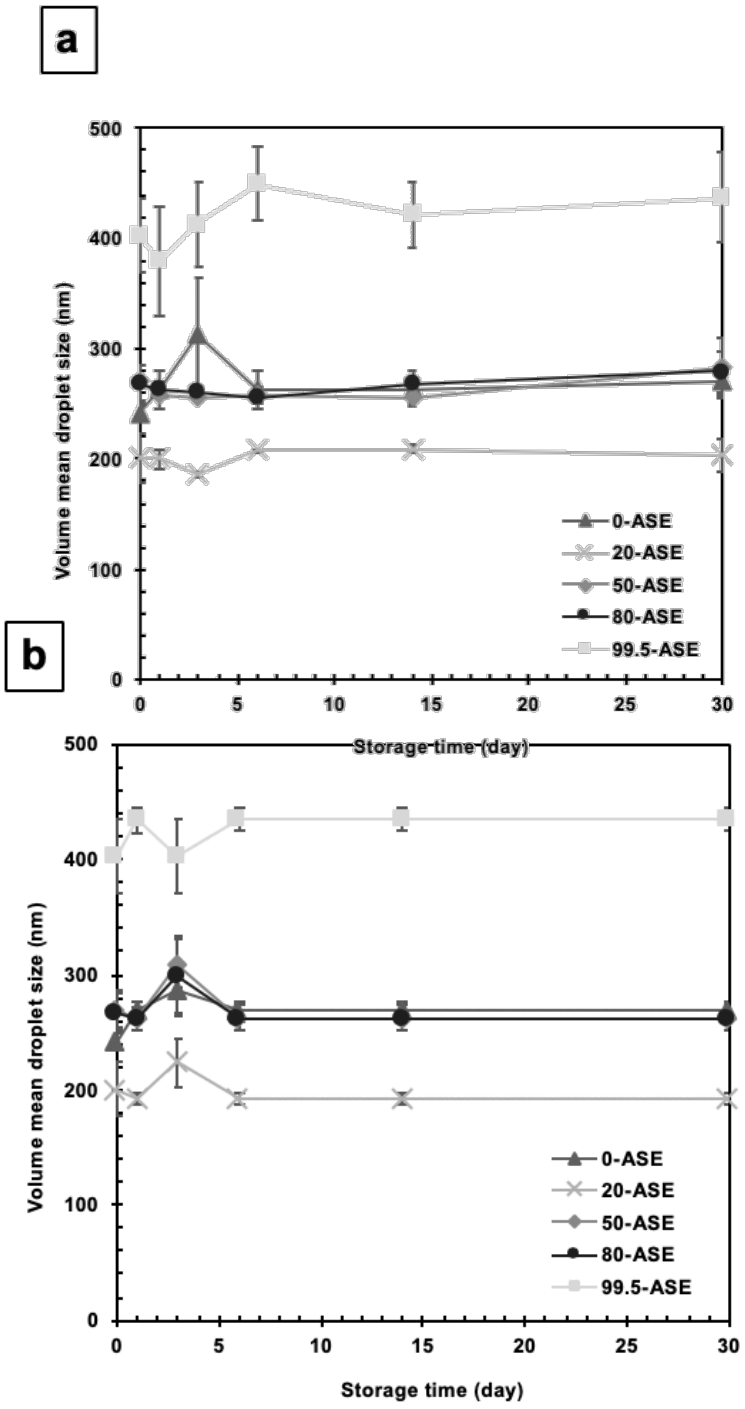

Figure 6 (a, b): Effect of storage time on emulsions volume-based mean droplet size (d_{43}) stabilized with 1 wt% of different ASE at (a) 5 ℃ and (b) 25 ℃ for 30 days.

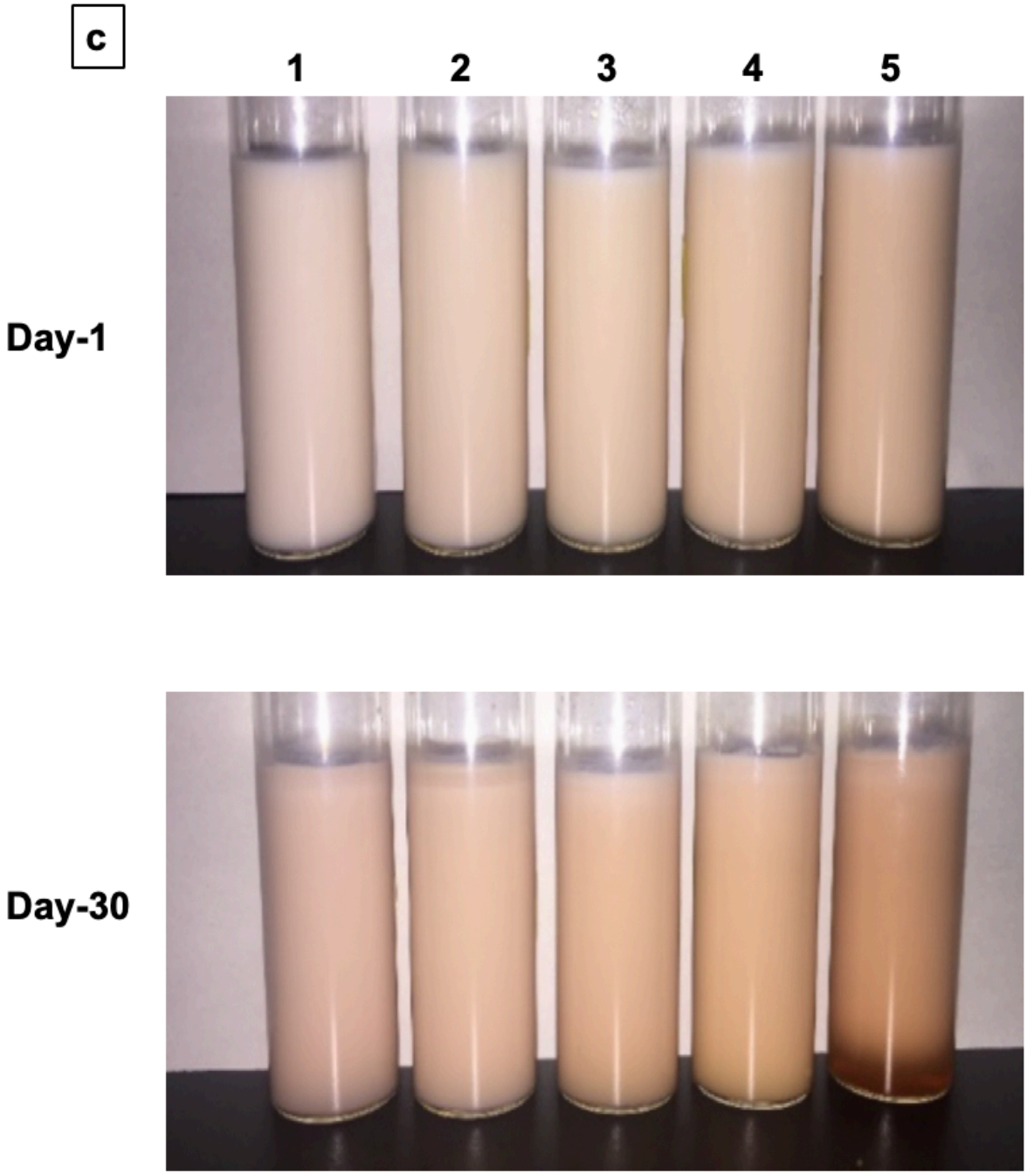

Figure 7 (c): Effect of storage time on emulsions volume-based mean droplet size (d_{43}) stabilized with 1 wt% of different ASE on the visual aspect of emulsions prepared with 0-ASE, 20-ASE, 50-ASE, 80-ASE or 99.5-ASE (from left to right, 1-5).

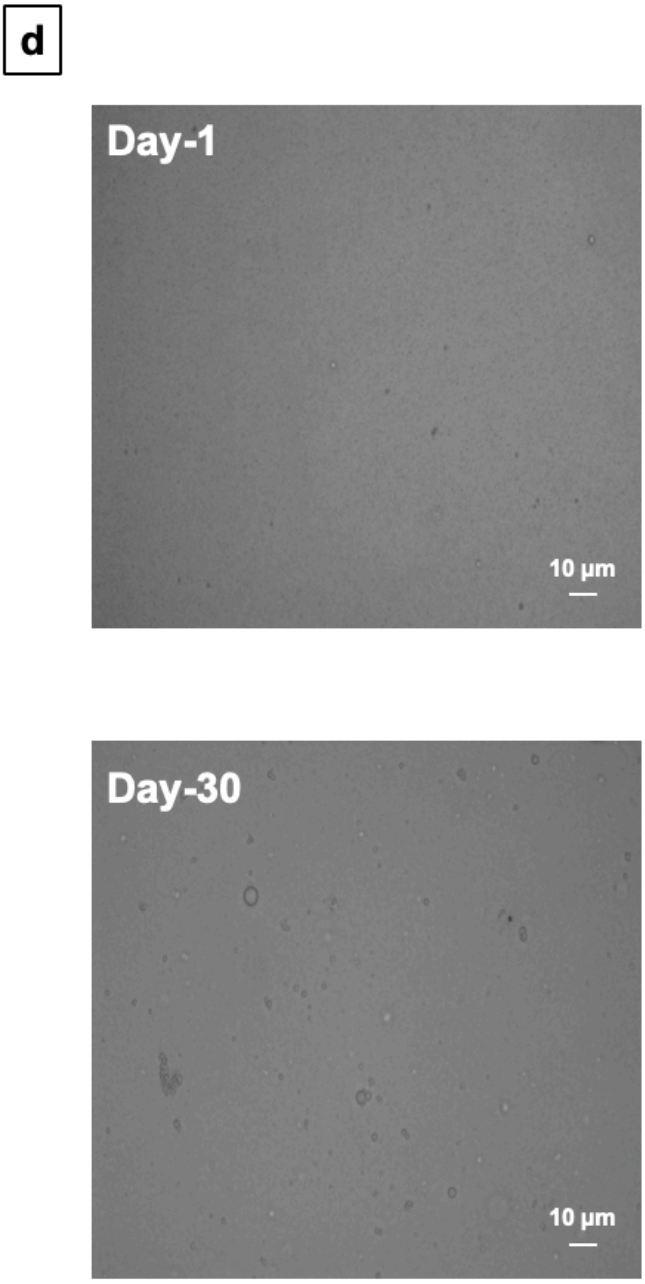

Figure 8 (d): Microscopic images of emulsions prepared with 20-ASE after 1 day and 30 days.

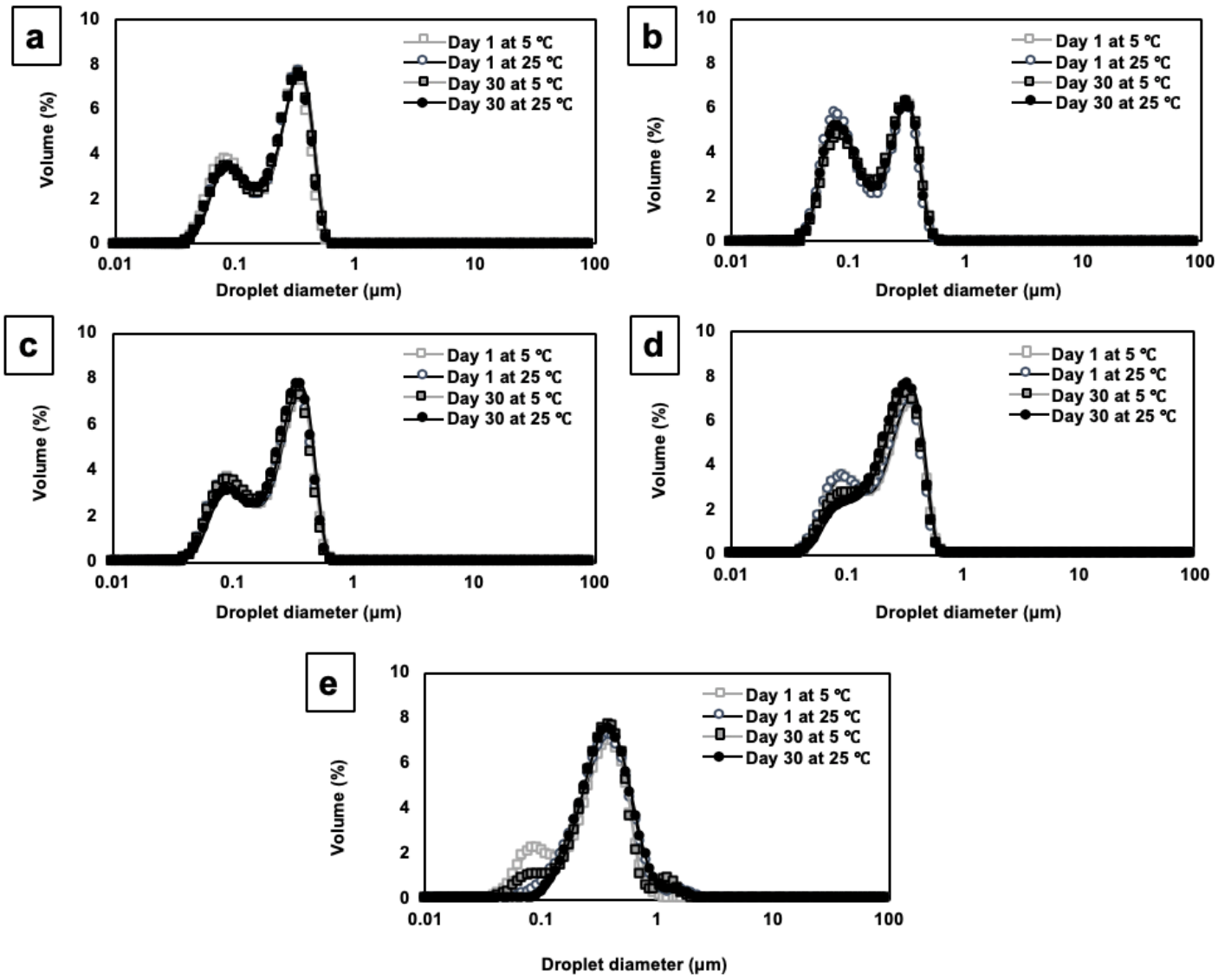

Figure 9: Droplet size distribution profiles of emulsions and after 1 days and 30 days storage at 5 ℃ and 25 ℃ using ASE (a) 0-ASE (b) 20-ASE (c) 50-ASE (d) 80-ASE (e) 99.5-ASE.

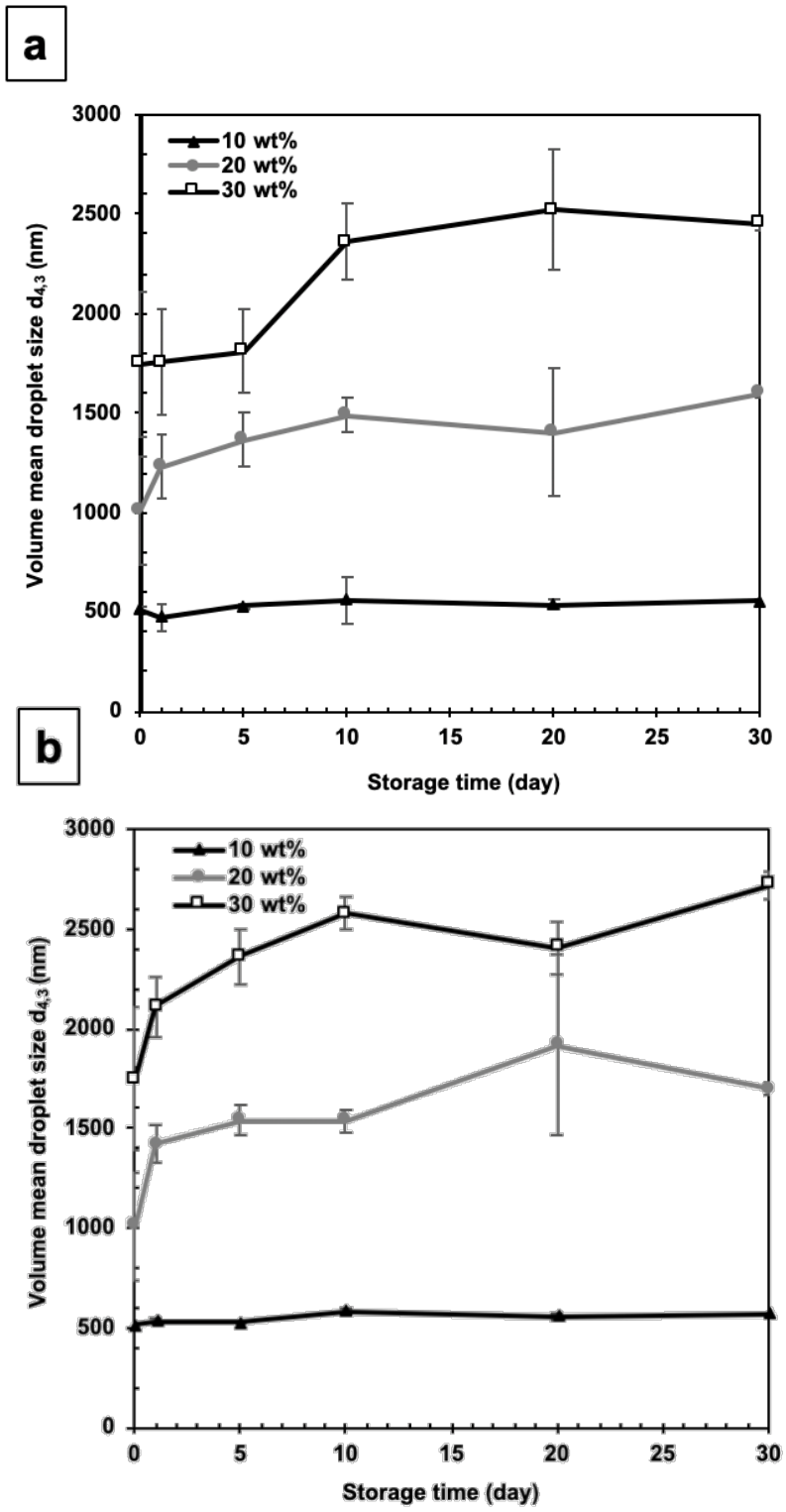

Figure 10 (a, b): Effect of storage time on volume-based mean droplet size (d_{43}) of emulsions containing 10 – 30 wt% soybean oil and stabilized by 20-ASE at (a) 5 ℃ and (b) 25 ℃ for 30 days.

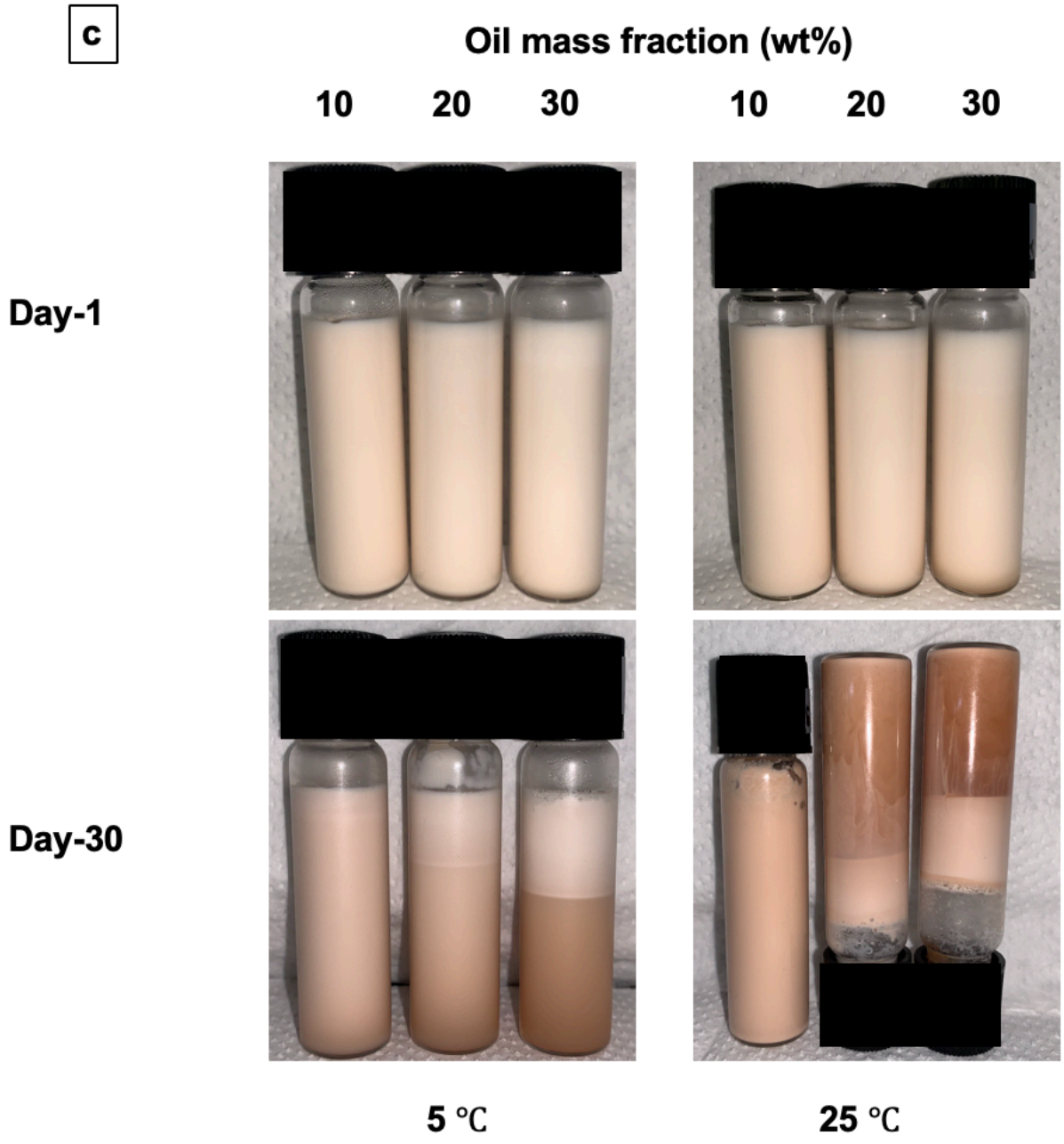

Figure 11 (c): Effect of storage time on the visual aspect of emulsions, prepared with 10 wt%, 20 wt% or 30 wt% after one day and after 30 days storage at 5 ℃ and 25 ℃.

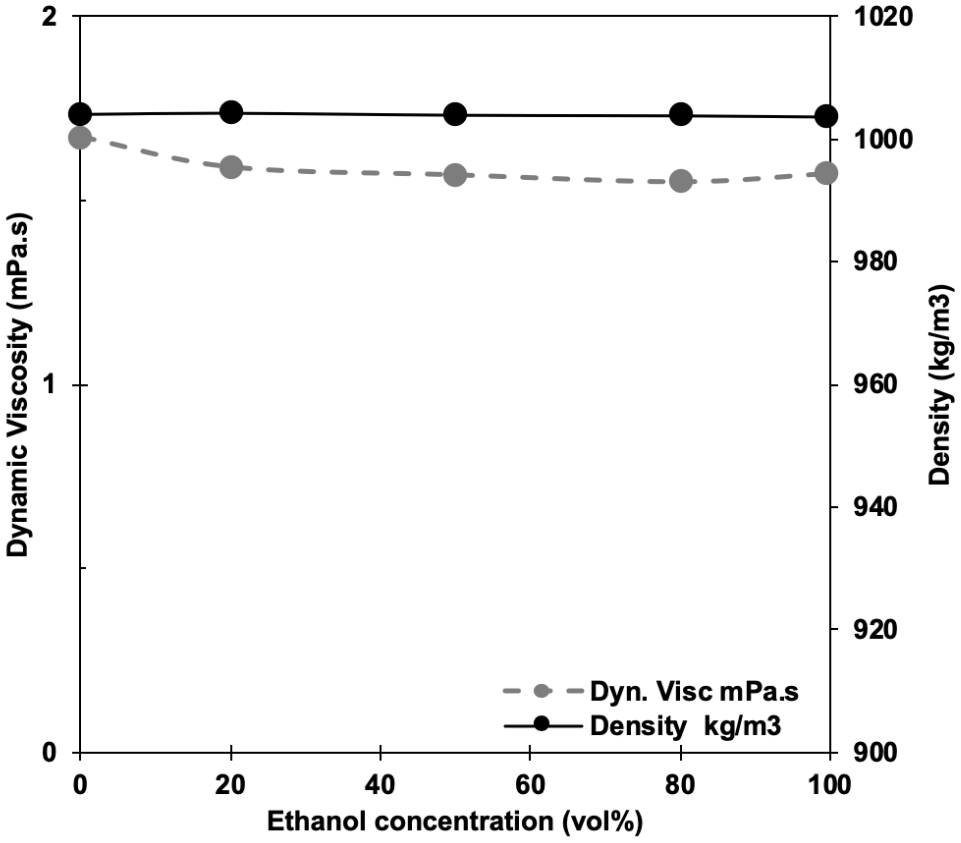

Figure 12: Dynamic viscosity and density of 1 wt% ASE in ultrapure water at 5 ℃.

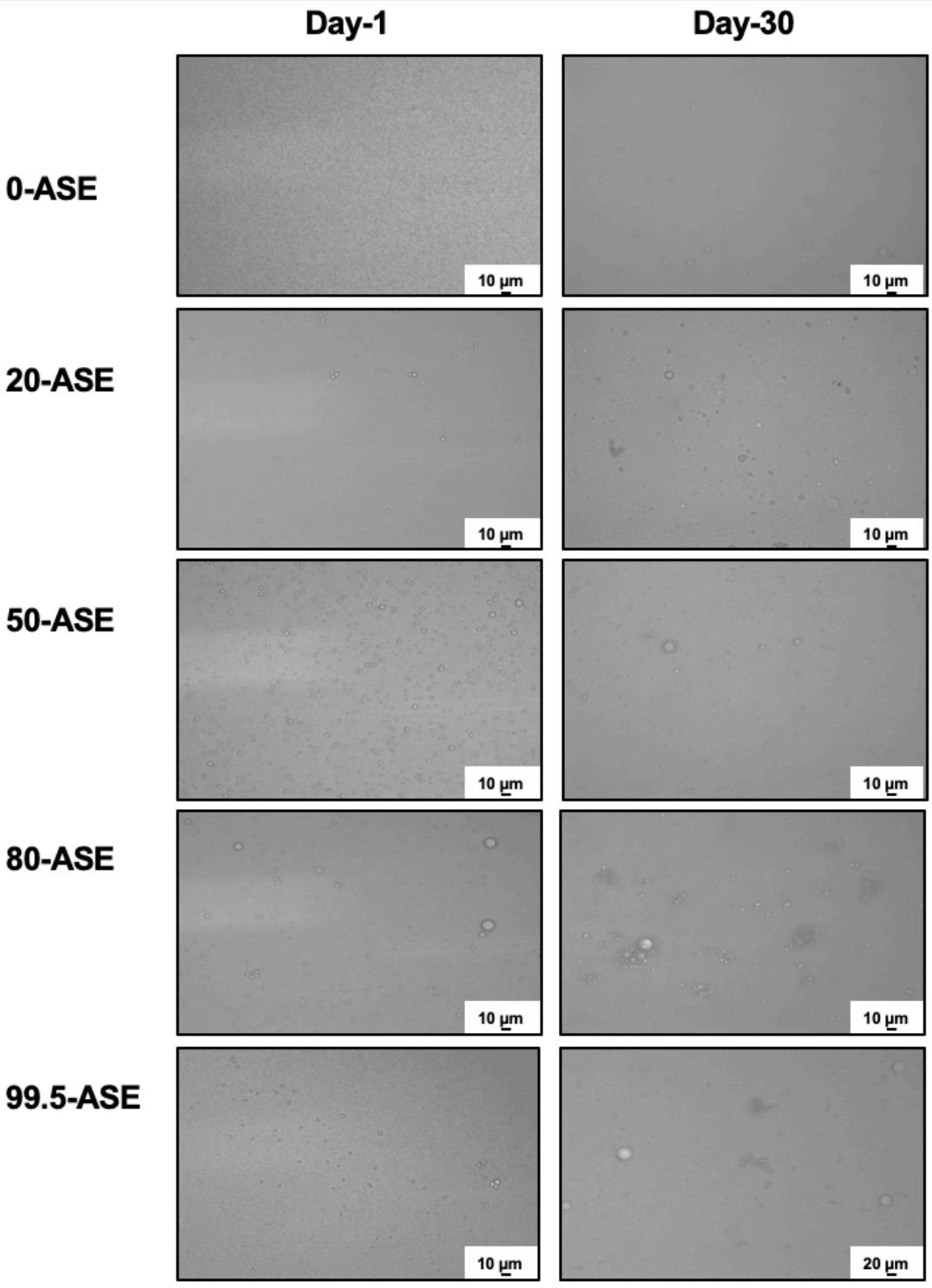

Figure 13: optical micrographs of emulsions stabilized with 0, 50, 80, 99.5-ASE after 1 day and 30 days storage.

Chapter 3 – Isolation and Characterization of Cellulose from Argan shell: Effect of Alkali treatment

---

Abstract

Cellulose was isolated from argan shell powder using a combination of alkali and bleaching treatments, 0.001 – 20% NaOH and H_2O_2 were used for this purpose. We studied the effect of alkali treatment on chemical, morphological and thermal properties of the produced residues. The resuls of hemicellulose, lignin and cellulose contents showed that there is an increase in cellulose content when increasing the concentration of NaOH. SEM micrographs did show a slight decrease in particle size of the residues and an entangled form of fibers that aggregates. FTIR analysis confirmed that alkali and bleaching treatments gradually removed hemicellulose and lignin from argan cell wall gradually with increasing NaOH concentration. In general, the purified cellulose isolated from argan shell have the potential for the preparation of microfibrillated cellulose using mechanical disintegration.

This chapter will be submitted for review as: Bouhoute, M., Taarji, N., de Oliveira, F. L., Habibi Y., Kobayashi I., Zahar M., Isoda H., Nakajima M., Neves M. (in preparation). Isolation and Characterization of Cellulose from Argan shell: Effect of Alkali treatment

3.1.Introduction

With the increasing concerns toward environmental issues, biomass-based resources are continuously attracting research and development to deliver more environmentally friendly products. Natural fibers as the main source of cellulose detain several advantages with regard to their high strength and low density in addition to the fact that they are renewable and biodegradable [67]. Endless resources of cellulose fibers can be found in nature from fibrous plants, such as jute, sisal, coir, bamboo, bagasse, pineapple leaf, etc. [68], therefore, cellulose characteristics and purity depends mainly on the origin and the natural source but also on the isolation process [69]. Cellulose is defined as a linear carbohydrate polymer of repeating $\beta(1,4)$ D-glucopyranose units. The monomers are linked by glycosidic oxygen bridges with a degree of polymerization varying between 10,000 and 15,000 in wood and cotton respectively [70].

Argan oil produced from *Argania spinosa,* an endemic species of south-west Morocco, is an internationally notorious cosmetic and edible oil driving attention due to its virtuous. However, only 3% of the species fruit represent the oil extracted from the kernel, the remaining parts are processing residues that are poorly valorized. Argan shell, endocarp protecting the fruit kernel, is an abundant biomass representing approximatively 52% of the fruit total mass (Figure 2) and is mostly composed of 73.6% fibers [71]. The utilization of argan shell is for now limited to its combustion by the local population as this biomass is able to burn for long time [25]. The commercial production of argan shell in southwestern Morocco generates an additional modest income to argan oil producers with a local selling price of (0.05 $/kg) [72]. Knowing the potential of this biomass to generate high value income products, led to few researches oriented toward argan shell valorization and utilization. Quaiss et al. (2015) reported about the incorporation of argan shell in the polymer matrix as a filler and demonstrated effective reinforcement of the polymer composite [73]. Bouqbis et al. (2016) described biochar from

argan shell to contain major nutrients and less heavy metals and recommended its utilization as soil amendment [74]. Laaziz et al. (2017) produced bio-composites based on polylactic acid and argan shell and reported about the effect of surface treatment on the morphology and thermal properties of the bio-composites [75]. El Moumen et al. (2020) presented a numerical model of the mechanical properties of bio-composites based on polypropylene and argan shell [76]. These studies demonstrate the tendency to utilize argan shell more efficiently to produce an effective material, however, none have reported about cellulose isolation and purification.

In the present work, we report about the effect of alkali treatment on argan shell fibers with various concentrations (0.001%, 1%, 10%, 20%) of sodium hydroxide when compared to untreated argan shell. We report also about the effect of a combined constant bleaching treatment on purified cellulose. We aim by this work to identify the successful chemical pretreatment to produce microfibrillated cellulose (chapter 3) to be successfully utilized as O/W Pickering emulsifier, thus, expanding the income of this endemic fruit.

3.2.Materials and methods

3.2.1. Materials

Argan shells were obtained from Agadir region in Morocco. Sodium hydroxyde (NaOH), potassium hydroxide (KOH), hydrogen preoxyde (30% H_2O_2), hydrochloric acid (HCl), sodium chrlorite ($NaClO_2$), were puchased from FUJIFILM Wako Pure Chemical Corporation (Osaka, Japan). Ultrapure water was produced using an Arium® pro system (Goettingen, Germany) and was used to prepare all solutions.

3.2.2. Cellulose purification

Argan shells size was reduced using hammer mill crashers (Masuko Sangyo Ltd., Saitama, Japan) the powder was then sieved to a homogeneous size ~ 62μm. The material was soaked

in an alkaline solution (0.001%, 1%, 10%, 20% NaOH) with a ratio of 1:10 for 24h and room temperature. The temperature was increased to 90°C for 3 hours before cooling down. The material was washed until neutral pH. Bleaching consisted in treating the residue of alkali treated argan shell using 3% H_2O_2 with a ratio of 1:5 at 90°C for 3 hours. Figure 11 represent the purification process of cellulose from argan shell.

3.2.3. Characterization of Argan fibers

3.2.3.1. *Cellulose, hemicellulose, lignin and ash contents*

The resulting residues from alkali and bleaching treatments were characterized with regards to their cellulose, hemicellulose, lignin and ash contents. First, lignin content was determined by delignifying the residues by acidification using sodium chlorite and acetic acid method [77]. Briefly, the dried powders were added to ultrapure water with a ratio 1:32 then $NaClO_2$ was added to the slurry with a powder: $NaClO_2$ ratio of 1:0.6. Acetic acid was then added gradually 0.2 ml/ hour and the reaction time continued for 6 hours at 72 ℃. Supernatant of the reaction represented the hydrolyzed lignin whereas the dried insoluble residue represented holocellulose. Hemicellulose was then extracted from the recovered holocellulose using alkali treatment [78]. Briefly, the recovered holocellulose powder was treated using 10% KOH at powder:solvent ratio of 1:20, the reaction was conducted for 10 hours at 35 ℃. The supernatant of the reaction represented hemicellulose and the insoluble residue represented cellulose content (Figure 12).

The carbohydrates mass balance was reported as %dry mass, the ash content was determined and subtracted from the cellulose content. Ash content was determined by placing the dried cellulose residue in muffle furnace at 500 ℃ for 12 hours.

3.2.3.2.Morphology and particle size

The alkali treated and bleached residues from argan shell powder were characterized for their particle size and aspect. After airdrying the samples Scanning Electron Microscope (Hitachi Miniscope TM-1000, Japan) was used to visualize the cellulosic particles

3.2.3.3.FTIR

Examination of changes in the chemical composition of Argan shell after alkali and bleaching treatments were carried out using Fourier transform infrared spectroscopy (FTIR). The samples were dried before mixing with KBr 1:100. Sample/KBr. The scan of each sample was recorded from 4000 cm^{-1} to 400 cm^{-1} with a resolution of 2 cm^{-1} in transmission mode.

3.2.3.4.DSC

Thermograms of untreated argan shell and alkali and bleached residue were determined using a differential scanning calorimetry (DSC 60 plus, Shimadzu, Japan). Briefly, 6 mg of each sample was heated in an aluminum pan from 25 ℃ to 300 ℃ and a heating rate of 10 ℃/min.

3.2.3.5.TGA

Thermogravimetric analysis (TGA) was performed using a 409 PC Luxx– Netzsch, Germany. The analyses were conducted under nitrogen atmosphere at a constant flow rate of 100 ml/min. Samples (10 - 15 mg) were heated from 30 to 800°C at a constant heating rate of 20°C min^{-1}.

3.3.Results and discussion

3.3.1. Composition of argan shell residues

Figure 13 shows the variation in hemicellulose, lignin and cellulose content after the chemical purification of argan shell using variable concentration of alkali solutions (0.001%-20%) and a constant bleaching treatment. Alkali treatment causes the hydrolysis of constituents such as starch, pectin but more importantly hemicellulose [79]. The bleaching treatment on the other hand induces de removal of lignin and phenols. A nucleophilic reaction between the aromatic rings of lignin and H_2O_2 generating hydroxyl, carboxyl and carbonyl groups facilitating lignin solubilization and therefore cellulose purification [79,80]. The effect of NaOH on cellulose isolation was highlighted. The results show that 20 % NaOH led to less hemicellulose and lignin contents. However, the purified cellulose in that case is considered alkali cellulose "mercerized cellulose" and therefore the natural structure of cellulose from argan shell was modified with higher alkali treatment.

3.3.2. Description of fiber's morphology

The chemical pretreatment that argan shell undergo leads to structural and chemical changes in the fibers. Morphological properties of argan shell residues along chemical treatment 0.001% - 20% NaOH followed by bleaching are shown in Figure 14 (a-d 1,2). The morphology of the fibers shows a small decrease of the dimension of particles at high alkali concentration and a constant bleaching treatment possibly resulting from a loss of matrix in the cell wall, aggregation of microfibrils could also be a possible explanation to this phenomenon. Pores were observed on the surface of treated particles which could be explained by a loss of lignin and hemicellulose. The particle size varied between 22 ± 12 and 42 ± 13 μm and the general aspect of the fibers show high entanglement and aggregation.

3.3.3. Chemical and thermal properties of treated argan shell residues

Figure 15 shows the changes in FTIR spectra of chemically purified argan shell using variable concentration of alkali solutions (0.001%-20%) and a constant bleaching treatment to identify the changes in functional groups present in the samples. A broad vibration was observed in all samples in the 3600-3000 cm^{-1} region, this adsorption band is attributed to -OH groups found in lignocellulosic materials [81]. The peaks at 1739 cm^{-1} correspond to C=O groups in acetyl and uronic ester groups of hemicellulose [82]. This first band disappears gradually with increasing alkali treatment from 0.001% NaOH until 20% NaOH. Therefore, increasing alkali concentration leads to an effective removal of hemicellulose from argan shell powder. The peak at 2900 cm^{-1} correspond to the aliphatic C–H stretching of lignin, and cellulose [83]. In addition the adsorption band in the 1670-1540 cm^{-1} region is attributed to the aromatic C=C stretch, therefore, aromatic rings and conjugated carbonyl groups found in lignin structure remained in the treated samples [84]. Alkali and bleaching treatments did not enable the removal of all lignin found in argan cell wall, thus the peak remained present when using further mechanical treatment.

Figure 16 shows the DSC curves obtained for untreated argan shell and alkali/bleaching treated (20% NaOH) residue. The samples were dried overnight before conducting the experiment therefore no peak was recorded between 100-120 °C corresponding to water evaporation. Two peaks were detected in both untreated and treated argan shell between 170-230 °C, these peaks are exothermic corresponding to the degradation of hemicellulose in the sample. Hemicellulose is composed of branched amorphous structure of various saccharides (xylose, mannose, glucose, galactose, etc.). The structure of hemicellulose leads to volatiles (CO, CO_2 and hydrocarbons) this peaks are therefore attributed to charring of the residues [83]. The degradation temperature of cellulose is known to occur between 290-375°C and this is due to

the unbranched glucose units forming the long polymer, thus, leading to higher stability [83]. In addition, lignin degrades over 500-900 °C [85]. Unfortunately, the DSC curves do not show the degradation of cellulose and lignin.

Figure 17 shows the thermogravimetric analysis (TGA) curves of untreated argan shell and chemically treated argan shell, the samples were dried prior to analysis. The weight loss of both samples stated at approximately the same temperature of 230 ℃ and reached a dominant peak at 370℃, 362℃ for untreated and treated argan shell respectively. This result may indicate that the treated sample had a similar degradation behavior compared to the raw material.

3.4.Conclusion

Cellulose have been successfully extracted combining alkali and bleaching treatments. Alkali concentration was the main parameter that was controlled in this study. We confirm that increasing NaOH concentration we improved the properties of the purified cellulose. Hemicellulose, lignin and cellulose contents reported in the different samples of argan shell residues (untreated and treated) showed that there is a slight increase in cellulose concentration in the sample however, hemicellulose and lignin still remain in all studied samples. Considering the high concentration of NaOH (20%), the purified cellulose obtained and selected for our study represents mercerized cellulose. SEM micrographs showed that alkali treatment improved the morphology of the fibers. FTIR analysis showed that the chemical treatment effectively removed hemicellulose and lignin from the samples. Further thermal analysis of TGA and DSC confirmed this tendency. This study could lead to a successful preparation of microfibrillated cellulose from argan shell for seeking it’s characterization and utilization as natural emulsifier.

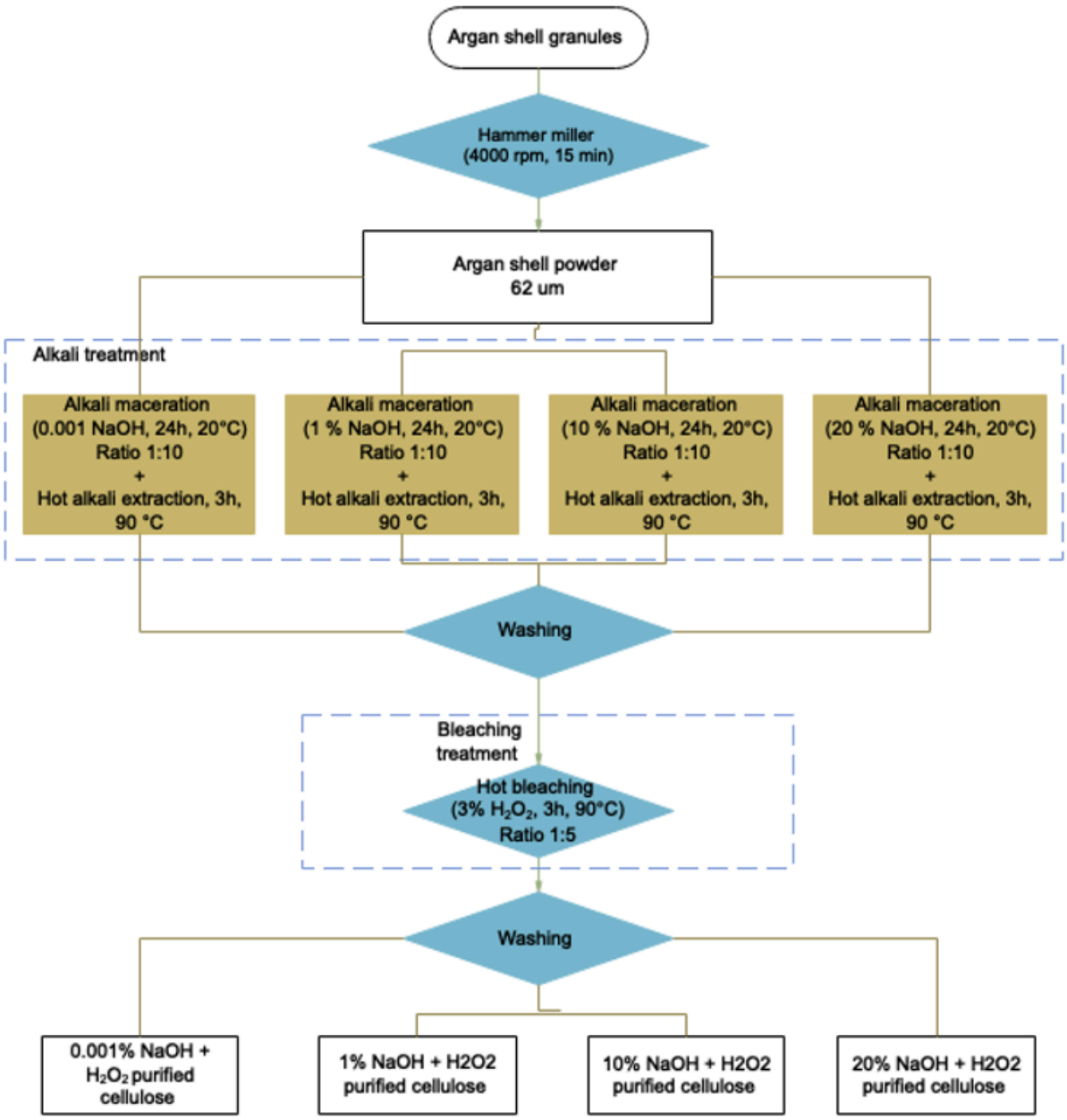

Figure 14: Process of purification of cellulose from Argan shell

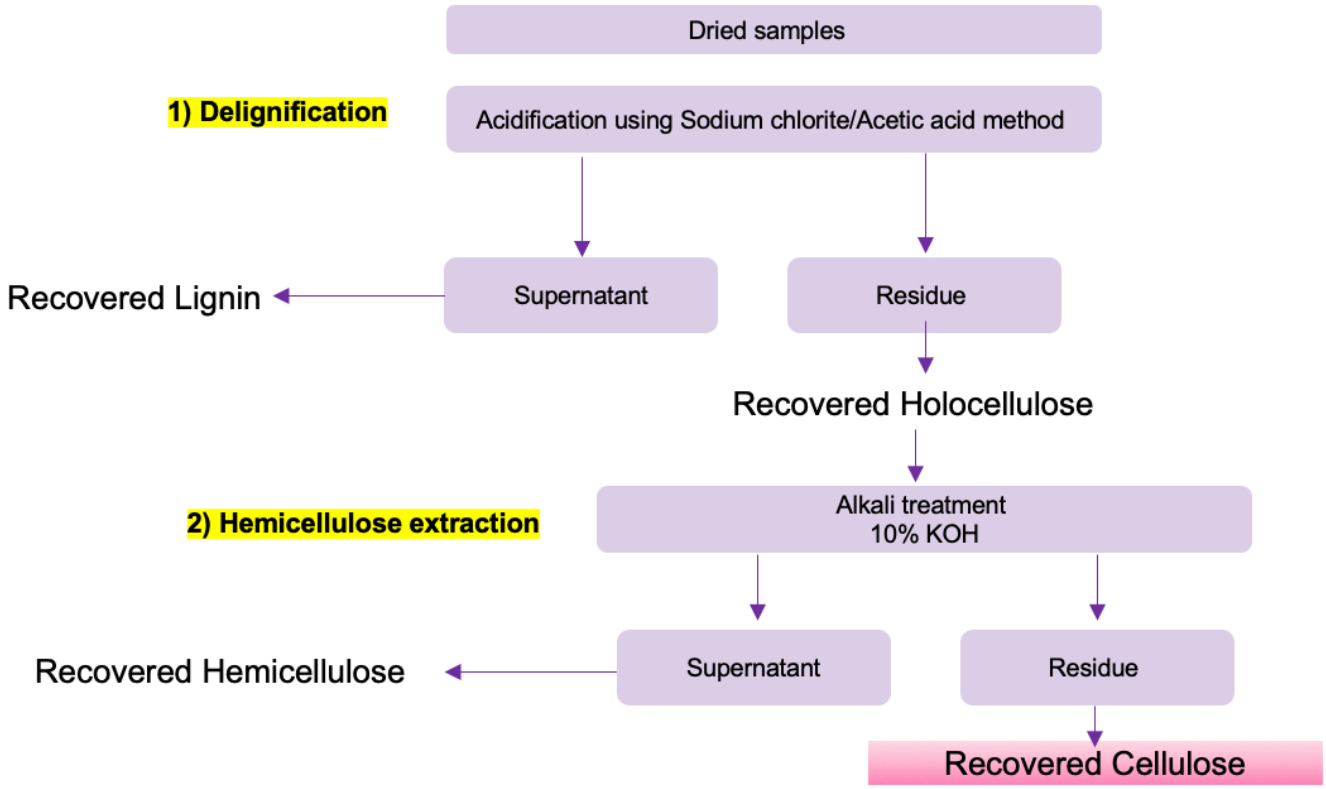

Figure 15: Description of delignification and hemicellulose extraction for characterization purposes of argan shell residues

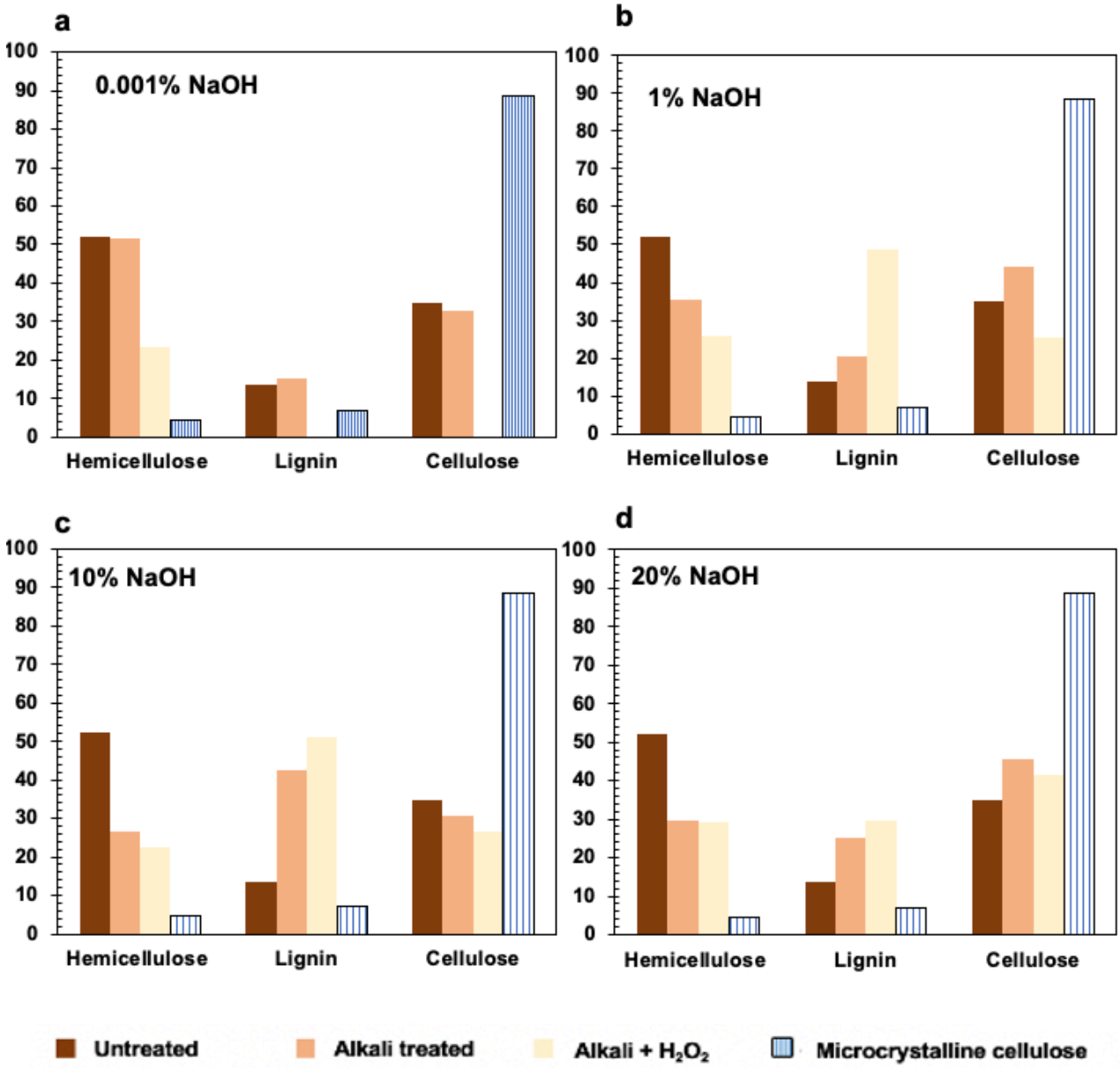

Figure 16: Hemicellulose, lignin and cellulose content in untreated, alkali treated and bleached argan shell and microcrystaline cellulose as control, the parameter that was varied is the concentration of NaOH (a) 0.001% NaOH (b) 1% NaOH (c) 10% NaOH (d) 20% NaOH

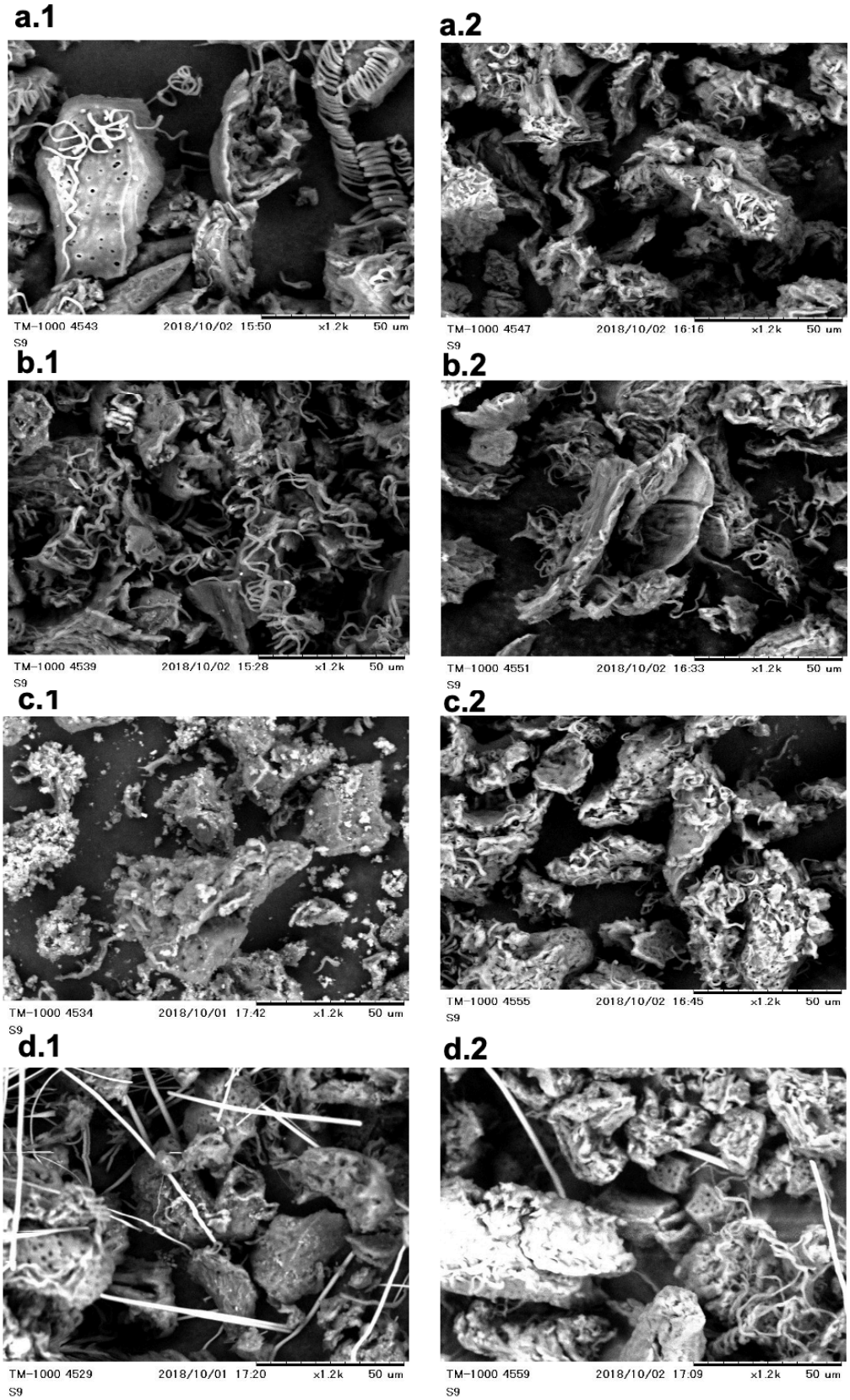

Figure 17: SEM micrographs of argan shell residues after (a.1, b.1, c.1, d.1) alkali treatment (o.001%, 1%, 10%, 20%) and bleaching treatment (a.2, b.2, c.2, d.2)

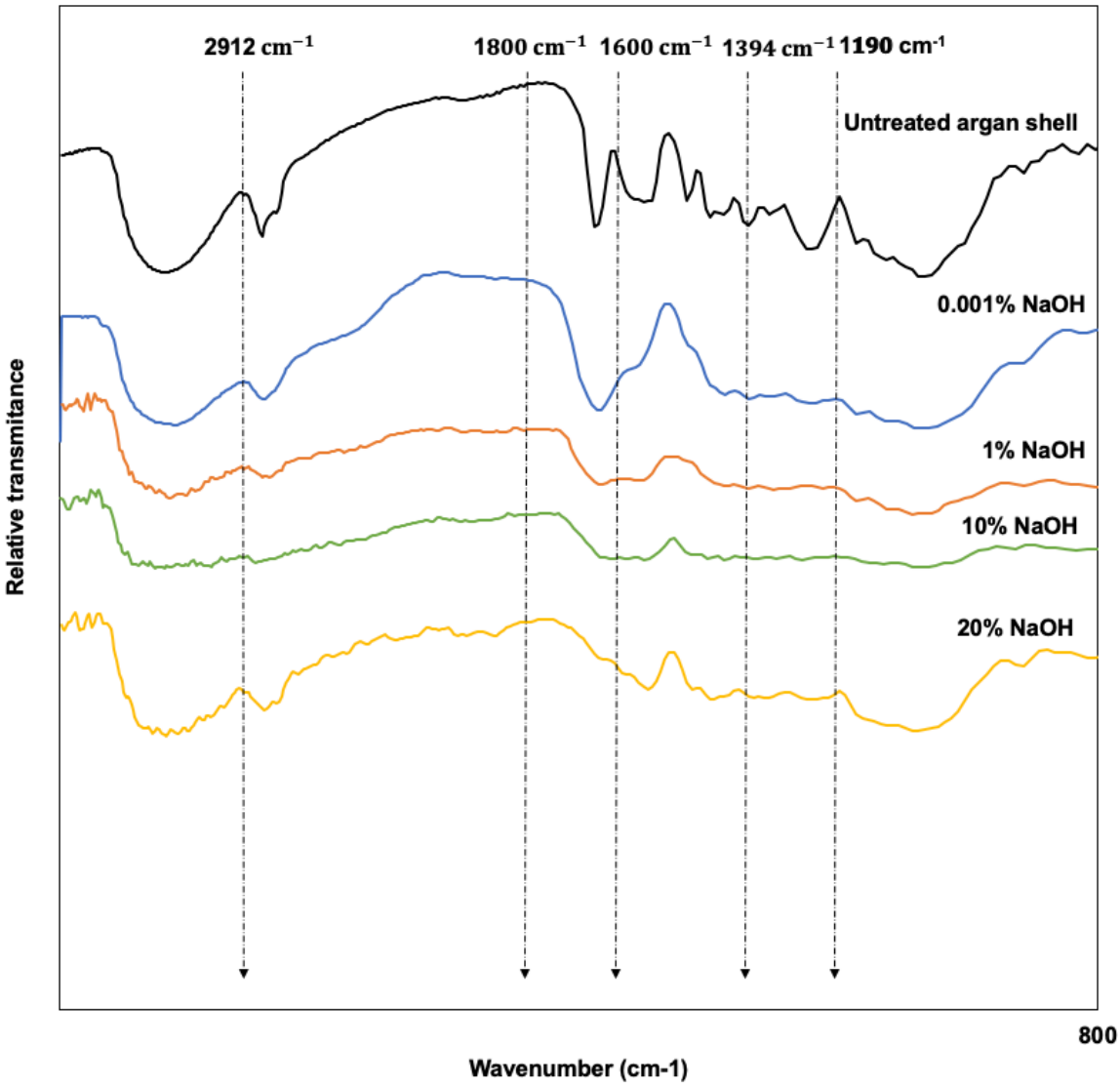

Figure 18: FTIR spectrum of untreated argan shell and alkali (0.001% -20% NaOH) and bleached residues

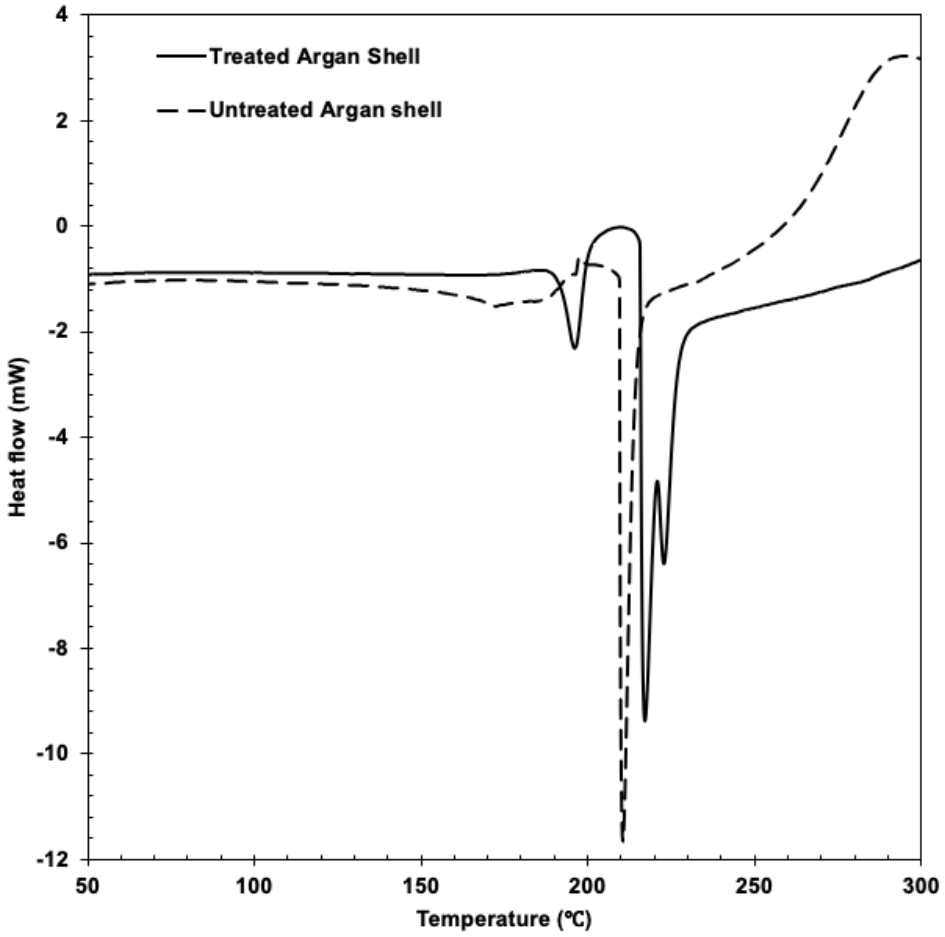

Figure 19: DSC curve of untreated argan shell vs 20% NaOH and bleached argan shell residue

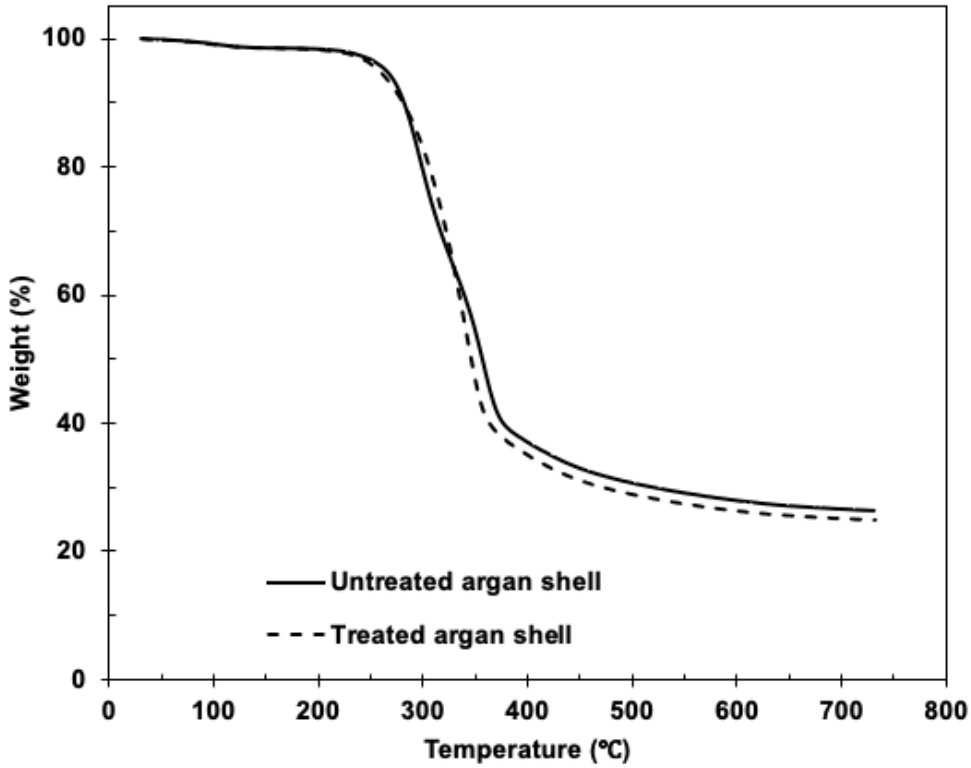

Figure 20: TGA thermogram of untreated argan shell vs 20% NaOH and bleached argan shell residue

Chapter 4 – Microfibrillated cellulose from *Argania spinosa* shell as sustainable solid particles for O/W Pickering emulsion

---

Abstract

Microfibrillated cellulose (MFC) from Argan (*Argania spinosa*) shells was prepared first by chemically purifying cellulose using alkali and bleaching treatments, then mechanical disintegration via high pressure homogenization to isolate elementary fibrils of cellulose. Chemical characterization of raw argan shell (AS-R), purified cellulose (AS-C), and argan shell MFC (AS-MFC) included FT-IR, XRD, NMR. Morphological characterization of AS-MFC was assessed using TEM and particle size was determined. The use of AS-MFC as oil-in-water (o/w) emulsions stabilizer was investigated. The effect of particles concentration was assessed and led to long term stability (15 days) of o/w emulsions at high concentration of AS-MFC confirmed by droplet size $d_{4,3}$ and creaming index. This study also shows the suitable oil concentration to reach the maximum volume of emulsion using 1% w/w AS-MFC. The results show AS-MFC could stabilize 70% w/w MCT oil without visual phase separation. Finally, CLSM shows the adsorption of AS-MFC at the oil-water interface and the formation of a 3D network surrounding oil droplets by larger fibrils confirming Pickering emulsion formation and stabilization with this new material.

This chapter was submitted for review as: Bouhoute, M., Taarji, N., de Oliveira, F. L., Habibi Y., Kobayashi I., Zahar M., Isoda H., Nakajima M., Neves M. (Under review). Microfibrillated cellulose from Argania spinosa shells as sustainable solid particles for O/W Pickering emulsions.

4.1.Introduction

Oil-in-water (O/W) emulsion is a system encountered in many commercial products such as food, cosmetic and pharmaceutic industries [9,57]. This system is thermodynamically unstable consisting of two immiscible liquids, one dispersed into the other, that would rapidly separate to the initial homogenized components in the absence of stabilizers [7]. Emulsion stabilizers can be categorized into surface-active emulsifiers (surfactants) and thickening or gelling agents depending on the mechanism of stability [86]. Furthermore, solid particles were also described to stabilize emulsions forming the so called 'Pickering emulsions' that were first reported by Pickering (1907). Pickering emulsions are formed when solid particles accumulate at the oil-water interface forming a steric barrier that prevent coalescence and Ostwald ripening [87]. Partial wetting of particles by the oil and the water phases is needed for an effective anchoring of the particles at the interface [88]. This shows enhanced properties in emulsion stabilization when compared to surface-active compounds that can easily be disrupted by the environmental conditions. In addition, this type of emulsions offer some advantages to reduce allergic effects and undesirable taste characteristics when compared to conventional surfactants [15].

Pickering emulsions stability, type, morphology and characters are highly influenced by the type of particles used [16]. Both organic and inorganic particles have been described to produce O/W Pickering emulsions. Particles such as silica (SiO_2) [17], calcium carbonate ($CaCO_3$) [18] and titanium dioxide (TiO_2) [19] maybe used in food as Pickering stabilizers. However, such particles face criticism due to the suitability for food and environmental related questions [20]. Therefore, sustainable food-grade particles such as starch granules, cellulose nanocrystals, bacterial cellulose nanocrystals, microfibrillated cellulose, nanofibrillated cellulose gained more attention in recent studies [20,86,89–94].

Cellulose is a biopolymer composed of linear chains of 1–4-linked β-D-glucopyranose structuring cellulose microfibrils. Microfibrillated cellulose (MFC) have been produced by

mechanical disintegration using different methods such as, homogenization [95] micro-fluidization [96] micro-grinding [97]. MFC typically shows interesting properties such as i) high specific surface area, ii) high strength and stiffness and iii) low weight that was reported as suitable for the formation and stabilization of Pickering emulsions [93,98]. Various lignocellulosic materials have been used for MFC isolation [99–104]. However, fewer studies applied the isolated fibers to formulate emulsions [93,94,105]. Thus, due to the growing demand for cellulosic fibers, research interest is now shifting toward sustainable and abundant sources such as agricultural by-products that have currently low value [106].

Argan (*Argania spinosa* L.) species endemically found in Morocco, produces a highly notorious fruit used for oil production. In early 21st century, argan oil made a breakthrough to international markets due to its virtues. Argan tree tolerance for hard climate conditions of dry arid lands and poor precipitations, procured to argan oil its high antioxidant, anti-cancer and anti-acne properties [107]. Nevertheless, argan oil represents only 3% of the industrial production, the remaining are by-products that are not valorized and used as cattle feed or combusted [23]. New applications for argan by-products have been proposed. For example, our research group reported the potential of saponins rich extract from argan press cake to produce highly stable O/W emulsion using both high and low energy emulsification processes [36,108]. Additionally, we showed the potential of argan shell crude extract to formulate and stabilize O/W emulsions by the presence of mixture of surface-active compounds (i.e. saponins, proteins and polyphenols) in its crude extracts [109]. However, despite this application with respect to argan shell, the recovery yield of aqueous-ethanolic extraction still remain low (~5%), thus, large amounts of lignocellulosic residue is yet to be valorized [109]. Hence, argan shell is proposed as potential candidate for MFC production as sustainable and abundant source of cellulose fibers. To the best of our knowledge, no previous study has

described the use of argan shell to produce MFC so far and applied it to formulate O/W Pickering emulsions.

In this study, we prepared for the first time, MFC from argan shell lignocellulosic residue via chemical purification of cellulose and mechanical disintegration using high pressure homogenizer. Then, we performed an extensive characterization of the produced fibers. Next we investigated the potential of using argan shell MFC in the formation and stabilization of Pickering emulsions. This study is of an importance to identify new sustainable sources of MFC with a suitable application in the formulation of Pickering emulsions.

4.2.Materials and methods

4.2.1. Materials

Argan shells were obtained from Agadir region in Morocco. All reagents were puchased from FUJIFILM Wako Pure Chemical Corporation (Osaka, Japan). Refined medium-chain triglyceride (MCT) oil was kindly provided by Taiyo Kagaku Co., Ltd. (Tokyo, Japan). Ultrapure water was produced using an Arium® pro system (Goettingen, Germany) and was used to prepare all solutions.

4.2.2. Preparation of Argan microfibrillated cellulose (MFC)

Argan shells were crashed using a Hammer miller operating at 2000 rpm (Masuko Sangyo Ltd., Saitama, Japan) the powder was sieved to a homogeneous size of 62 μm. Cellulose purification consisted on extractives removal using 20% ethanol solution as described by [109] then washing and soaking the remaining lignocellulosic residue in an alkaline solution (20% NaOH) with a ratio of 1:10 for 24h at room temperature. Next the temperature was increased to 90°C for 3 h before cooling down. The material was washed until neutral pH and bleaching treatment was conducted using 3% H_2O_2 with a ratio of 1:5 at 90°C for 3 h and the slurry was washed

and stored until further use. Argan shell MFC was prepared using high pressure homogenization, briefly, 1% of argan cellulose dispersion was passed in high-pressure homogenizer (NanoVater, NV200, Yoshida Kikai, Nagoya, Japan) at 100 MPa for 10 passes. Raw argan shell material, argan shell cellulose and argan shell MFC were denoted AS-R, AS-C, AS-MFC respectively in this study.

4.2.3. Characterization of Argan fibers

4.2.3.1.*Particles size and morphology*

AS-MFC particle size distribution was acquired using laser diffraction particle size analyzer (Beckman Coulter, Brea, California). The morphology of AS-MFC was assessed using Transmission Electron Microscope (TEM) H-7650 (Hitachi, Tokyo, Japan) at 80 kV. Briefly, 5 μl of 0.01 % (w/w) AS-MFC dispersion was deposited on a dried carbon-coated grid 200 mesh. The sample was dried at 50 ℃ for 10 min then visualized under 25,000x magnification.

4.2.3.2.FTIR

Fourier transform infrared (FTIR) analysis of argan samples was carried out using Bruker Tensor 27 FT-IR, Germany, to examine the changes in functional groups of argan fibers after each treatment. The samples were dried before mixing with KBr 1:100. Sample/KBr compressed pellets were further dried under vacuum. The scan of each sample was recorded from 4000 cm^{-1} to 400 cm^{-1} with a resolution of 2 cm^{-1} in transmission mode.

4.2.3.3.XRD

X-ray diffraction (XRD) was performed with an X-ray diffractometer using a Bruker Discover D8, Germany, to evaluate the argan fibers structure and determine the crystallinity index (CrI) of the samples after different treatments. The samples were grounded in powder and compacted

into a sample holder. Measures were conducted in a 2θ range between 5° and 50°. The CrI of the samples was evaluated according to the Segal method [110] and calculated using Eq. (1)

$$CrI = \frac{Ic - IAm}{Ic} \, x \, 100 \qquad (1)$$

where, I_{Am} is the minimum intensity of the peak 101 (amorphous band) and I_c is the crystalline portion of the peak 002, 2θ = 18° and 2θ = 22° respectively.

4.2.3.4.NMR

Nuclear magnetic resonance (NMR) spectrums were recorded on a Bruker Avance III HD 600MHz NMR spectrometer, Germany, equipped with standard bore magnet and a 4 mm dual channel probe. ^{13}C Crosspolarisation (CP) spectrum was recorded using optimized conditions, i.e. 1.5 ms spin-lock using a 50-100 ramp at 8 kHz centered on the first spinning side band (MAS-rate 8kHz) with high-power decoupling at 62.5 kHz and a relaxation delay of 9 s.

4.2.3.5.Interfacial properties

1% AS-MFC dispersion in ultrapure water was prepared to measure dynamic interfacial tension (γ_{OW}) at the MCT/water interface for 10 min. Pendant drop method was carried out in an interfacial tensiometer (Kyowa, Saitama, Japan). Briefly, Dispersions were placed in a syringe and a drop was formed by a 22 G needle to form a 54 μl drop. Then, interfacial tension was calculated automatically by FAMAS software based on the drop shape using the Young-Laplace equation during 5 min.

AS-MFC hydrophilicity was assessed by measuring the contact angle of one water drop (10 μl) on AS-MFC film that was prepared using 0.5% AS-MFC and dried over night at 50 ℃ in a petri dish.

4.2.4. Preparation of O/W emulsions

O/W emulsions were prepared by homogenizing the oil phase (MCT oil) with an aqueous phase consisting of 0.05 – 1 % (w/w) AS-MFC in phosphate buffer (pH 7). Sodium azide 0.02% (w/w) was added to all emulsions to inhibit microbial proliferation during the storage. First, coarse emulsions were prepared using high shear blending at 10,000 rpm for 5 min (Kinematica-AG, Luzern, Switzerland). The coarse emulsions were then passed through high-pressure homogenization (Yoshida Kikai Co., Ltd., Tokyo, Japan) at 100 MPa for 4 passes.

4.2.5. Caracterization of emulsions

4.2.5.1.*Droplet size measurement*

The droplet size of emulsions was monitored using a laser diffraction particle size analyzer (Beckman Coulter, Brea, California). Droplet size was expressed as volume mean diameter, d_{43} ($= \sum n_i \ {d_i}^4 / \sum n_i \ {d_i}^3$) where n_i is the number of droplets with diameter d_i.

4.2.6. Creaming index

10 g of emulsions were transferred to a glass test tube (17 mm diameter and 75 mm height) immediately after their preparation. The tubes were stored at 25 ℃ and creaming was assessed for different time periods. Creaming index (CI) was reported using Eq. (2)

$$CI = \frac{H_S}{H_T} \ x \ 100 \qquad (2)$$

where, H_S is the serum layer height and H_T is the total height of the emulsion in the tube.

4.2.6.1.Rheological measurement

Thixotropic-loop test was performed using DV2T viscometer operating with spindle 18 (Brookfield, Middleborough, USA). Shear stress and viscosity versus the shear rate (2 – 80 s^-

^{1}) were plotted for concentrations of 0.5, 0.8 and 1 % w/w of AS-MFC dispersions. The viscosity of emulsions prepared with 10 % w/w MCT oil and 0.05 – 0.5 % w/w AS-MFC was also recorded at a fixed shear rate of 264 s^{-1}.

4.2.6.2.ζ-potential measurement

ζ-potential of emulsions was determined using electrophoresis instrument (Malvern Instruments Ltd., Worcestershire, UK). pH and ionic strength of prepared emulsions was adjusted to different levels of pH (2 - 9) or NaCl (0 – 200 mM) by adding appropriate amount of HCl, NaOH or NaCl solution. Samples were stored for 24 h before the measurement.

4.2.6.3.Microstructural analysis

The localization of AS-MFC at the oil-water interface was assessed using Confocal scanning laser microscopy (CSLM) (Leica DM6000B GmBH, Wetzlar, Germany). Prior to the observation, the fresh emulsions were stained using Congo red dye at a final concentration of 0.8 mg dye/ml. The added dye was thoroughly mixed with the emulsions, then the samples were incubated overnight in the dark at room temperature. Stained samples were then visualized by CLSM using an emission wavelength of 580 nm. Fluorescence was excited with 488 nm line and observation was carried out with 40x magnification and digital zoom-in when appropriate.

4.2.7. Statistical analysis

All experiments were conducted at least duplicate with a minimum 3 replicates, mean and standard deviation are reported in the current study.

4.3.Results and discussion

4.3.1. Characterization of argan shell fibers

Figure 18a shows the changes in FTIR spectra of AS-C and AS-MFC compared to AS-R to identify the changes in functional groups present in the samples. A broad vibration was observed in all samples in the 3600-3000 cm^{-1} region, this adsorption band is attributed to -OH groups found in lignocellulosic materials [81]. The peaks at 1739 cm^{-1} and 1039 cm^{-1} correspond to C=O groups in acetyl and uronic ester groups of hemicellulose [82]. The absence of the first one in the AS-C and AS-MFC confirms that the alkali treatment was effective at removing hemicellulose from argan shell cell wall corresponding to breaking C-O-C bound linking the monomers [111]. However, the formal peak remains present in all samples, this can be attributed to hemicellulose found strongly bound within the cellulose fibrils (Costa et al., 2018). The peak at 2900 cm^{-1} in the three analyzed samples correspond to the aliphatic C–H stretching of lignin, and cellulose [83]. In addition the adsorption band in the 1670-1540 cm^{-1} region is attributed to the aromatic C=C stretch, therefore, aromatic rings and conjugated carbonyl groups found in lignin structure remained in the treated samples [84]. Alkali and bleaching treatments did not enable the removal of all lignin found in argan cell wall, thus the peak remained present when using further mechanical treatment.

In this section, we assess the crystalline behavior of AS-R and the influence of treatment conditions on crystallinity index of AS-C and AS-MFC using wide angle XRD (Figure 18b). Distinctive peaks were observed at 16.0° and 22.0° two theta for all samples. These peaks correspond to cellulose I, the crystal form of native cellulose [112]. Upon alkali treatment the crystalline state of argan shell cellulose is expected to undergo polymorphic modification from cellulose I to cellulose II. This means that cellulose chains rearrange from parallel configuration (cellulose I) to antiparallel configuration (cellulose II) [113]. Mechanical

treatment on the other hand generates highly individualized cellulose nanofibers with smaller diameter [114]. The crystallinity index increases from 30% in the AS-R to 46% in AS-C, this further confirms the removal of non-crystalline hemicellulose and part of lignin due to alkali and bleaching treatments. However, after mechanical treatment crystallinity index drastically decreased to 23%, this might indicate that the mechanical treatment significantly induced intermolecular hydrogen bonds breakage in cellulose structure, causing the collapse of some crystalline domains. Isolation of MFC from sugarcane bagasse, prickly pear fruit peels and mangosteen rinds showed similar results in the decrease of crystallinity index with mechanical treatment [93,115,116].

Samples of argan shell fibers were examined by ^{13}C-CP/MAS NMR (Figure 18c). AS-R sample, lower figure, shows typical signals for raw biomass. Signals belonging to acetate (180, 20 ppm), aromatic region of lignin (120 ppm), methoxy group (55 ppm), and cellulose (104, 88,82,73,63 ppm) were detected [117]. The chemical shifts of 104 ppm and between 80 and 90 ppm are associated with C1 and C4, respectively. The cluster between 70 and 80 ppm is assigned to C2, C3 and C5. The region between 60 and 70 ppm is linked to C6 [118,119]. From the ^{13}C signals the region between 86 and 92 ppm is attributed to the crystalline domain of cellulose, whereas the region between 80 and 86 ppm is related to the amorphous domain of cellulose (Ek, Wormald, Östelius, Iversen, & Nyström, 1995). In the spectrum of AS-R we notice the presence of crystalline and amorphous peak at 88 and 81 ppm respectively. After chemical treatment, AS-C showed similar chemical shift in that region indicating that chemical treatment did not affect the crystallinity of the AS-MFC, thus, confirming the results of XRD. Finally, the C6 peak show a sharp peak at 63 ppm attributed to native cellulose I in AS-R, the chemical shifts of 61 ppm of chemically and mechanically treated samples confirms mercerization of cellulose I to an antiparallel configuration (cellulose II) [121].

Morphology and size distribution of argan shell MFC are presented in Figure 19 TEM analysis show that the fibers have a diameter of 48 ± 15 nm, however, when they entangle, they form a unit of 719 ± 88 nm diameter. The length of argan shell MFC is estimated to be 3 – 5 μm. The size distribution measured for a diluted dispersion of argan shell MFC in water allows a rapid estimation of the particle size of the sample. It seems that in accordance with the results of TEM, argan shell MFC contain small particles varying between 44 and 452 nm, AS-MFC entangle to form colloidal system with a second peak and sharp distribution in the range of 1.6 – 36 μm (Figure 19b). The results are similar to those reported by Iwamoto et al., 2005 for Kraft pulp treated mechanically, the research group reported a length of several micrometer and a diameter of 50 – 100 nm.

4.3.2. Effect of AS-MFC concentration on emulsion formation

1% AS-MFC versus MCT oil did not lead to a significant reduction in interfacial tension, hence, dynamic interfacial tension measurement reached 18 mN/m after 5 min from droplet formation (Figure 26). Therefore, in order to assess the effect of AS-MFC on emulsion formation we proceed by testing the effect of different concentrations of AS-MFC (0.05 – 1 % w/w) on volume mean diameter ($d_{4,3}$) (Figure 20 a). After 24 h storage with low AS-MFC concentration (0.05 % w/w), large droplets were obtained with a mean value $d_{4,3}$ = 28.77 ± 0.33 μm, however, the volume mean diameter gradually decreased when increasing AS-MFC concentrations. The decrease in droplet size is related to the availability of more particles allowing the stability of smaller droplets with higher interfacial area. When enough particles are available, the formulated oil droplet by high pressure homogenizer are stabilized immediately and are no longer prone to coalescence. Our results are in good agreement with previously reported Pickering emulsions stabilized using solid particles showing that droplet size of emulsions decreases with increasing the particles concentration in the continuous phase

[90,122]. However, they are different from those reported for MFC from mangosteen rind stabilized emulsions [94]. The authors report an increase in droplet size of emulsions with increasing MFC concentration and relate it to higher aspect ratio of MFC. Stability of emulsions against coalescence using different concentrations of AS-MFC was assessed by monitoring $d_{4,3}$ variation after 15 days storage at 25 °C. We confirmed that emulsions prepared with AS-MFC above 0.5 % w/w were stable toward coalescence. Furthermore, Figure 20b show the creaming index of the samples after a 1 and 15 days storage. Creaming index drastically decreased when increasing the AS-MFC concentration, thus, emulsion volume increased. The small size of emulsion droplets induce a higher volume of emulsion [123]. Overall, no oiling-off was observed in all emulsions after 15 days storage. Finally, it was also observed that the viscosity of emulsions increases sharply when increasing the MFC concentration. Increasing the thickening is known to enhance emulsions stability [88]. Therefore, increasing AS-MFC concentration generates higher viscosity of emulsions leading to stable emulsions during storage.

To further understand the mechanism of AS-MFC to stabilize emulsions, we conducted microscopic observations using CSLM. Staining AS-MFC using Congo red allows the visualization of the particles at the oil-water interface as well as in the continuous phase. Microscopic observations of two emulsions prepared by 0.1 % w/w AS-MFC (Figure 21a) and by 0.8 % w/w AS-MFC (Figure 21b) are reported. In both cases we can observe clearly the adsorption of MFC at the oil-water interface in a round-shaped fluorescence indicating the oil drop (Figure 21, white arrows), the size of this drops varies depending on the MFC concentration, which is in agreement with the results reported on droplet diameter ($d_{4,3}$). Another observation is the presence of free AS-MFC fibers in the continuous phase (Figure 21, colored arrows). These are more present in the high concentrated continuous phases. Basically, the availability of particles leads to the adsorption of AS-MFC on oil droplets in addition to an

interconnection between the non-adsorbed and adsorbed fibers creating a 3D network surrounding the oil droplets. Therefore, AS-MFC exabits excellent emulsion stability against coalescence via i) single adsorption on oil droplet ii) 3D network surrounding oil droplets. This is in good agreement with results reported previously of the enhanced stability of emulsions using MFC particles [124].

4.3.3. The relevance of MCT oil concentration on emulsion formation

In this section we discuss the effect of varying MCT oil content, from 5 % w/w to 80 % w/w at a constant AS-MFC concentration (1 % w/w) on emulsion formation. The reason behind conducting this experiment was to determine the concentration of the dispersed phase where full emulsification of oil is achieved. Figure 22a shows the effect of oil concentration on $d_{4,3}$ and CI. We observe two distinctive domains, the first one with oil mass fraction less than 30 % w/w where the droplet size is constant ($d_{4,3}$ = 12.4 $\pm$ 1.3 μm), nevertheless, the creaming index is decreasing to achieve 84 % of emulsion volume when we use 30 % w/w of oil. Above 50 % w/w of MCT oil, $d_{4,3}$ values gradually increased, and 92% of emulsion was achieved. Full emulsification was reached up to 70 % w/w oil content. Higher concentration of oil (i.e. 80 % w/w) induced emulsification failure and oiling off due to poor coverage of oil droplets by AS-MFC. Furthermore, droplet size distribution of emulsions confirms that with oil concentration above 50 % w/w, monomodal distribution is recorded (Figure 22b). The droplet size of emulsions varied between 27 and 160 μm when using 70 % w/w oil. The large mean droplet size can be explained by the limitations of AS-MFC to adsorb rapidly to the oil-water interface. Therefore, strong coalescence occurs due to the high number of oil droplets generated without a protective layer inhibiting coalescence during the homogenization. We can clearly state based on our results that the dispersed phase content influenced strongly the creaming of emulsions (Figure 22b,c). Creaming velocity is known to decrease with increasing droplet

concentration once a critical dispersed phase fraction has been exceeded [9]. In addition, the increase in packing fraction of oil droplets improves emulsion stability with respect to creaming, and, this can be achieved by increasing the oil content [125]. Results of CLSM confirms that with increasing the oil content up to 70 % w/w a clear close packing of oil droplets is observed (Figure 23d,e), and a strong 3D network was formed protecting oil droplets from coalescence. AS-MFC dispersed in water acts as a non-Newtonian fluid which has a shear-thinning behavior (Figure 25). We conclude from the CLSM results combined to the viscosity results of the continuous phase that AS-MFC adsorb to the oil-water interface leading the formation of Pickering emulsions. AS-MFC dispersions acts also as thickening agent exhibiting high apparent shear.

4.3.4. Effect of change in electrolytes and pH

In order to understand the importance of electrostatic interactions in AS-MFC stabilized emulsions, we proceed by measuring the electrical charge of oil droplets in different ionic environments. Figure 24a. shows pH dependent ζ-potential measurement of stabilized emulsions (50 % w/w MCT oil, 1 % w/w AS-MFC). Emulsion sample shows a high negative charge at high pH (pH 9) and gradually increase upon decreasing the pH of the emulsion sample to become positive (pH < 3). The surface charge of MFC is known to be dependent on the chemical treatments and the fiber source [126,127]. Alkali treatment used in this study facilitate the access to cellulose carboxyl groups. In addition, the bleaching treatment allows the oxidation of hydroxyl groups of cellulose for example at C6, it can also oxidize the glucoside bonds at C1 thus producing carboxyl groups [128,129]. An isoelectric point (IEP) between pH 3 and pH 4 was identified for AS-MFC, this result is slightly different from reported IEP for flax, hemp and cellulose fibers witch was ranging between pH 1.6 and pH 2.2 [130]. The swelling behavior due to the high polarity of cellulose fibers leads to the protonation of

carboxylic groups thus leading to the dramatic decrease of negative ζ-potential at low pH [131]. The contact angle of water on AS-MFC surface was 32 ± 4 ° shows a hydrophilic behavior of the particles (Figure 26b). Additionally, we tested the effect of ionic strength (0 - 200 mM NaCl) on ζ-potential of emulsion droplets (Figure 24b). Our results show a gradual increase in the magnitude of ζ-potential with increasing the concentration of NaCl from -18 mV to -9.5 mV, this behavior confirms the availability of charged $-COO^-$ groups on the surface of oil droplets and their electrostatic interaction with counter-ions Na^+. Through these results we conclude that emulsions prepared with AS-MFC and MCT oil are stabilized by the adsorption of AS-MFC fibers at the oil water interface, thus leading to the formation of Pickering emulsion inducing electrostatic repulsions.

4.4.Conclusion

In summary, successful preparation of MFC from argan shell was demonstrated with defined chemical and morphological characteristics. Long-term Pickering emulsions were stabilized exclusively by AS-MFC with limited creaming when the concentration of particles in the continuous phase is ≥ 0.5 % w/w. Full emulsification of oil droplets without phase separation were achieved when using 70 % w/w of oil stabilized using 1 % w/w MFC. We confirm via CLSM that the main stability mechanism is related to the adsorption of AS-MFC particles to the oil-water interface thus leading to Pickering type emulsions formation. Excess of AS-MFC particles induce 3D network formation surrounding oil droplet thus inhibiting oil movement and collision. Furthermore, close packing was observed when highly concentrated emulsions were formulated. Finally, electrostatic repulsions between adsorbed AS-MFC particles were also reported to enhance the stability. This study provided a new source of MFC from agricultural waste with excellent emulsifying properties which have great potential for application in food, cosmetics, and pharmaceutical industries.

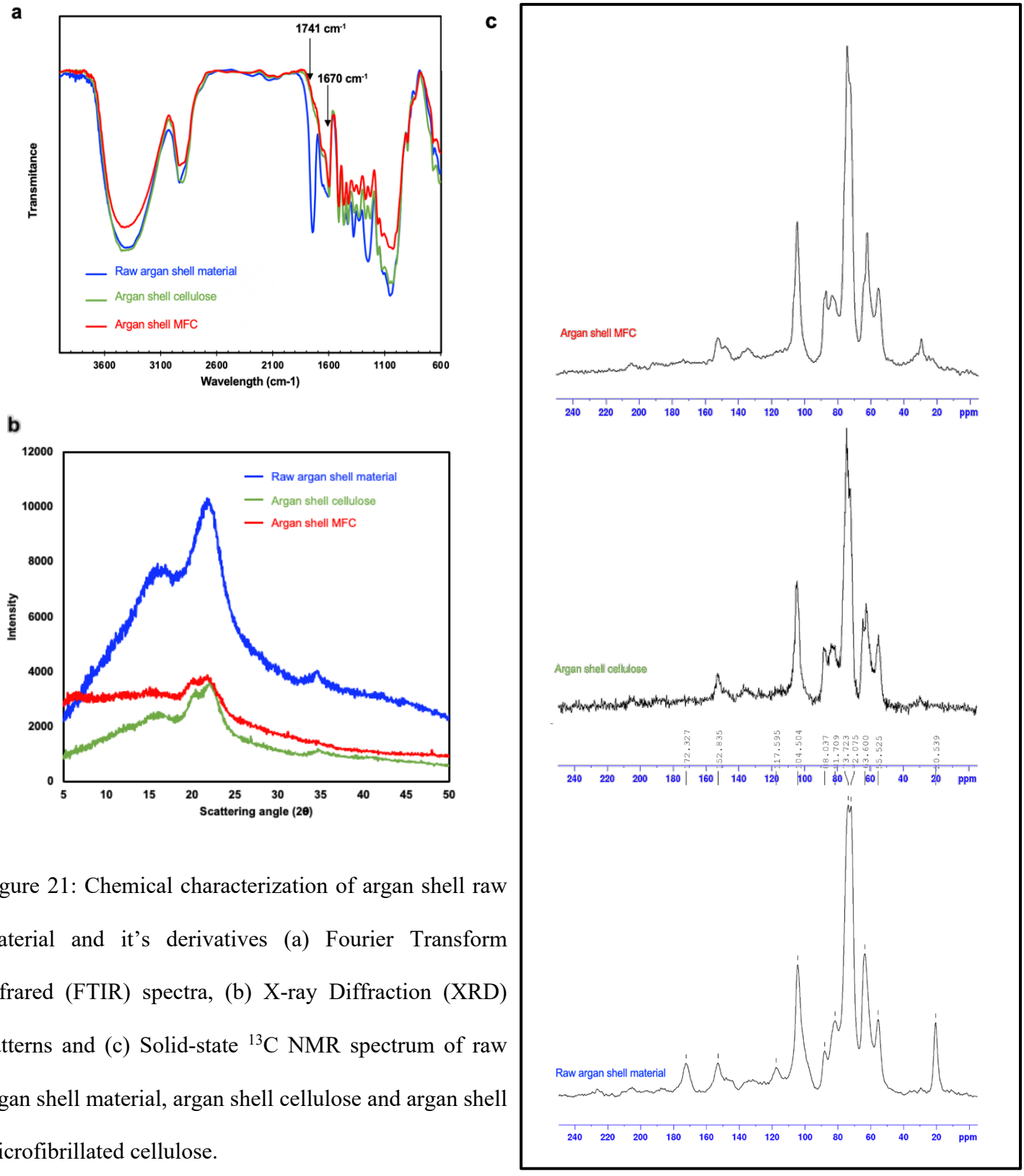

Figure 21: Chemical characterization of argan shell raw material and it's derivatives (a) Fourier Transform Infrared (FTIR) spectra, (b) X-ray Diffraction (XRD) patterns and (c) Solid-state ^{13}C NMR spectrum of raw argan shell material, argan shell cellulose and argan shell microfibrillated cellulose.

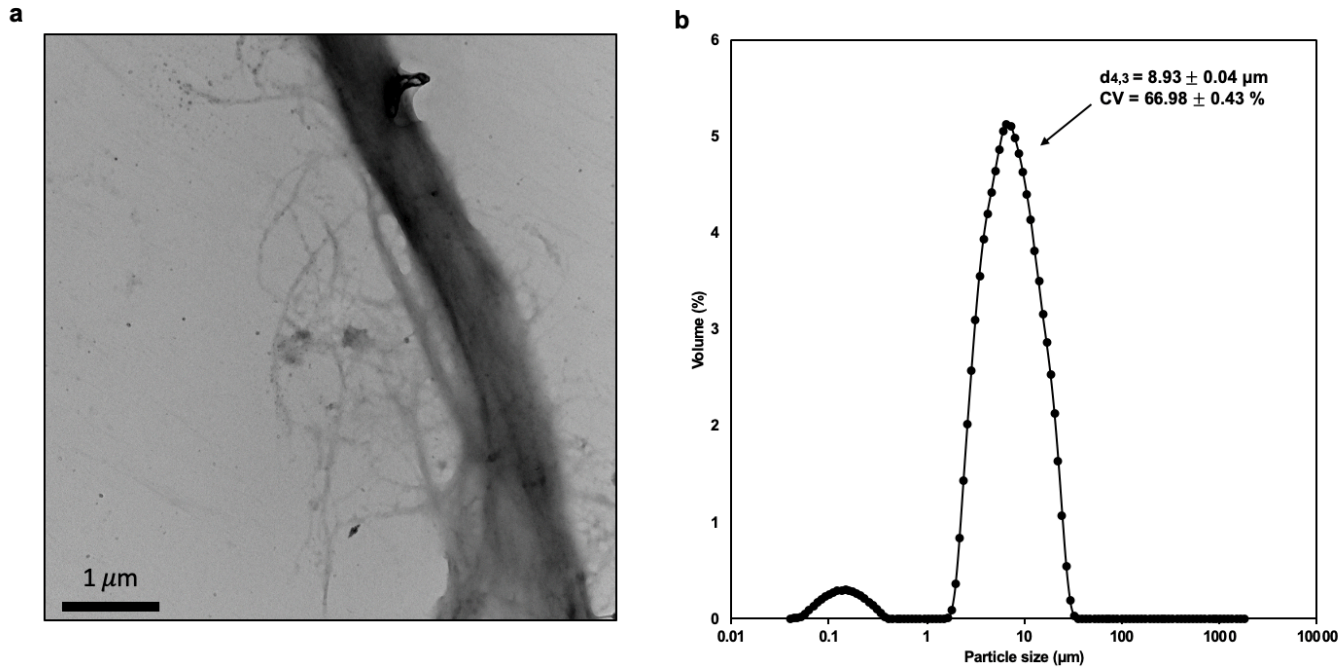

Figure 22: (a) Transmission electron micrograph from diluted suspension of argan shell microfibrillated cellulose and (b) particle size distribution using laser diffraction particle size analyzer.

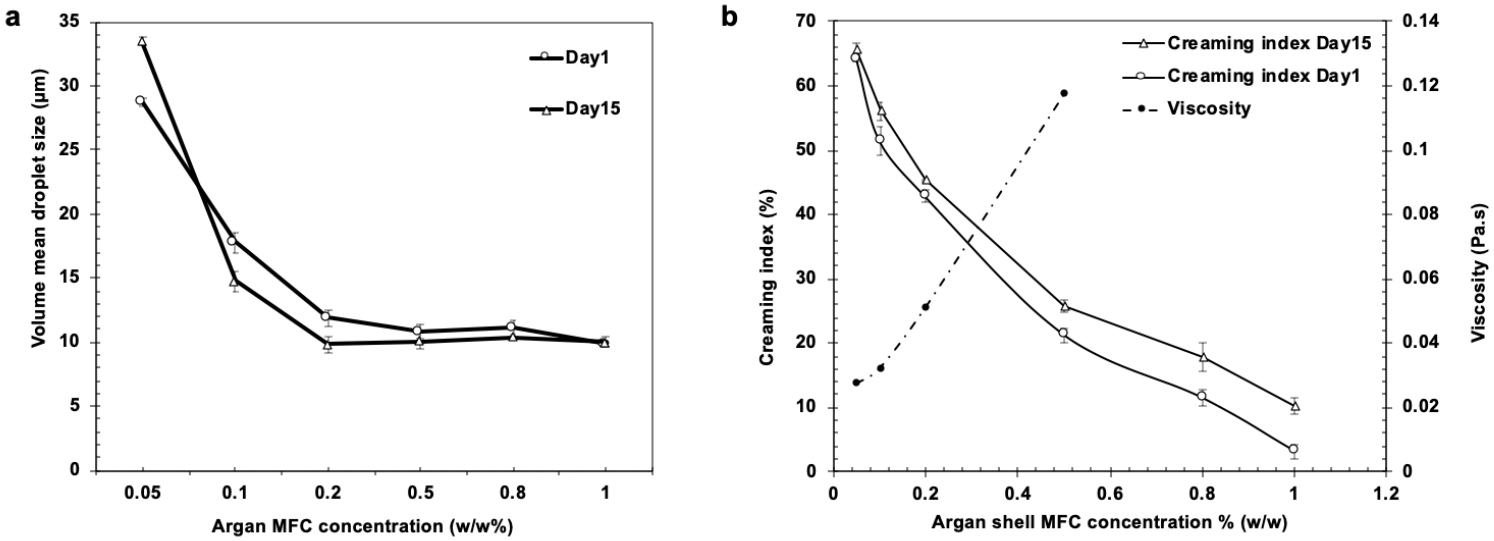

Figure 23: Effect of argan shell microfibrillated cellulose concentration on (a) volume mean droplet size (d4,3) and (b) creaming index and viscosity of O/W emulsions (10% w/w MCT oil) under standardized conditions (100 MPa, 4 Passes) stored at 25 °C for 15 days.

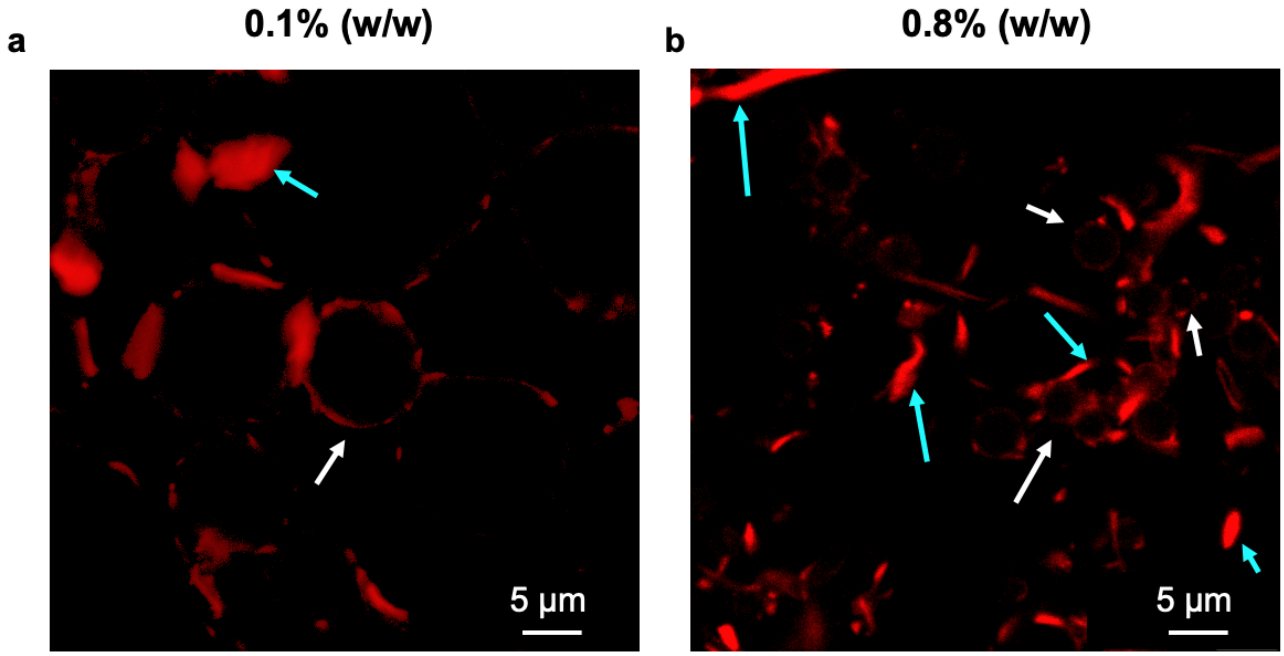

Figure 24: Confocal laser scanning micrographs of fresh O/W emulsions (10% w/w MCT oil) stabilized by (a) 0.1% w/w MFC or (b) 0.8% w/w MFC in aqueous phase).

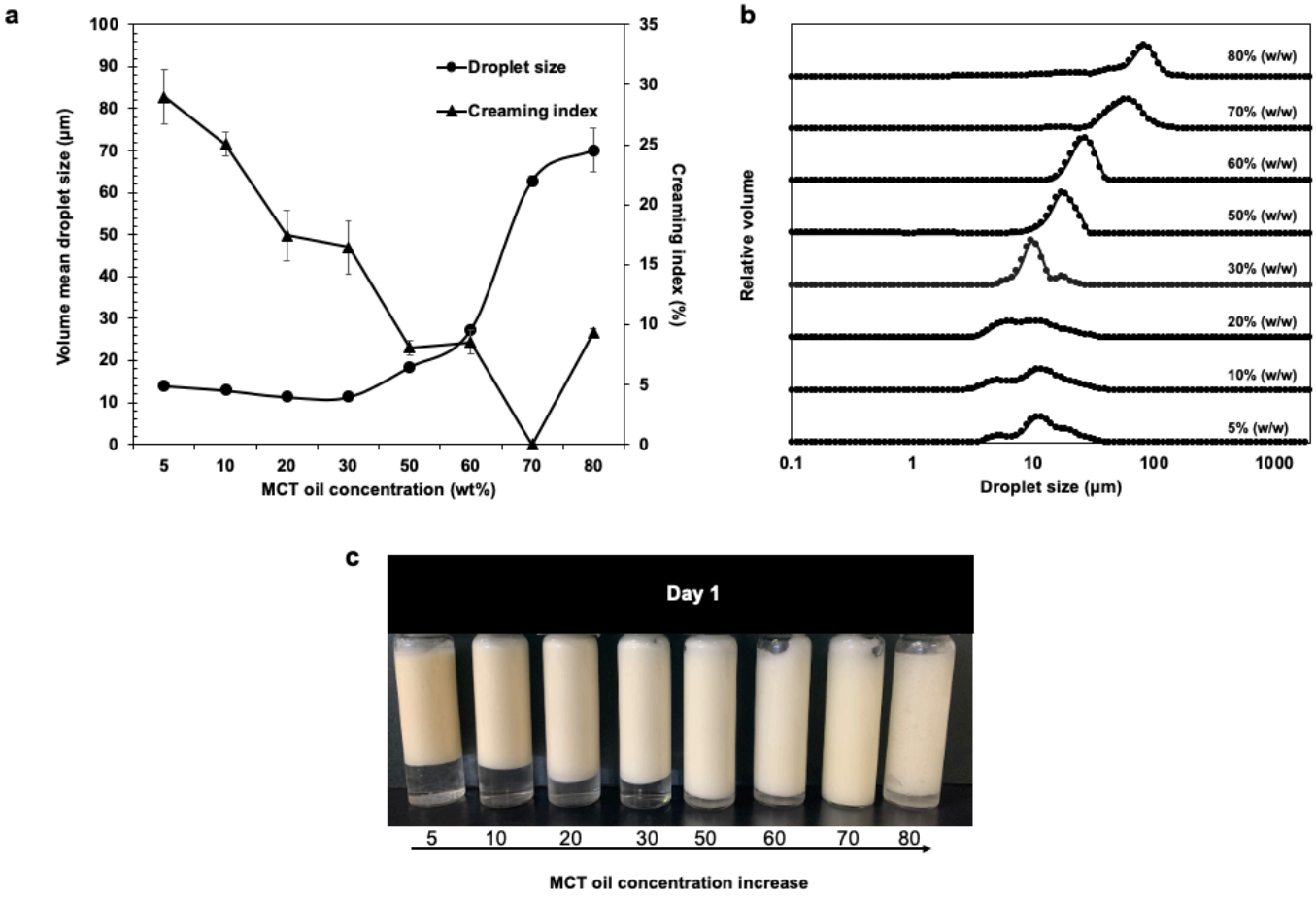

Figure 25: Effect of oil concentration on (a) volume mean droplet size ($d_{4,3}$) and creaming index (b) size distribution and (c) visual aspect of O/W emulsions prepared by (5 – 80% w/w MCT oil, 1% w/w MFC in aqueous phase)

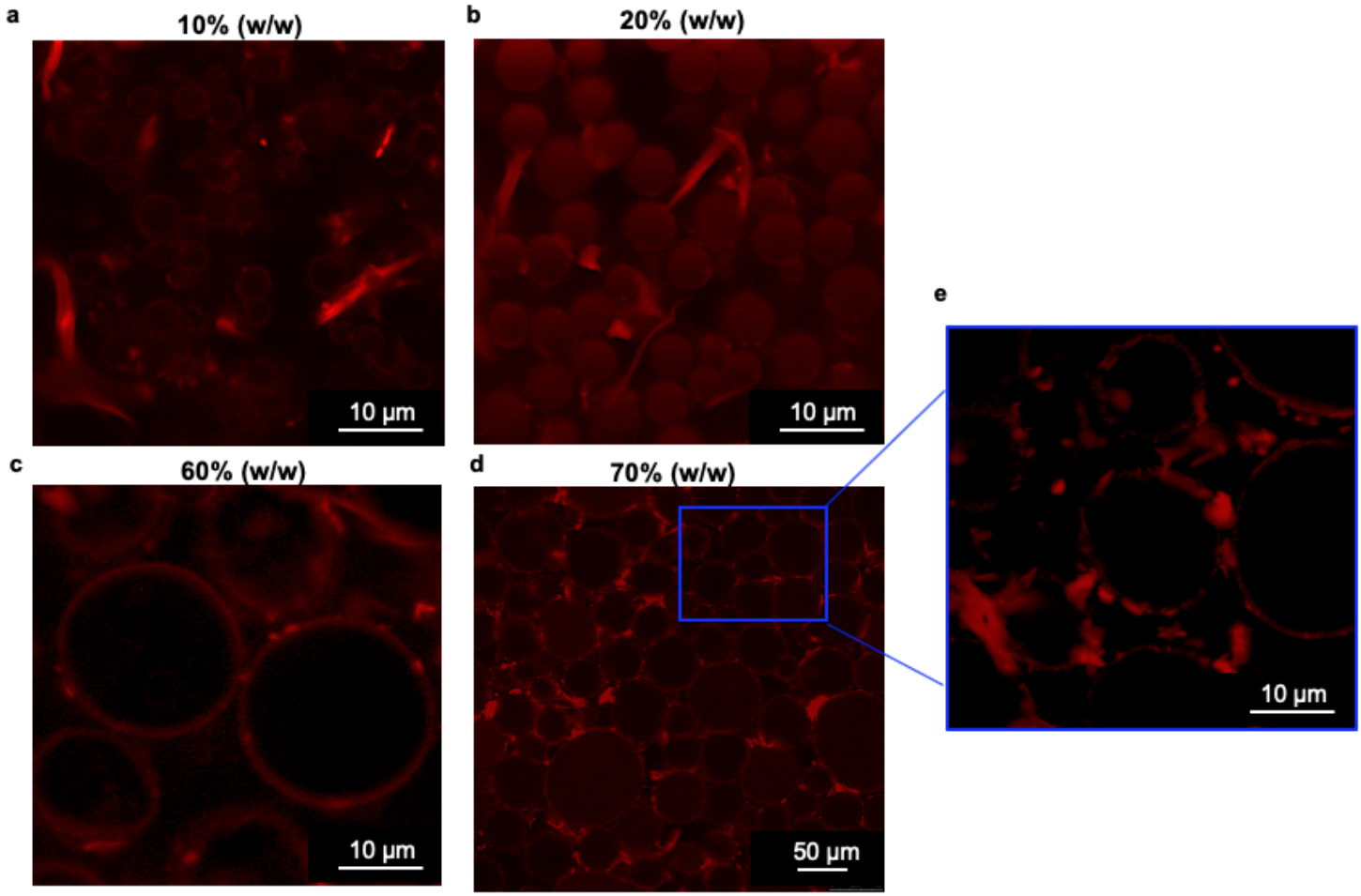

Figure 26: Confocal laser scanning micrographs of fresh O/W emulsions stabilized using 1% w/w MFC in aqueous phase and a concentration of MCT oil of (a) 10% w/w (b) 20% w/w (c) 60% w/w (d) 70% w/w (e) digital zoom in of blue square.

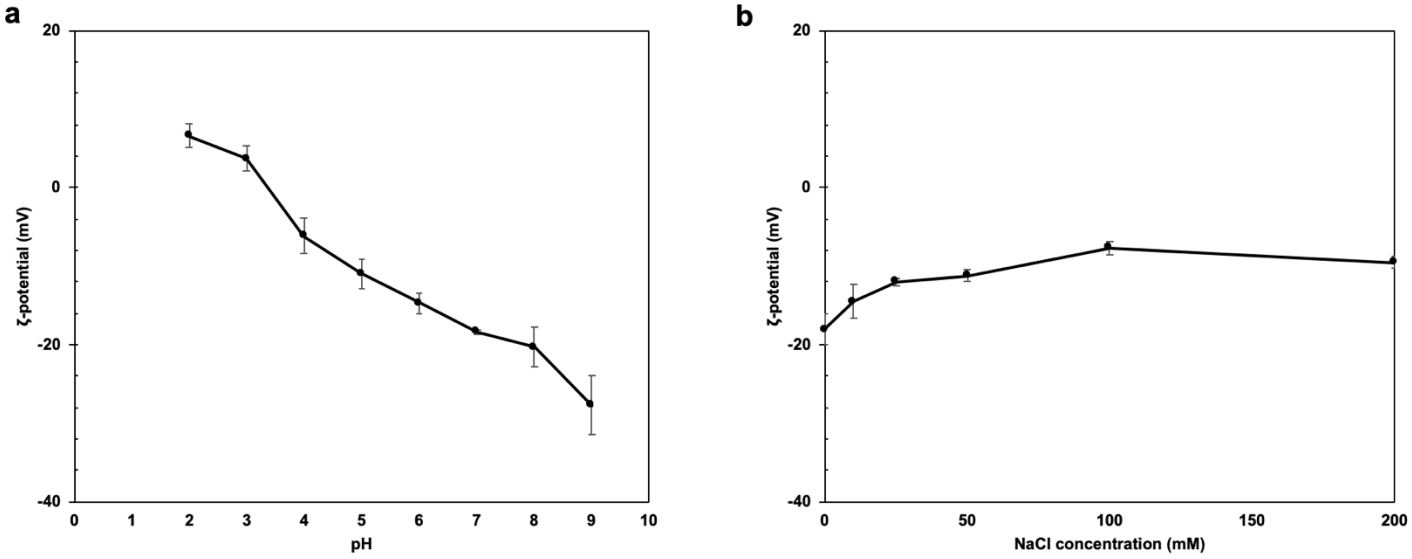

Figure 27: Effects of (a) pH and (b) NaCl concentration on ζ-potential of argan shell microfibrillated cellulose stabilized O/W emulsions (50% w/w MCT oil, 1% w/w MFC in aqueous phase).

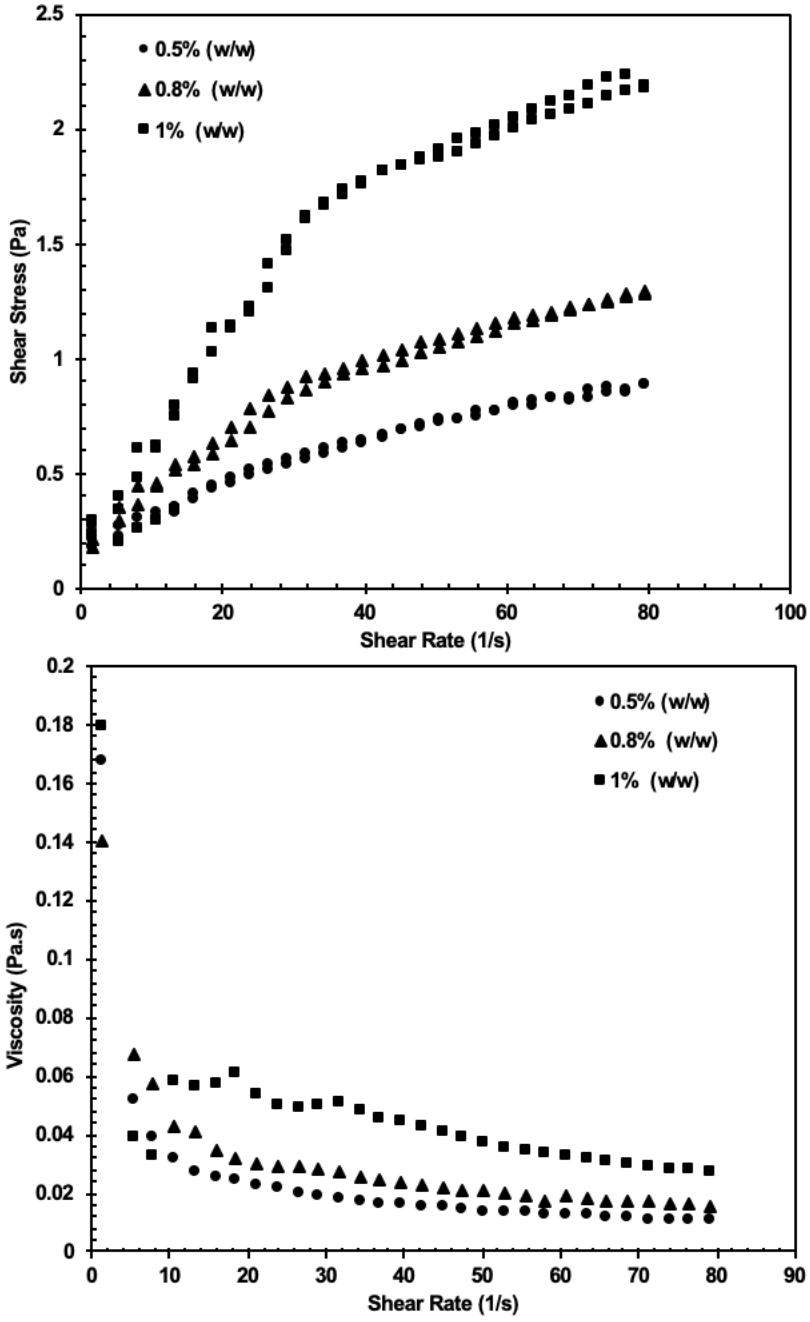

Figure 28: Shear stress and viscosity as a function of shear rate of argan shell microfibrillated dispersions containing different concentration 0.5 – 1% w/w of particles.

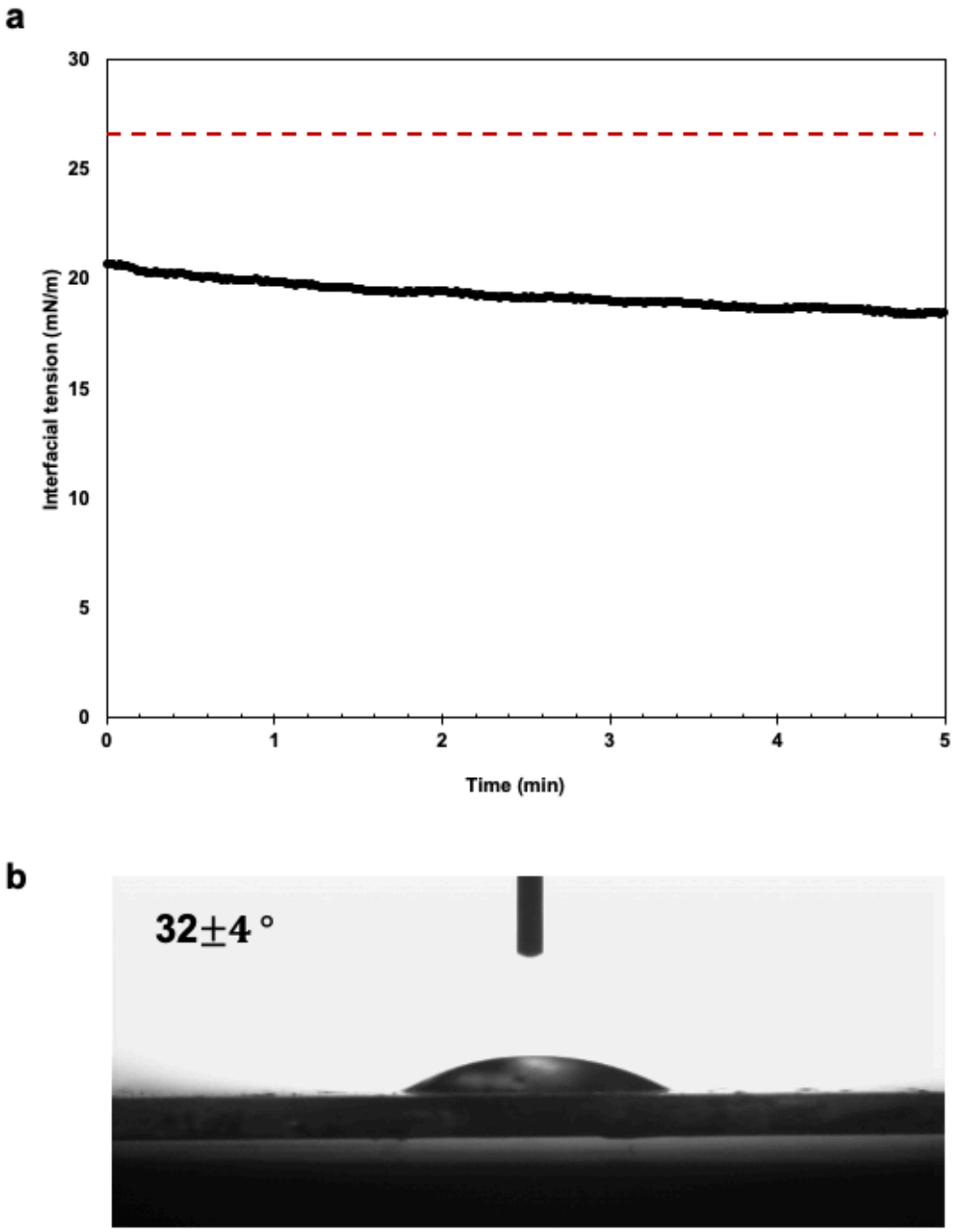

Figure 29: (a) Dynamic interfacial tension of 1% w/w argan shell microfibrillated cellulose in water against MCT oil and (b) contact angle of one drop of water on 1% w/w argan shell microfibrillated cellulose film.

Chapter 5 – General conclusion and perspectives

The utilization of natural ingredients derived from biomass is a promising path toward sustainability. In recent years, consumers are more aware about the resources and ingredients formulating their products and the challenges facing today's food engineering field is to provide healthy sustainable products while regaining consumer trust. Sustainability approach is based on three main pillars, environment, social and economic. For a product to be sustainable, it has to satisfy those three pillars. In addition, the development of functional food, dietary supplements, nutraceuticals and product reformulation for favorable health impact (salt reduction, calorie reduction) for an aging population is also a challenge toward healthiness. Finally, to regain consumer trust, food formulations require the incorporation of natural ingredients and providing clean label products.

Considering the above-mentioned aspects, the choice of argan oil industry made a lot of sense for this study to tackle the challenges of product formulation. This industry is unique to the Moroccan country because the species *Argania spinosa* is endemic to its desert. Argan tree plays an important environmental role in the region, because of its high resistance to environmental stress (water draught, arid land) therefore procuring a barrier to desertification and erosion of the soil. Argan plays also an important socio-economical role in the region, considering that Argan is a wild species that have been present for centuries in southwestern Morocco. Today, 2-3 million people rely on argan tree as a source of income, in fact, all the parts of the tree are used today by the local population. The main product of argan fruit is the oil, however, this product represents only 3% of the total mass of the fruit. The remaining are, agan press cake, argan pulp and argan shell that are considered by-products and are used by the locals as cattle feed (press care and pulp) or burned for heat generation (shell).

Argan shell is a lignocellulosic biomass rich in fibers, which led to few research centered toward this material to prepare composites or to be used as biochar [73–76]. However, considering that argan oil made a real breakthrough to international markets (argan oil is known for its unique cosmetic and edible features) , this thesis was inspired to valorize argan by-product (argan shell) within food, cosmetic or pharmaceutic industries. By providing new compounds acting as natural emulsifiers.

Emulsifiers global market represents 8.4 billion $, this market is divided between food market (30%), cosmetics (20%) and pharmaceutic and agrochemicals (50%). This market is expected to grow by 5.6 points in 2050. Mostly, when considering emulsifiers, it is more common to find a synthetic emulsifier used rather than a natural one. In fact, synthetic emulsifiers represent 70% of emulsifiers against only 30% of natural emulsifiers in the global market. The reason behind this difference is the inhomogeneous and high cost of natural emulsifiers when compared to their synthetic counterparts. Therefore, industrial are less attracted to their utilization when formulating products. But this trend is now changing, and industrials and manufacturers have to adapt to the new aspirations of consumers, thus, providing acceptable products for them to use.

This thesis highlighted an exhaustive extraction of natural compounds from argan shell biomass and applied them in the formulation of O/W emulsions. The first extraction consisted on solid-liquid extraction using aqueous-ethanol as solvent. Five extracts were characterized in this study then compared for their emulsifying performance.

The obtained residue of aqueous-ethanol extraction was used for the preparation and purification of cellulose. The pulping process consisted of alkali treatment and we studied the effect of four different concentration of sodium hydroxide on argan shell purified cellulose.

After reaching satisfying properties of argan shell cellulose microfibrillated cellulose was prepared using mechanical disintegration.

The exhaustive extraction of surface-active compounds and microfibrillated cellulose from argan shell led the utilization of those compounds separately to formulate and stabilize O/W emulsions. Both extracts were capable at adsorbing at the oil-water interface and we proved two distinctive mechanisms of emulsion stabilization. The first mechanism was the surface-activity of saponin, protein and polyphenol rich extract that was able to reduce the interfacial tension between oil and water phases thus leading to the formation of submicron emulsions that were stabilized via electrostatic and steric repulsions. The second mechanism that was elucidated in this thesis is emulsion stabilization by solid particles (i.e. microfibrillated cellulose from argan shell) thus leading to Pickering emulsions.

Taking a look back at the scientific evidence provided in this thesis, we predict an added value of argan shell for food, cosmetic or pharmaceutic industries. However, more research is required regarding toxicity of the compounds extracted from argan shell. In addition, for an industrial use, an economical based study is required for scaling up the production and reaching homogeneous compounds ready for utilization by the above-mentioned industries.

Besides the industrial application of surface-active compounds and microfibrillated cellulose, there are many scientific topics in which argan shell may offer new research opportunities. First, the chemical stability of bio-active compounds encapsulated by surface-active compounds or microfibrillated cellulose could be elucidated. Next, digestive stability of emulsions can be studied. Furthermore, it would be interesting to study the interfacial composition of emulsions stabilized by argan shell extracts. Another intersting topic would be the complexation of microfibrillated cellulose and surface-active compounds to deliver enhanced emulsifying properties.

On the same path of preparation of microfibrillated cellulose, the preparation of cellulose nanocrystals and the identification of its properties could be an interesting for research and development of functional materials from this biomass.

References

[1] S.U. Pickering, Pickering : Emulsions, J. Chem. Soc. Trans. (1907) 2001–2021.

[2] P. Becher, Food Emulsions An Introduction, Microemulsions Emuls. Foods. (1991) 1–6. http://pubs.acs.org/doi/pdfplus/10.1021/bk-1991-0448.ch001.

[3] W. Ostwald, Beiträge zur Kenntnis der Emulsionen, Zeitschrift Für Chemie Und Ind. Der Kolloide. 6 (1910) 103–109. https://doi.org/10.1007/BF01465754.

[4] J.H. Schulman, J.B. Montagne, Formation of Microemulsions by Amino Alkyl Alcohols, Langmuir. (1961).

[5] D.J. McClements, C.E. Gumus, Natural emulsifiers — Biosurfactants, phospholipids, biopolymers, and colloidal particles: Molecular and physicochemical basis of functional performance, Adv. Colloid Interface Sci. 234 (2016) 3–26. https://doi.org/10.1016/j.cis.2016.03.002.

[6] D.J. McClements, E. Decker, Interfacial Antioxidants: A Review of Natural and Synthetic Emulsifiers and Coemulsifiers That Can Inhibit Lipid Oxidation, J. Agric. Food Chem. 66 (2018) 20–25. https://doi.org/10.1021/acs.jafc.7b05066.

[7] D.J. McClements, L. Bai, C. Chung, Recent Advances in the Utilization of Natural Emulsifiers to Form and Stabilize Emulsions, (2017) 1–32. https://doi.org/10.1146/annurev-food-030216-030154.

[8] A. Benichou, A. Aserin, N. Garti, Double emulsions stabilized with hybrids of natural polymers for entrapment and slow release of active matters, Adv. Colloid Interface Sci. 108–109 (2004) 29–41. https://doi.org/10.1016/j.cis.2003.10.013.

[9] D.J. McClements, Food Emulsions, Third, CRC Press, 2016. https://doi.org/10.1201/b18868.

[10] D.J. McClements, Emulsion Design to Improve the Delivery of Functional Lipophilic Components, Annu. Rev. Food Sci. Technol. 1 (2010) 241–269. https://doi.org/10.1146/annurev.food.080708.100722.

[11] J. Thomas, The Global Food Additives Market, 6th Editio, Food Research Leatherhead, 2014.

[12] M. Andres-Brull, The Quest for Natural Emulsifiers Evaluating the Effectiveness of Natural Emulsifiers, 2016.

[13] B. Ozturk, D.J. McClements, Progress in natural emulsifiers for utilization in food emulsions, Curr. Opin. Food Sci. 7 (2016) 1–6. https://doi.org/10.1016/j.cofs.2015.07.008.

[14] E. Dickinson, Towards more natural emulsifiers, Trends Food Sci. Technol. 4 (1993) 330–334.

[15] S. Boostani, S.M.H. Hosseini, G. Yousefi, M. Riazi, A.M. Tamaddon, P. Van der Meeren, The stability of triphasic oil-in-water Pickering emulsions can be improved by physical modification of hordein- and secalin-based submicron particles, Food Hydrocoll. 89 (2019) 649–660. https://doi.org/10.1016/j.foodhyd.2018.11.035.

[16] Y. Yang, Z. Fang, X. Chen, W. Zhang, Y. Xie, Y. Chen, Z. Liu, W. Yuan, An overview of pickering emulsions: Solid-particle materials, classification, morphology, and applications, Front. Pharmacol. 8 (2017) 1–20. https://doi.org/10.3389/fphar.2017.00287.

[17] N.G. Eskandar, S. Simovic, C.A. Prestidge, Synergistic effect of silica nanoparticles and charged surfactants in the formation and stability of submicron oil-in-water emulsions, Phys. Chem. Chem. Phys. 9 (2007) 6426–6434. https://doi.org/10.1039/b710256a.

[18] Z.G. Cui, C.F. Cui, Y. Zhu, B.P. Binks, Multiple phase inversion of emulsions stabilized by in situ surface activation of CaCO 3 nanoparticles via adsorption of fatty acids, Langmuir. 28 (2012) 314–320. https://doi.org/10.1021/la204021v.

[19] C.P. Whitby, D. Fornasiero, J. Ralston, Structure of oil-in-water emulsions stabilised by silica and hydrophobised titania particles, J. Colloid Interface Sci. 342 (2010) 205–209. https://doi.org/10.1016/j.jcis.2009.10.068.

[20] I. Capron, B. Cathala, Surfactant-free high internal phase emulsions stabilized by cellulose nanocrystals, Biomacromolecules. 14 (2013) 291–296. https://doi.org/10.1021/bm301871k.

[21] Z. Charrouf, D. Guillaume, Secondary metabolites from Argania spinosa (L.) Skeels, Phytochem. Rev. 1 (2002) 345–354. https://link.springer.com/content/pdf/10.1023%2FA%3A1026030100167.pdf (accessed June 29, 2018).

[22] A. Karmaoui, Ecosystem Services of the Argan Forest , the Current State and Trends, 8 (2016) 1–13. https://doi.org/10.9734/AIR/2016/21353.

[23] G. Lizard, Y. Filali-Zegzouti, A. El Midaoui, Benefits of Argan Oil on Human Health—May 4–6 2017, Errachidia, Morocco, Int. J. Mol. Sci. 18 (2017) 1383. https://doi.org/10.3390/ijms18071383.

[24] F. Zahrae, A. Benali, M. Rachid, K. El, E. Maadoudi, M. Bouksaim, A. Essamri, Typical characterization of argane pulp of various Moroccan areas : A new biomass for the second generation bioethanol production, J. Saudi Soc. Agric. Sci. (2018). https://doi.org/10.1016/j.jssas.2018.09.004.

[25] B. Bouzemouri, Colloque International L'arganier : levier du développement humain du milieu rural marocain, in: Problématique La Conserv. Du Développement l'arganeraie Benhammou, Rabat, 2007: pp. 15–19.

http://www.biodiv.be/maroc/biodiversity/ecosyst/les-arganeraies/larganier-levier-de-developpement-humain-du.

[26] H. El Monfalouti, Z. Charrouf, S. Belviso, D. Ghirardello, Analysis and antioxidant capacity of the phenolic compounds from argan fruit (Argania spinosa (L .) Skeels), Eur. J. Lipid Sci. Technol. (2012) 446–452. https://doi.org/10.1002/ejlt.201100209.

[27] A. Alaoui, Z. Charrouf, M. Soufiaoui, V. Carbone, A. Malorni, C. Pizza, S. Piacente, Triterpenoid saponins from the shells of Argania spinosa seeds, J. Agric. Food Chem. 50 (2002) 4600–4603. https://doi.org/10.1021/jf0200117.

[28] L. Mao, Y.H. Roos, C.G. Biliaderis, S. Miao, Food Emulsions as Delivery Systems for Flavor Compounds — A Review, Crit. Rev. Food Sci. Nutr. 8398 (2015). https://doi.org/10.1080/10408398.2015.1098586.

[29] G.P. Savage, Saponins, Encycl. Food Sci. Nutr. (Second Ed. (2003) 5095–5098. https://doi.org/10.1016/B0-12-227055-X/01402-4.

[30] Y. Yang, M.E. Leser, A.A. Sher, D.J. McClements, Formation and stability of emulsions using a natural small molecule surfactant: Quillaja saponin (Q-Naturale®), Food Hydrocoll. 30 (2013) 589–596. https://doi.org/10.1016/j.foodhyd.2012.08.008.

[31] D. Kregiel, J. Berlowska, I. Witonska, H. Antolak, C. Proestos, M. Babic, L. Babic, B. Zhang, Additional, Saponin-Based, Biological-Active Surfactants from Plants, 2017. https://doi.org/10.5772/68062.

[32] T. Ralla, H. Salminen, M. Edelmann, C. Dawid, T. Hofmann, J. Weiss, Stability of Emulsions Using a New Natural Emulsifier: Sugar Beet Extract (Beta vulgaris L.), Food Biophys. 12 (2017) 269–278. https://doi.org/10.1007/s11483-017-9482-7.

[33] T. Ralla, H. Salminen, M. Edelmann, C. Dawid, T. Hofmann, J. Weiss, Oat bran extract (Avena sativa L.) from food by-product streams as new natural emulsifier, Food Hydrocoll. 81 (2018) 253–262. https://doi.org/10.1016/j.foodhyd.2018.02.035.

[34] T. Ralla, H. Salminen, J. Tuosto, J. Weiss, Formation and stability of emulsions stabilised by Yucca saponin extract, Int. J. Food Sci. Technol. (2017) 1–8. https://doi.org/10.1111/ijfs.13715.

[35] T. Ralla, H. Salminen, T. Wolfangel, M. Edelmann, C. Dawid, T. Hofmann, J. Weiss, Value addition of red beet (Beta vulgaris L.) by-products: Emulsion formation and stability, Int. J. Food Sci. Technol. (2018) 1–7. https://doi.org/10.1111/ijfs.13886.

[36] N. Taarji, C.A. Rabelo da Silva, N. Khalid, C. Gadhi, A. Hafidi, I. Kobayashi, M.A. Neves, H. Isoda, M. Nakajima, Formulation and stabilization of oil-in-water nanoemulsions using a saponins-rich extract from argan oil press-cake, Food Chem. 246 (2018) 457–463. https://doi.org/10.1016/j.foodchem.2017.12.008.

[37] D. Guillaume, Z. Charrouf, Saponines et métabolites secondaires de l'arganier (Argania, Cah. Agric. 14 (2005) 509–516.

[38] Z. bao Xiang, C. hong Tang, G. Chen, Y. song Shi, Studied On Corlorimetric Determination Of Oleanolic Acid In Chinese Quince, Nat. Prod. Res. Dev. 4 (2001).

[39] F. Mariotti, D. Tomé, P.P. Mirand, Converting nitrogen into protein - Beyond 6.25 and Jones' factors, Crit. Rev. Food Sci. Nutr. 48 (2008) 177–184. https://doi.org/10.1080/10408390701279749.

[40] V.L. Singleton, R. Orthofer, R.M. Lamuela-Raventós, Analysis of total phenols and other oxidation substrates and antioxidants by means of folin-ciocalteu reagent, Methods Enzymol. 299 (1998) 152–178. https://doi.org/10.1016/S0076-6879(99)99017-1.

[41] C.Y. Cheok, H.A.K. Salman, R. Sulaiman, Extraction and quantification of saponins: A review, Food Res. Int. 59 (2014) 16–40. https://doi.org/10.1016/j.foodres.2014.01.057.

[42] T. Van Ngo, C.J. Scarlett, M.C. Bowyer, P.D. Ngo, Q. Van Vuong, Impact of Different Extraction Solvents on Bioactive Compounds and Antioxidant Capacity from the Root of *Salacia chinensis* L., J. Food Qual. 2017 (2017) 1–8. https://doi.org/10.1155/2017/9305047.

[43] S. Gafner, C. Bergeron, M.M. McCollom, L.M. Cooper, K.L. McPhail, W.H. Gerwick, C.K. Angerhofer, Evaluation of the Efficiency of Three Different Solvent Systems to Extract Triterpene Saponins from Roots of Panax quinquefolius Using High-Performance Liquid Chromatography, J. Agric. Food Chem. 52 (2004) 1546–1550. https://doi.org/10.1021/jf0307503.

[44] S.R. Ko, S.C. Kim, K.J. Choi, Extract yields and saponin contents of red ginseng extracts prepared with various concentrations of ethanol, Korean J. Pharmacogn. 23 (1992) 24–28.

[45] Y. Shishikura, S. Khokhar, B.S. Murray, Effects of tea polyphenols on emulsification of olive oil in a small intestine model system, J. Agric. Food Chem. 54 (2006) 1906–1913. https://doi.org/10.1021/jf051988p.

[46] Ö. Guclu-Ustundag, G. Mazza, Saponins: Properties, applications and processing, Crit. Rev. Food Sci. Nutr. 47 (2007) 231–258. https://doi.org/10.1080/10408390600698197.

[47] Q.D. Do, A.E. Angkawijaya, P.L. Tran-Nguyen, L.H. Huynh, F.E. Soetaredjo, S. Ismadji, Y.H. Ju, Effect of extraction solvent on total phenol content, total flavonoid content, and antioxidant activity of Limnophila aromatica, J. Food Drug Anal. 22 (2014) 296–302. https://doi.org/10.1016/j.jfda.2013.11.001.

[48] S. Tan, C. Stathopoulos, S. Parks, P. Roach, An Optimised Aqueous Extract of Phenolic Compounds from Bitter Melon with High Antioxidant Capacity, Antioxidants. 3 (2014) 814–829. https://doi.org/10.3390/antiox3040814.

[49] T. Ralla, E. Herz, H. Salminen, M. Edelmann, C. Dawid, T. Hofmann, J. Weiss, Emulsifying Properties of Natural Extracts from Panax ginseng L, Food Biophys. 12 (2017) 479–490. https://doi.org/10.1007/s11483-017-9504-5.

[50] T. Ralla, H. Salminen, M. Edelmann, C. Dawid, T. Hofmann, J. Weiss, Sugar Beet Extract (Beta vulgaris L.) as a New Natural Emulsifier: Emulsion Formation, J. Agric. Food Chem. 65 (2017) 4153–4160. https://doi.org/10.1021/acs.jafc.7b00441.

[51] R. Pichot, F. Spyropoulos, I.T. Norton, Competitive adsorption of surfactants and hydrophilic silica particles at the oil – water interface : Interfacial tension and contact angle studies, J. Colloid Interface Sci. 377 (2012) 396–405. https://doi.org/10.1016/j.jcis.2012.01.065.

[52] C.J. Beverung, C.J. Radke, H.W.U. Blanch, Protein adsorption at the oil/water interface : characterization of adsorption kinetics by dynamic interfacial tension measurements, Biophys. Chem. 81 (1999) 59–80.

[53] S. Böttcher, J. Keppler, S. Drusch, Mixtures of Quillaja saponin and beta-lactoglobulin at the oil/water-interface: adsorption, interfacial rheology and emulsion properties, Colloids Surfaces A Physicochem. Eng. Asp. 518 (2017) 46–56. https://doi.org/10.1016/j.colsurfa.2016.12.041.

[54] L.A. Pugnaloni, E. Dickinson, R. Ettelaie, A.R. Mackie, P.J. Wilde, Competitive adsorption of proteins and low-molecular-weight surfactants: Computer simulation and microscopic imaging, Adv. Colloid Interface Sci. 107 (2004) 27–49. https://doi.org/10.1016/j.cis.2003.08.003.

[55] X. Xu, Q. Sun, D.J. McClements, Enhancing the formation and stability of emulsions using mixed natural emulsifiers : Hydrolyzed rice glutelin and quillaja saponin, Food Hydrocoll. 89 (2019) 396–405. https://doi.org/10.1016/j.foodhyd.2018.11.020.

[56] M. Rámirez, J. Bullón, J. Andérez, I. Mira, J.-L. Salager, Drop Size Distribution Bimodality and Its Effect on O / W Emulsion Viscosity, J. Dispers. Sci. Technol. 23(1–3) (2002) 309–321. https://doi.org/10.1080/01932690208984207 To.

[57] D.J. McClements, S.M. Jafari, Improving emulsion formation, stability and performance using mixed emulsifiers: A review, Adv. Colloid Interface Sci. 251 (2018) 55–79. https://doi.org/10.1016/j.cis.2017.12.001.

[58] D.J. McClements, Comments on viscosity enhancement and depletion flocculation by polysaccharides, Food Hydrocoll. 14 (2000) 173–177. https://doi.org/S0268-005X(99)00065-X.

[59] Á. Bravo-núñez, M. Golding, T.K. Mcghie, M. Gómez, L. Matía-merino, Emulsification properties of garlic aqueous extract, Food Hydrocoll. 93 (2019) 111–119. https://doi.org/10.1016/j.foodhyd.2019.02.029.

[60] J.N. Losso, A. Khachatryan, M. Ogawa, J.S. Godber, F. Shih, Random centroid optimization of phosphatidylglycerol stabilized lutein-enriched oil-in-water emulsions at acidic pH, Food Chem. 92 (2005) 737–744. https://doi.org/10.1016/j.foodchem.2004.12.029.

[61] I. Roland, G. Piel, L. Delattre, B. Evrard, Systematic characterization of oil-in-water

emulsions for formulation design, Int. J. Pharm. 263 (2003) 85–94. https://doi.org/10.1016/S0378-5173(03)00364-8.

[62] M. Pathak, Nanoemulsions and Their Stability for Enhancing Functional Properties of Food Ingredients, Nanotechno, 2017. https://doi.org/10.1016/B978-0-12-811942-6.00005-4.

[63] E. Dickinson, Structure , stability and rheology of flocculated emulsions, Curr. Opin. Colloid Interface Sci. 3 (1998) 633–638. https://doi.org/10.1016/S1359-0294(98)80092-7.

[64] E. Dickinson, Hydrocolloids as emulsifiers and emulsion stabilizers, Food Hydrocoll. 23 (2009) 1473–1482. https://doi.org/10.1016/j.foodhyd.2008.08.005.

[65] L. Jourdain, M.E. Leser, C. Schmitt, M. Michel, E. Dickinson, Stability of emulsions containing sodium caseinate and dextran sulfate : Relationship to complexation in solution, Food Hydrocoll. 22 (2008) 647–659. https://doi.org/10.1016/j.foodhyd.2007.01.007.

[66] C.L. Reichert, H. Salminen, G. Badolato, C. Schäfer, Influence of concentration ratio on emulsifying properties of Quillaja saponin - protein or lecithin mixed systems, Colloids Surfaces A. 561 (2018) 267–274. https://doi.org/10.1016/j.colsurfa.2018.10.050.

[67] H. Chen, W. Zhang, X. Wang, H. Wang, Y. Wu, T. Zhong, B. Fei, Effect of alkali treatment on wettability and thermal stability of individual bamboo fibers, J. Wood Sci. 64 (2018) 398–405. https://doi.org/10.1007/s10086-018-1713-0.

[68] M. Das, C. Debabrata, Evaluation of Improvement of Physical and Mechanical Properties of Bamboo Fibers Due to Alkali Treatment Mahuya, J. Appl. Polym. Sci. 107 (2008) 522–527. https://doi.org/10.1002/app.

[69] H. Hazwan, D. Trache, C.T. Hui Chuin, M.R. Nurul Fazita, M.K. Mohamad Haafiz, M. Sohrab Hossain, Extraction of cellulose nanofibers and their eco-friendly polymer composites, 2019. https://doi.org/10.1007/978-3-030-05399-4_23.

[70] D. Trache, M.H. Hussin, C.T. Hui Chuin, S. Sabar, M.R.N. Fazita, O.F.A. Taiwo, T.M. Hassan, M.K.M. Haafiz, Microcrystalline cellulose: Isolation, characterization and bio-composites application—A review, Int. J. Biol. Macromol. 93 (2016) 789–804. https://doi.org/10.1016/j.ijbiomac.2016.09.056.

[71] Z. Charrouf, D. Pioch, Projet UE / MEDA / ADS « Appui à l'amélioration de la situation de l'emploi de la femme rurale et gestion durable de l'arganeraie dans le sud-ouest du Maroc », 2009.

[72] Y. Rahib, A. Elorf, B. Sarh, S. Bonnamy, J. Chaoufi, M. Ezahri, Experimental Analysis on Thermal Characteristics of Argan Nut Shell (ANS) Biomass as a Green Energy Resource, Int. J. Renew. Energy Res. 9 (2019) 1606–1615.

[73] A. Qaiss, R. Bouhfid, H. Essabir, Characterization and Use of Coir, Almond, Apricot,

Argan, Shells, and Wood as Reinforcement in the Polymeric Matrix in Order to Valorize These Products, 2015. https://doi.org/10.1007/978-3-319-13847-3.

[74] L. Bouqbis, S. Daoud, H.W. Koyro, C.I. Kammann, L.F.Z. Ainlhout, M.C. Harrouni, Biochar from argan shells: production and characterization, Int. J. Recycl. Org. Waste Agric. 5 (2016) 361–365. https://doi.org/10.1007/s40093-016-0146-2.

[75] S.A. Laaziz, M. Raji, E. Hilali, H. Essabir, D. Rodrigue, R. Bouhfid, A. el kacem Qaiss, Bio-composites based on polylactic acid and argan nut shell: Production and properties, Int. J. Biol. Macromol. 104 (2017) 30–42. https://doi.org/10.1016/j.ijbiomac.2017.05.184.

[76] A. El Moumen, F. N'Guyen, T. Kanit, A. Imad, Mechanical properties of poly–propylene reinforced with Argan nut shell aggregates: Computational strategy based microstructures, Mech. Mater. 145 (2020) 103348. https://doi.org/10.1016/j.mechmat.2020.103348.

[77] R. Kumar, F. Hu, C.A. Hubbell, A.J. Ragauskas, C.E. Wyman, Comparison of laboratory delignification methods, their selectivity, and impacts on physiochemical characteristics of cellulosic biomass, Bioresour. Technol. 130 (2013) 372–381. https://doi.org/10.1016/j.biortech.2012.12.028.

[78] J. Bian, F. Peng, X.P. Peng, F. Xu, R.C. Sun, J.F. Kennedy, Isolation of hemicelluloses from sugarcane bagasse at different temperatures: Structure and properties, Carbohydr. Polym. 88 (2012) 638–645. https://doi.org/10.1016/j.carbpol.2012.01.010.

[79] H. Chen, Biotechnology of lignocellulose: Theory and practice, 2014. https://doi.org/10.1007/978-94-007-6898-7.

[80] A. Dufresne, J. Cavaillé, M.R. Vignon, Mechanical behavior of sheets prepared from sugar beet cellulose microfibrils, J. Appl. Polym. Sci. 64 (1997) 1185–1194. https://doi.org/10.1002/(sici)1097-4628(19970509)64:6<1185::aid-app19>3.3.co;2-2.

[81] S.Y. Oh, I.Y. Dong, Y. Shin, C.K. Hwan, Y.K. Hak, S.C. Yong, H.P. Won, H.Y. Ji, Crystalline structure analysis of cellulose treated with sodium hydroxide and carbon dioxide by means of X-ray diffraction and FTIR spectroscopy, Carbohydr. Res. 340 (2005) 2376–2391. https://doi.org/10.1016/j.carres.2005.08.007.

[82] B.M. Cherian, L.A. Pothan, T. Nguyen-Chung, G. Mennig, M. Kottaisamy, S. Thomas, A novel method for the synthesis of cellulose nanofibril whiskers from banana fibers and characterization, J. Agric. Food Chem. 56 (2008) 5617–5627. https://doi.org/10.1021/jf8003674.

[83] F.M. Pelissari, P.J.D.A. Sobral, F.C. Menegalli, Isolation and characterization of cellulose nanofibers from banana peels, Cellulose. 21 (2014) 417–432. https://doi.org/10.1007/s10570-013-0138-6.

[84] H. Tibolla, F.M. Pelissari, M.I. Rodrigues, F.C. Menegalli, Cellulose nanofibers produced from banana peel by enzymatic treatment: Study of process conditions, Ind.

Crops Prod. 95 (2017) 664–674. https://doi.org/10.1016/j.indcrop.2016.11.035.

[85] M. Brebu, C. Vasile, Thermal degradation of lignin - A review, Cellul. Chem. Technol. 44 (2010) 353–363.

[86] C. Costa, B. Medronho, A. Filipe, I. Mira, B. Lindman, H. Edlund, M. Norgren, Emulsion formation and stabilization by biomolecules: The leading role of cellulose, Polymers (Basel). 11 (2019) 1–18. https://doi.org/10.3390/polym11101570.

[87] R. Aveyard, B.P. Binks, J.H. Clint, Emulsions stabilised solely by colloidal particles, Adv. Colloid Interface Sci. 100–102 (2003) 503–546. https://doi.org/10.1007/978-3-642-04417-5_2.

[88] Y. Chevalier, M.A. Bolzinger, Emulsions stabilized with solid nanoparticles: Pickering emulsions, Colloids Surfaces A Physicochem. Eng. Asp. 439 (2013) 23–34. https://doi.org/10.1016/j.colsurfa.2013.02.054.

[89] T. Winuprasith, P. Khomein, W. Mitbumrung, M. Suphantharika, A. Nitithamyong, D.J. McClements, Encapsulation of vitamin D3in pickering emulsions stabilized by nanofibrillated mangosteen cellulose: Impact on in vitro digestion and bioaccessibility, Food Hydrocoll. 83 (2018) 153–164. https://doi.org/10.1016/j.foodhyd.2018.04.047.

[90] I. Kalashnikova, H. Bizot, B. Cathala, I. Capron, New pickering emulsions stabilized by bacterial cellulose nanocrystals, Langmuir. 27 (2011) 7471–7479. https://doi.org/10.1021/la200971f.

[91] X. Lu, H. Zhang, Y. Li, Q. Huang, Fabrication of milled cellulose particles-stabilized Pickering emulsions, Food Hydrocoll. 77 (2018) 427–435. https://doi.org/10.1016/j.foodhyd.2017.10.019.

[92] C. Miao, M. Tayebi, W.Y. Hamad, Investigation of the formation mechanisms in high internal phase Pickering emulsions stabilized by cellulose nanocrystals, Philos. Trans. R. Soc. A Math. Phys. Eng. Sci. 376 (2018). https://doi.org/10.1098/rsta.2017.0039.

[93] T. Winuprasith, M. Suphantharika, Microfibrillated cellulose from mangosteen (Garcinia mangostana L.) rind: Preparation, characterization, and evaluation as an emulsion stabilizer, Food Hydrocoll. 32 (2013) 383–394. https://doi.org/10.1016/j.foodhyd.2013.01.023.

[94] T. Winuprasith, M. Suphantharika, Properties and stability of oil-in-water emulsions stabilized by microfibrillated cellulose from mangosteen rind, Food Hydrocoll. 43 (2015) 690–699. https://doi.org/10.1016/j.foodhyd.2014.07.027.

[95] F.W. Turbak, A.F., Snyder, K.R. Sandberg, Microfibrillated cellulose, 1983.

[96] A. Ferrer, I. Filpponen, A. Rodríguez, J. Laine, O.J. Rojas, Valorization of residual Empty Palm Fruit Bunch Fibers (EPFBF) by microfluidization: Production of nanofibrillated cellulose and EPFBF nanopaper, Bioresour. Technol. 125 (2012) 249–255. https://doi.org/10.1016/j.biortech.2012.08.108.

[97] S. Panthapulakkal, M. Sain, Preparation and characterization of cellulose nanofibril films from wood fibre and their thermoplastic polycarbonate composites, Int. J. Polym. Sci. 2012 (2012). https://doi.org/10.1155/2012/381342.

[98] N. Lavoine, I. Desloges, A. Dufresne, J. Bras, Microfibrillated cellulose - Its barrier properties and applications in cellulosic materials: A review, Carbohydr. Polym. 90 (2012) 735–764. https://doi.org/10.1016/j.carbpol.2012.05.026.

[99] A. Bhatnagar, M. Sain, Processing of Cellulose Nanofiber-reinforced Composites, J. Reinf. Plast. Compos. 24 (2005) 1259–1268. https://doi.org/10.1177/0731684405049864.

[100] S. Janardhnan, M.M. Sain, Isolation of cellulose microfibrils - An enzymatic approach, BioResources. 1 (2006) 176–188. https://doi.org/10.15376/biores.1.2.176-188.

[101] S. Iwamoto, A.N. Nakagaito, H. Yano, M. Nogi, Optically transparent composites reinforced with plant fiber-based nanofibers, Appl. Phys. A Mater. Sci. Process. 81 (2005) 1109–1112. https://doi.org/10.1007/s00339-005-3316-z.

[102] A. Alemdar, M. Sain, Isolation and characterization of nanofibers from agricultural residues – Wheat straw and soy hulls, Bioresour. Technol. 99 (2008) 1664–1671. https://doi.org/https://doi.org/10.1016/j.biortech.2007.04.029.

[103] W. Yang, Y. Feng, H. He, Z. Yang, Environmentally-friendly extraction of cellulose nanofibers from steam-explosion pretreated sugar beet pulp, Materials (Basel). 11 (2018). https://doi.org/10.3390/ma11071160.

[104] R. Grande, E. Trovatti, M.T.B. Pimenta, A.J.F. Carvalho, Microfibrillated cellulose from sugarcane bagasse as a biorefinery product for ethanol production, J. Renew. Mater. 6 (2018) 195–202. https://doi.org/10.7569/JRM.2018.634109.

[105] A.L.R. Costa, A. Gomes, H. Tibolla, F.C. Menegalli, R.L. Cunha, Cellulose nanofibers from banana peels as a Pickering emulsifier: High-energy emulsification processes, Carbohydr. Polym. 194 (2018) 122–131. https://doi.org/10.1016/j.carbpol.2018.04.001.

[106] I. Siró, D. Plackett, Microfibrillated cellulose and new nanocomposite materials: A review, Cellulose. 17 (2010) 459–494. https://doi.org/10.1007/s10570-010-9405-y.

[107] D. Guillaume, Z. Charrouf, Argan oil, Altern. Med. Rev. 16 (2011). https://doi.org/10.1525/gfc.2003.3.4.68.

[108] N. Taarji, S. Vodo, M. Bouhoute, N. Khalid, A. Hafidi, I. Kobayashi, M.A. Neves, H. Isoda, M. Nakajima, Preparation of monodisperse O/W emulsions using a crude surface-active extract from argan by-products in microchannel emulsification, Colloids Surfaces A Physicochem. Eng. Asp. 585 (2020) 124050. https://doi.org/10.1016/j.colsurfa.2019.124050.

[109] M. Bouhoute, N. Taarji, S. Vodo, I. Kobayashi, M. Zahar, H. Isoda, M. Nakajima, M.A. Neves, Formation and stability of emulsions using crude extracts as natural emulsifiers

from Argan shells, Colloids Surfaces A Physicochem. Eng. Asp. 591 (2020) 124536. https://doi.org/10.1016/j.colsurfa.2020.124536.

[110] L. Segal, J.J. Creely, A.E. Martin, C.M. Conrad, An Empirical Method for Estimating the Degree of Crystallinity of Native Cellulose Using the X-Ray Diffractometer, Text. Res. J. 29 (1959) 786–794. https://doi.org/10.1177/004051755902901003.

[111] A. Oushabi, S. Sair, F. Oudrhiri Hassani, Y. Abboud, O. Tanane, A. El Bouari, The effect of alkali treatment on mechanical, morphological and thermal properties of date palm fibers (DPFs): Study of the interface of DPF–Polyurethane composite, South African J. Chem. Eng. 23 (2017) 116–123. https://doi.org/10.1016/j.sajce.2017.04.005.

[112] M.M. Andrade-Mahecha, F.M. Pelissari, D.R. Tapia-Blácido, F.C. Menegalli, Achira as a source of biodegradable materials: Isolation and characterization of nanofibers, Carbohydr. Polym. 123 (2015) 406–415. https://doi.org/10.1016/j.carbpol.2015.01.027.

[113] N.H. Kim, T. Imai, M. Wada, J. Sugiyama, Molecular directionality in cellulose polymorphs, Biomacromolecules. 7 (2006) 274–280. https://doi.org/10.1021/bm0506391.

[114] Y. Jiang, X. Liu, Q. Yang, X. Song, C. Qin, S. Wang, K. Li, Effects of residual lignin on mechanical defibrillation process of cellulosic fiber for producing lignocellulose nanofibrils, Cellulose. 25 (2018) 6479–6494. https://doi.org/10.1007/s10570-018-2042-6.

[115] J. Li, X. Wei, Q. Wang, J. Chen, G. Chang, L. Kong, J. Su, Y. Liu, Homogeneous isolation of nanocellulose from sugarcane bagasse by high pressure homogenization, Carbohydr. Polym. 90 (2012) 1609–1613. https://doi.org/10.1016/j.carbpol.2012.07.038.

[116] Y. Habibi, M. Mahrouz, M.R. Vignon, Microfibrillated cellulose from the peel of prickly pear fruits, Food Chem. 115 (2009) 423–429. https://doi.org/10.1016/j.foodchem.2008.12.034.

[117] L. Fu, S.A. McCallum, J. Miao, C. Hart, G.J. Tudryn, F. Zhang, R.J. Linhardt, Rapid and accurate determination of the lignin content of lignocellulosic biomass by solid-state NMR, Fuel. 141 (2015) 39–45. https://doi.org/10.1016/j.fuel.2014.10.039.

[118] A. Idström, S. Schantz, J. Sundberg, B.F. Chmelka, P. Gatenholm, L. Nordstierna, 13C NMR assignments of regenerated cellulose from solid-state 2D NMR spectroscopy, Carbohydr. Polym. 151 (2016) 480–487. https://doi.org/10.1016/j.carbpol.2016.05.107.

[119] T. Sparrman, L. Svenningsson, K. Sahlin-Sjövold, L. Nordstierna, G. Westman, D. Bernin, A revised solid-state NMR method to assess the crystallinity of cellulose, Cellulose. 26 (2019) 8993–9003. https://doi.org/10.1007/s10570-019-02718-0.

[120] R. Ek, P. Wormald, J. östelius, T. Iversen, C. Nyström, Crystallinity index of microcrystalline cellulose particles compressed into tablets, Int. J. Pharm. 125 (1995) 257–264. https://doi.org/10.1016/0378-5173(95)00139-A.

[121] J. Cai, L. Zhang, Rapid dissolution of cellulose in LiOH/urea and NaOH/urea aqueous solutions, Macromol. Biosci. 5 (2005) 539–548. https://doi.org/10.1002/mabi.200400222.

[122] M. Rayner, D. Marku, M. Eriksson, M. Sjöö, P. Dejmek, M. Wahlgren, Biomass-based particles for the formulation of Pickering type emulsions in food and topical applications, Colloids Surfaces A Physicochem. Eng. Asp. 458 (2014) 48–62. https://doi.org/10.1016/j.colsurfa.2014.03.053.

[123] I. Kalashnikova, H. Bizot, B. Cathala, I. Capron, Modulation of cellulose nanocrystals amphiphilic properties to stabilize oil/water interface, Biomacromolecules. 13 (2012) 267–275. https://doi.org/10.1021/bm201599j.

[124] K. Xhanari, K. Syverud, G. Chinga-Carrasco, K. Paso, P. Stenius, Structure of nanofibrillated cellulose layers at the o/w interface, J. Colloid Interface Sci. 356 (2011) 58–62. https://doi.org/10.1016/j.jcis.2010.12.083.

[125] E. Dickinson, M. Golding, Depletion flocculation of emulsions containing unadsorbed sodium caseinate, Food Hydrocoll. 11 (1997) 13–18. https://doi.org/10.1016/S0268-005X(97)80005-7.

[126] K. Junka, I. Filpponen, T. Lindström, J. Laine, Titrimetric methods for the determination of surface and total charge of functionalized nanofibrillated/microfibrillated cellulose (NFC/MFC), Cellulose. 20 (2013) 2887–2895. https://doi.org/10.1007/s10570-013-0043-z.

[127] M. Reischl, K. Stana-Kleinschek, V. Ribitsch, Electrokinetic investigations of oriented cellulose polymers, Macromol. Symp. 244 (2006) 31–47. https://doi.org/10.1002/masy.200651203.

[128] N.L. Vanier, S.L.M. El Halal, A.R.G. Dias, E. da Rosa Zavareze, Molecular structure, functionality and applications of oxidized starches: A review, Food Chem. 221 (2017) 1546–1559. https://doi.org/10.1016/j.foodchem.2016.10.138.

[129] B. Bissaro, Å.K. Røhr, G. Müller, P. Chylenski, M. Skaugen, Z. Forsberg, S.J. Horn, G. Vaaje-Kolstad, V.G.H. Eijsink, Oxidative cleavage of polysaccharides by monocopper enzymes depends on H2O2, Nat. Chem. Biol. 13 (2017) 1123–1128. https://doi.org/10.1038/nchembio.2470.

[130] A. Bismarck, I. Aranbefwi-Askargorta, J. Springer, T. Lampke, B. Wielage, A. Stamboulis, I. Shenderovich, H.-H. Limbach, Cellulose Fibers ; Surface Properties and the the Water Uptake Behavior, Polym. Compos. 23 (2002) 872–894. https://doi.org/10.1002/PC.10485.

[131] C. Bellmann, A. Caspari, V. Albrecht, T.T. Loan Doan, E. Mäder, T. Luxbacher, R. Kohl, Electrokinetic properties of natural fibres, Colloids Surfaces A Physicochem. Eng. Asp. 267 (2005) 19–23. https://doi.org/10.1016/j.colsurfa.2005.06.033.